TEKTONIKA

A Field Guide to the High Arctic Large Igneous Province in and Around Isfjorden, Svalbard

Kim Senger *[1], **Fenna Ammerlaan** [2], **Peter Betlem** [3], **Carmen Gaina** [4], **Olivier Galland** [5], **Sten-Andreas Grundvåg** [6], **Rafael Horota** [1], **Hans Jørgen Kjøll** [5], **Morgan T. Jones** [7,8], **Denise Kulhanek** [9], **Harmon Maher** [10], **Krzysztof Michalski** [11], **Kei Ogata** [12], **Snorre Olaussen** [1], **Sverre Planke** [8,13], **Ole Rabbel** [5], **Nil Rodes** [1], **Anna M. R. Sartell** [14,1], **Grace E. Shephard** [15,4], **Aleksandra Smyrak-Sikora** [2], **Christian Tegner** [16]

[1]Department of Arctic Geology, The University Centre in Svalbard, PO Box 156, 9171 Longyearbyen, Norway | [2]Department of Geosciences, Norwegian University of Science and Technology; S. P. Andersens veg 15a, 7031 Trondheim, Norway | [3]Norwegian Geotechnical Institute, NGI, Postboks 3930 Ullevål Stadion, 0806 Oslo, Norway | [4]Centre for Planetary Habitability, Department of Geosciences, University of Oslo, Norway | [5]Njord Centre, Department of Geosciences, University of Oslo, PO Box 1048, 0316 Oslo Norway | [6]Department of Geosciences, UiT The Arctic University of Norway, P.O. Box 6050 Langnes, 9037 Tromsø, Norway | [7]Department of Ecology, Environment and Geoscience (EMG), Umeå University, Umeå, Sweden | [8]Department of Geosciences, University of Oslo, 0315 Oslo, Norway | [9]Institute of Geosciences, Kiel University, Ludewig-Meyn-Straße 14, 24118 Kiel, Germany | [10]Department of Geography and Geology, University of Nebraska at Omaha, Omaha, NE 68189, USA | [11]Institute of Geophysics, Polish Academy of Sciences, Ks. Janusza 64, 01-452 Warszawa, Poland | [12]Dipartimento di Scienze della Terra, dell'Ambiente e della Vita (DiSTAV), Università degli Studi di Genova, Corso Europa 26, 16132 - Genova, Italy | [13]Volcanic Basin Energy Research AS, Oslo, Norway | [14]Department of Geosciences and Geography, University of Helsinki, Gustaf Hällströmin katu 2, 00014 Helsinki, Finland | [15]Research School of Earth Sciences, Australian National University, Australia | [16]Department of Geoscience, Aarhus University, Aarhus, Denmark

Abstract The High Arctic Large Igneous Province (HALIP) is a major tectono-magmatic element that affected large parts of the Arctic during the Cretaceous (magmatism occurred from 126 to 78 million years ago [Ma]). In Svalbard, HALIP intrusive and extrusive rocks are grouped and classified as the Diabasodden Suite. Sills and dykes are present throughout Svalbard, emplaced in units stratigraphically ranging from crystalline basement to Jurassic-Cretaceous siliciclastics. Time-equivalent lava flows are exposed on Kong Karls Land in eastern Svalbard. In this contribution, we firstly define and introduce major features of the circum-Arctic HALIP. Secondly, we zoom into Svalbard where we document and summarize the attributes of HALIP outcrops (i.e., the Diabasodden Suite) located in and around Isfjorden, the most accessible location that is reachable on day trips using boats from Longyearbyen. For each of the 15 sites we focus on specific aspects of HALIP characterization, including geochronology, geochemistry and geometry of volcanic and intrusive rocks. We complement field descriptions of the sites with digital geoscientific data, including digital outcrop models and photospheres. Finally, we synthesize the Isfjorden study area in the context of data and knowledge gaps for the HALIP in general. We hope that this contribution will stimulate further HALIP research in Isfjorden and beyond.

Executive Editor:
Graeme Eagles
Associate Editor:
Chiara Montomoli
Technical Editor:
Mohamed Gouiza

Reviewers:
Enrico Tavarnelli
Anonymous Reviewer

Submitted:
15 December 2025
Accepted:
7 July 2026
Published:
18 September 2026

1 Introduction

Large igneous provinces (LIPs) are characterized by voluminous volcanic and magmatic activity over a geologically speaking short period of time having short-lived intense pulses of activity. *Bryan and Ernst* (2008) classify LIPs as "...magmatic provinces with areal extents > 0.1 million km^2, igneous volumes > 0.1 million km^3 and maximum lifespans of ~50 million years (Myr) that have intraplate tectonic settings or geochemical affinities, and are characterized by igneous pulse(s) of short duration (~1–5 Myr), during which a large proportion (> 75%) of the total igneous volume has been emplaced." They are typically caused by the arrival of a mantle plume head that has been derived from the deep interior.

LIPs may have profound effects on the global climate, having been linked as the main driver of many mass extinctions (e.g., *Svensen et al.*, 2004; *Bond and Grasby*, 2017; *Ernst and Youbi*, 2017; *Zhou et al.*, 2024), including the largest mass extinction also known as "The Great Dying" at the end of the Permian (End-Permian Mass Extinction, EPME; e.g., *Zuchuat et al.*, 2020; *Shen et al.*, 2011). Characterizing the influence of both extruded lava and greenhouse gases generated through contact metamorphism within the igneous plumbing system and subsequent release by hydrothermal venting is crucial to

* kims@unis.no

understanding how the Earth system responds to such major perturbations.

On the regional scale, LIP emplacement is often associated with regional uplift linked to the arrival of a mantle plume (e.g., *Dam et al.*, 1998) that exerts a strong control on sedimentation patterns. However, regional uplift and subsidence may occur because of lithospheric heterogeneities (*Burov et al.*, 2007). Finally, LIPs are often associated with ore-forming processes, and many LIP-related regionsare thus investigated for associated mineral resources (*Ernst and Jowitt*, 2013).

There are many LIPs worldwide and the northernmost one, located in the high Arctic, remains one of the least well studied and understood. John Tarduno coined the term High Arctic Large Igneous Province (HALIP) in 1998 at the 3rd International Conference on Arctic Margins (ICAM) meeting in Celle, Germany (*Tarduno et al.*, 1998), based on his studies in the Canadian Arctic (*Tarduno et al.*, 1998). While there is no formal definition of the HALIP, it is generally accepted to refer to basaltic magmatic rocks emplaced within the circum-Arctic (a region bounded by the 60°N latitude) during the Cretaceous (*Sartell et al.*, 2025). Since the labelling of the Arctic Cretaceous magmatic province, HALIP rocks have been investigated in Svalbard (i.e., Diabasodden Suite; *Maher*, 2001; *Nejbert et al.*, 2011; *Senger et al.*, 2024; *Senger and Galland*, 2022), Franz Josef Land (*Ntaflos and Richter*, 2003; *Simonov et al.*, 2019), the Barents Shelf (*Polteau et al.*, 2016), Arctic Canada (*Bédard et al.*, 2021a,b; *Deegan et al.*, 2023; *Dockman et al.*, 2025; *Evenchick et al.*, 2015; *Kingsbury et al.*, 2018), the central Arctic basin (*Døssing et al.*, 2013, 2017), the Chukchi Plateau (*Coakley et al.*, 2016; *Mukasa et al.*, 2020), northern Greenland (*Estrada et al.*, 2001; *Kontak et al.*, 2001; *Thórarinsson et al.*, 2015; *Tegner et al.*, 2011) and the De Long Islands (*Nikishin et al.*, 2024). Several major questions regarding the nature of the HALIP remain, including the apparent multi-phased magmatism, the linkage to the opening of the Amerasian Basin, and its influence on global climate.

In this contribution we provide a thematic field guide to some of the most accessible HALIP exposures on the shores of Isfjorden, central Spitsbergen (Spitsbergen being the largest island of the Norwegian Svalbard archipelago). We place these field stops in both a regional and, where relevant, circum-Arctic HALIP perspective. Furthermore, we provide an overview of existing geological and geophysical data sets regionally and for each stop to stimulate further research, and provide some perspectives on the knowledge and data gaps with respect to the HALIP in Isfjorden and beyond.

2 The High Arctic Large Igneous Province

The HALIP is interesting also due to its striking longevity compared to other LIPs, with radiometric dates ranging over a 48 Myr period from 126-78 Ma (e.g., *Dockman et al.*, 2025; *Sartell et al.*, 2025; *Tegner et al.*, 2011), and three main magmatic pulses at ~123, ~92 and ~81 Ma defined on the basis of robust U-Pb dating (*Sartell et al.*, 2025). There is a partly contemporaneous or formative link to the adjacent Amerasia Basin (*Døssing et al.*, 2013), and a connection between the protracted nature of the HALIP and mantle plume-lithosphere interactions (*Heyn et al.*, 2024). Furthermore, the HALIP has a strong control on circum-Arctic sedimentation (e.g., *Grundvåg et al.*, 2017; *Ineson et al.*, 2021) and may have influenced the global climate (e.g., *Galloway et al.*, 2022; *Naber et al.*, 2020). In this section we briefly review some of the wider observations and inferences about the HALIP, before focussing on the HALIP on Svalbard.

2.1 Zooming out to the Larger Scale - Arctic Ocean Opening

The Arctic Ocean can be subdivided into two sub-basins, the older Amerasia Basin and the younger Eurasia Basin (Figure 1; *Glebovsky et al.*, 2006; *Nikishin et al.*, 2018). The two basins are separated along the Lomonosov Ridge (Figure 1). The Eurasia Basin has been opening since ~56 Ma (Paleogene) and opening continues today along the ultra-slow seafloor spreading of the Gakkel Ridge. This basin therefore separates the Barents and Kara shelves, including the Svalbard and Franz Josef Land archipelagos, from the other HALIP localities (Figure 1). However, the HALIP Cretaceous configuration can be restored by a plate tectonic reconstruction that takes into account the age of rifting and seafloor spreading between the Lomonosov Ridge and Eurasian continental margin (Figure 2). It is the timing and nature of opening of the Amerasia Basin which has more pertinent implications for the emplacement of the HALIP (e.g., *Døssing et al.*, 2013, 2017; *Hadlari*, 2024).

The Amerasia Basin can be subdivided into several regions with discrete geometries and characteristics. The Canada Basin is thought to have the only true oceanic lithosphere, which is surrounded by crust of hyperextended or transitional nature (Figure 3; e.g., *Chian et al.*, 2016; *Priyanto and Coakley*, 2025). The elevated continental Chukchi Plateau extends from the Siberian Shelf. To the north lies the Alpha-Mendeleev Ridge, an underwater mountain chain, which is thought to be dominantly magmatic in nature, potentially with some underlying component of continental crust (*Oakey and Saltus*, 2016). The Makarov and Podvodnikov basins lie adjacent to the Lomonosov Ridge, and at least for the Makarov Basin have been suggested to be related to a discrete later oceanic spreading episode (*Gaina et al.*, 2025).

The timing of Amerasia Basin opening is broadly described as Mesozoic, with evidence of rifting from the early Jurassic (*Grantz et al.*, 1998) through to opening sometime in the Early Cretaceous. In the Canada Basin, a central gravity low and set of conjugate magnetic anomalies indicates a fossil spreading ridge and suggest that opening must have occurred before (or after) the Cretaceous Normal Superchron (121-83 Ma). Depending on the timescale used, recent magnetic isochron interpretations from *Døssing et al.* (2020)

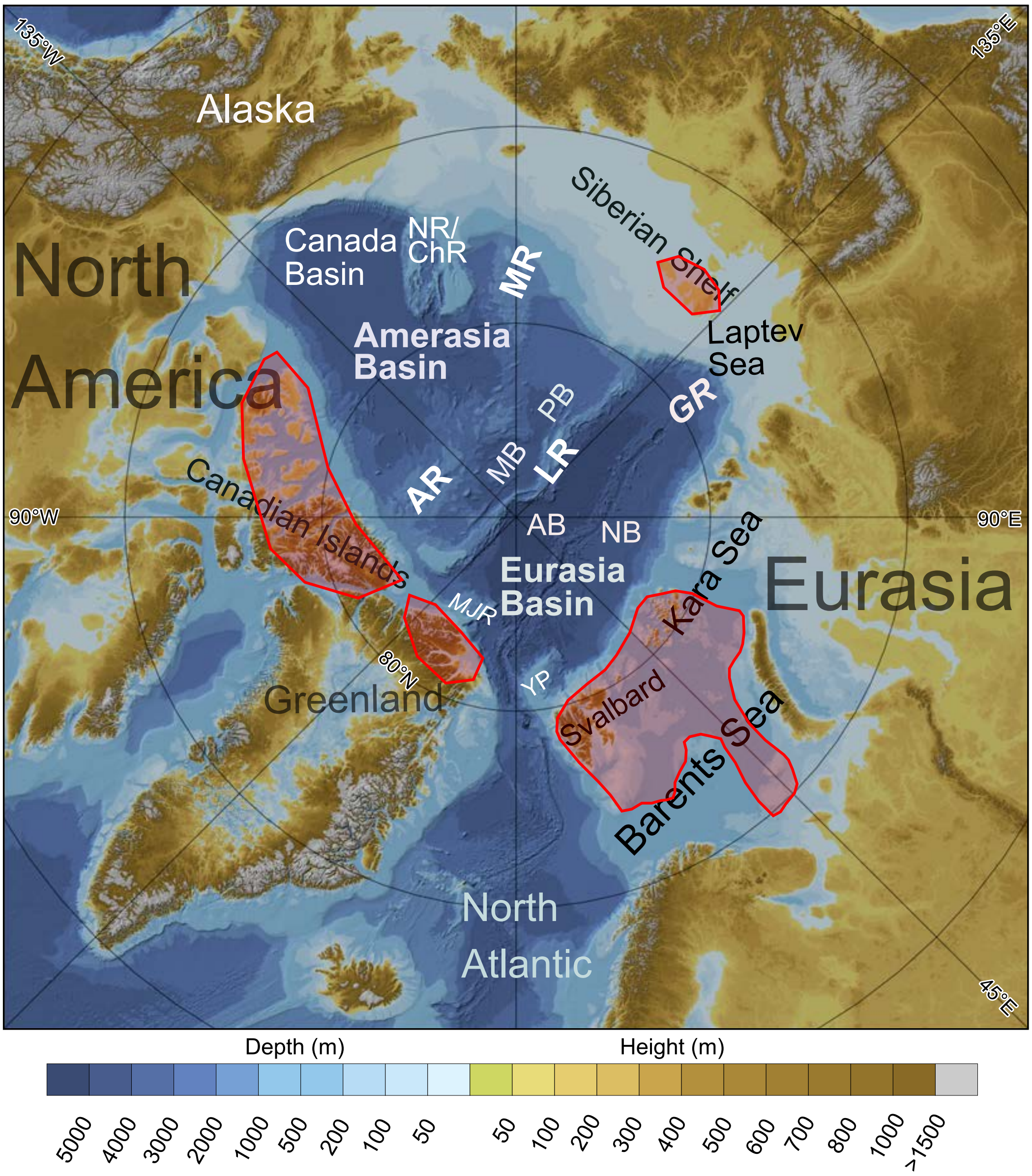

Figure 1 – Map of the main High Arctic Large Igneous Province (HALIP) elements at present-day (red polygons; may also include parts of the Alpha Ridge) and the major geographic names of the Arctic. AB = Amundsen Basin; AR = Alpha Ridge; GR = Gakkel Ridge; LR = Lomonosov Ridge; MB = Makarov Basin; MJR = Morris Jesup Rise; MR = Mendeleev Ridge; NB = Nansen Basin; NR/ChR = Northwind Ridge and Chukchi Rise; PB = Podvodnikov Basin; YP = Yermak Plateau.

suggest seafloor spreading to have occurred between 127-120 (alternatively 131-126 Ma; c.f. 140-128 or 142-133 Ma by *Zhang et al.*, 2019). Incorporating these constraints, and a wide range of onshore and offshore geological, geochronological, geophysical data, several conceptual or fully kinematic tectonic models have emerged (e.g., *Shephard et al.*, 2013; *Miller et al.*, 2018; *Hutchinson et al.*, 2017). The kinematics of opening can be largely ascribed to either a suite of counter-clockwise "windshield-wiper" rotational models, or more recent translational models which account for NE-trending anomalies (e.g., *Hutchinson et al.*, 2017; *Døssing et al.*, 2020). Accounting for the various Amerasia Basin sub-domains, e.g., motion of the Chukchi Plateau, the potential continuation of the Canada Basin spreading axis to the north, and restoring any extended continental crust in the Alpha Ridge domain, is a challenge for any consistent, time-dependent plate reconstruction.

Nonetheless, because the HALIP has been ascribed to ~126-78 Ma, including the first pulse at ca. 123 ± 3 Ma in Svalbard (*Sartell et al.*, 2025), it is likely that the Amerasia Basin had dominantly opened or was in the final stages of opening (i.e., before 120 Ma) when the HALIP was emplaced. In other words, an underlying mantle plume likely impinged on recently opened or actively opening lithosphere. It is worth acknowledging that younger opening times for parts of the Amerasia Basin, including the Alpha-Mendeleev ridge and Makarov Basin, have also been presented (e.g., *Chernykh et al.*, 2018; *Døssing et al.*, 2017).

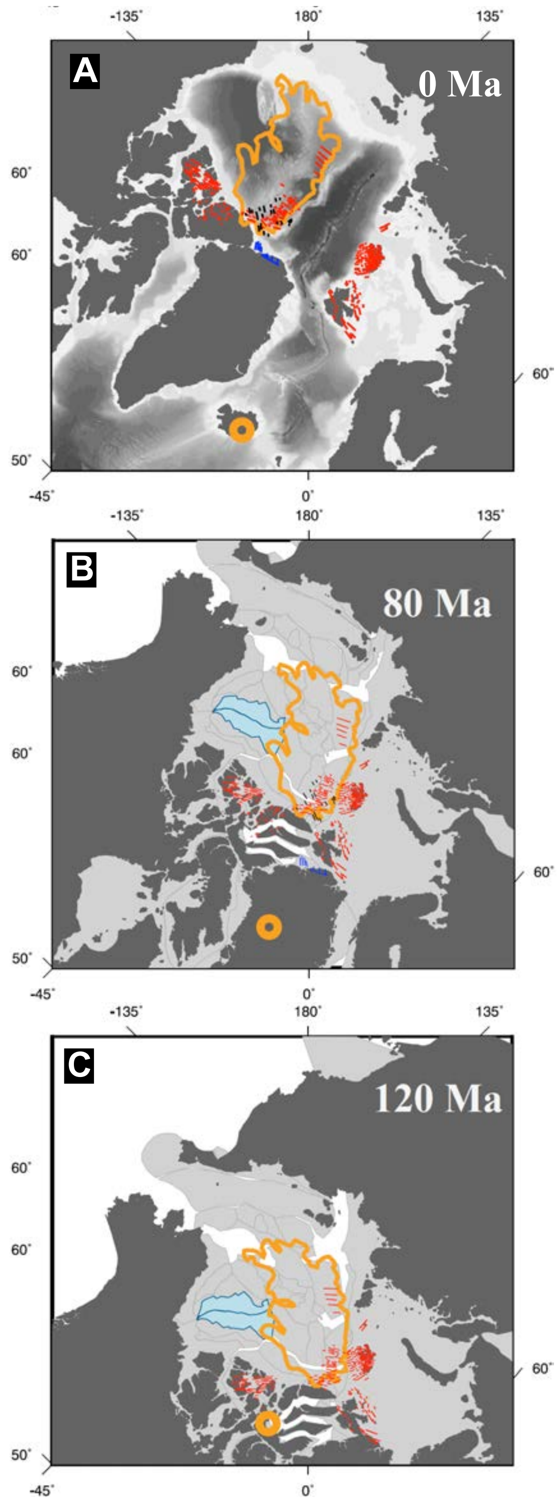

Figure 2 – A) Present day location of dykes (red lines) and interpreted extent of magmatism in the Alpha -Mendeleev region (purple; based on the High Arctic Magnetic Domain - HAMD from Oakey and Saltus, 2016) B) and C) Plate tectonic reconstructions (modified after *Døssing et al.*, 2020) in an absolute reference frame (*Steinberger and Torsvik*, 2008) showing the distribution of HALIP elements at 120 Ma (corresponding to the oldest HALIP pulse) and 80 Ma (youngest HALIP pulse). The present-day location of the Iceland mantle plume is shown by the orange circle. The blue polygon shows the extent of oceanic crust in the Canada Basin.

2.2 Geochronology - Circum-Arctic Perspective

The HALIP exhibits a wide range of radiometric dates from 126 to 78 Ma (Figure 4). Furthermore, based largely on the Canadian samples, the HALIP is thought to include three main pulses (Figure 4; *Dockman et al.*, 2018, 2025; *Heyn et al.*, 2024; *Sartell et al.*, 2025). Not all HALIP sub-provinces exhibit the full range of magmatic episodes. Robust U-Pb dating in Svalbard, for instance, suggests that only the oldest pulse (123 ± 3 Ma) is present locally (*Corfu et al.*, 2013; *Sartell et al.*, 2025). In the first 2D numerical mantle convection models of their kind, *Heyn et al.* (2024) showed that a mantle plume interacting with variable lithospheric thicknesses (e.g., from the Amerasia Basin to Sverdrup Basin to cratonic Greenland) could account for some of the first-order elements of the HALIP. Namely, the spatially and temporally variable melt volumes, and at least two of the pulsations.

2.3 Geochemistry - Circum-Arctic Perspective

Numerous studies address the geochemistry of the HALIP throughout the Arctic, including Svalbard (*Nejbert et al.*, 2011), Franz Jozef Land (*Ntaflos and Richter*, 2003), the De Long Islands (*Silantyev et al.*, 2004), the Canadian Arctic (e.g., *Estrada et al.*, 2016; *Deegan et al.*, 2023; *Bédard et al.*, 2021a,b; *Naber et al.*, 2020), northern Greenland (*Thorarinsson et al.*, 2011a) and dredged samples from the Alpha-Mendeleev Ridge (*Van Wagoner et al.*, 1986; *Williamson et al.*, 2026).

Initial studies focused on correlating the intrusions geochemically, largely classified as basaltic dolerites (Figure 5). By far the most extensive and systematic geochemical studies of HALIP rocks have been conducted in Arctic Canada, primarily driven by mapping initiatives led bv the Geological Survey of Canada. *Bédard et al.* (2021b) conduct an updated classification of HALIP rocks from Canada to decipher when, how and where the various magmatic types were generated.

The HALIP is dominated by tholeiites (Figure 5), with some alkaline igneous rocks particularly in the younger complexes seen in the Canadian Arctic (*Bédard et al.*, 2021a). The geochemical data provide evidence for multiple magma components and crustal contamination, as well as constraints on melting depths. On a regional scale, the geochemical data suggests depth-controlled melting for the upper tholeiitic and lower alkalic suites. Magma was then transported laterally across hundreds of kilometers to the Sverdrup Rim and Sverdrup Basin through a series of sills and dykes (*Dockman et al.*, 2025).

2.4 Sedimentology - Circum-Arctic Perspective

The emplacement of the High Arctic Large Igneous Province (HALIP) during the Cretaceous triggered regional-scale thermal uplift and major shifts in source areas and drainage patterns across the Arctic (Figure 6). This initial pulse, occurring approximately 123–122 Ma,

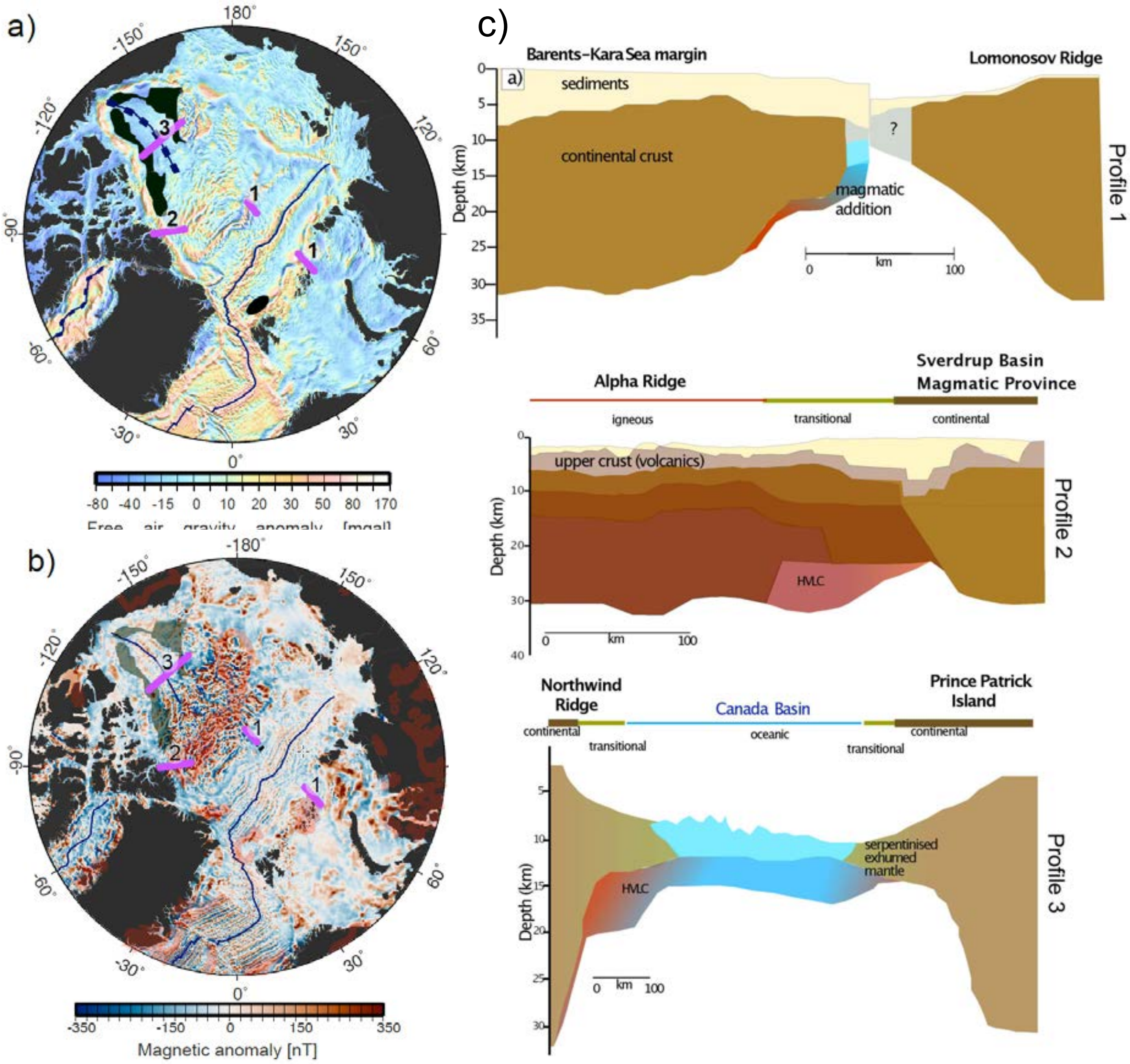

Figure 3 – Circum-Arctic geophysical maps and regional crustal-scale profiles illustrating the main tectono-magmatic elements of the Arctic. A) Free air gravity anomaly (*Andersen et al.*, 2014) and B) magnetic anomaly (*Gaina et al.*, 2011) maps of the Circum-Arctic. Magenta lines numbered 1 to 3 indicate crustal profiles illustrated in (C). C) Crustal transects continental margins of Eurasia Basin (a), northern Sverdrup Basin and Alpha Ridge (b), and of Canada Basin (c). Profile 1 is modified after profile D of *Minakov et al.* (2012); profile 2 is modified after *Funck et al.* (2011), and Profile 3 is modified after *Chian et al.* (2016). HVLC = high-velocity lower crust.

coincided with the opening of the Canada Basin, where seafloor spreading is estimated to have occurred between 127 and 120 Ma.

This widespread uplift created diachronous unconformities across various basins, including the Sverdrup, Wandel Sea, and Barents Shelf (Figure 7). For example, a major Hauterivian break-up unconformity is documented in Alaska and Arctic Canada, while central and southern Spitsbergen exhibit a Barremian-age unconformity at the base of the Helvetiafjellet Formation (*Śliwińska et al.*, 2020). These variations reflect regional differences in the rate and magnitude of uplift, exhumation, and isostatic response to HALIP activity.

Prior to the main HALIP activity, Jurassic to Early Cretaceous clastic wedges in the Agardhfjellet and Rurikfjellet formations suggest early basin margin uplift related to incipient rifting. During the main HALIP pulse, the Helvetiafjellet Formation on Svalbard transitioned from quartz arenites to volcanic arenites (*Edwards*, 1979), reflecting an influx of volcanic sediment. This period was also characterized by bentonite layers, dolerite intrusions, and basaltic lavas (*Senger et al.*, 2014a). Similar fluvio-deltaic to marine successions are recorded in Northeast Greenland and the Sverdrup Basin (*Ineson et al.*, 2021; *Tullius et al.*, 2014). Notably, the early Aptian Oceanic Anoxic Event (OAE) 1a is preserved in organic-rich marine mudstones across these regions, marking a broad transgression following the uplift (*Midtkandal et al.*, 2016).

Later HALIP pulses continued to influence Arctic stratigraphy. On Spitsbergen, a low-angle unconformity spanning the late Albian to lowermost Paleocene

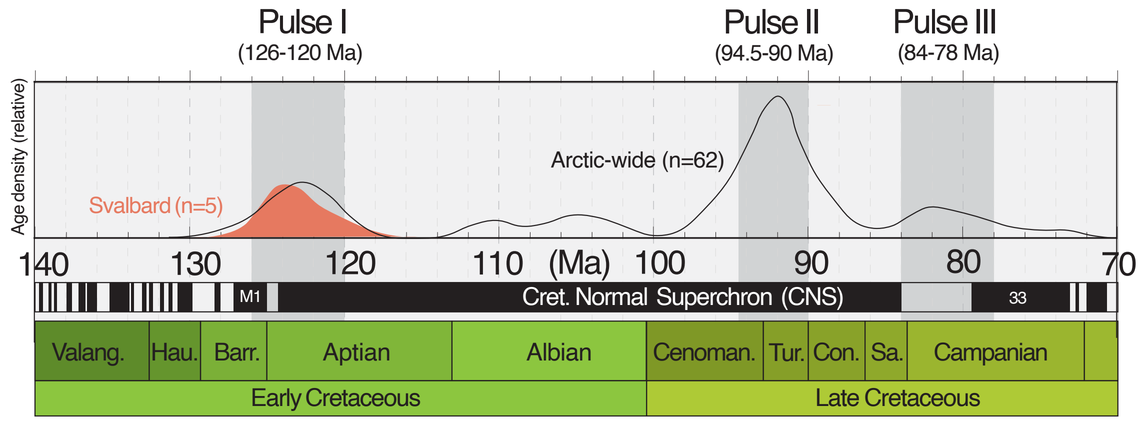

Figure 4 – Summary of circum-Arctic geochronological data from the HALIP, three pulses based on *Sartell et al.* (2025) timings, alternatively 124-120 Ma, 99-91 Ma and 85-77 Ma based on *Dockman et al.* (2018). Figure modified from *Heyn et al.* (2024) and *Sartell et al.* (2025), where the maximum peak in age density for the Svalbard samples (n=5) is 0.2 and all verified Arctic-wide samples (n=62) is 0.08.

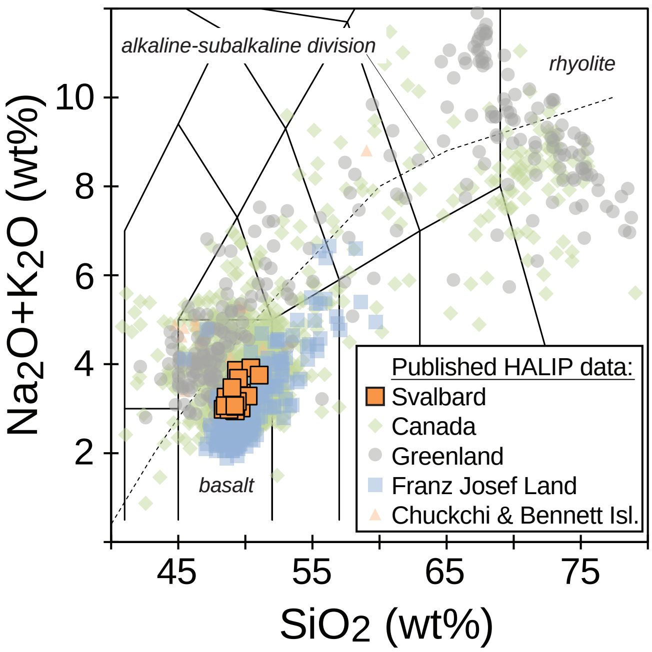

Figure 5 – Geochemical characterization of the HALIP. Silica vs. total alkalis classification plot for a compilation of HALIP rocks. This compilation is based on published data (*Amundsen et al.*, 1998; *Brown et al.*, 1987; *Bédard et al.*, 2020; *Dockman et al.*, 2018; *Dostal and MacRae*, 2018; *Estrada*, 2000; *Estrada et al.*, 2001, 2006; *Estrada*, 2015; *Estrada et al.*, 2016; *Estrada and Henjes-Kunst*, 2004; *Estrada et al.*, 2010; *Estrada and Piepjohn*, 2019; *Evenchick et al.*, 2015, 2019; *Jowitt et al.*, 2014; *Kingsbury et al.*, 2016; *Korago et al.*, 2010; *Nejbert et al.*, 2011; *Osadetz and Moore*, 1988; *Saumur et al.*, 2016; *Shipilov and Karyakin*, 2010; *Sklyarov et al.*, 2016; *Thorarinsson et al.*, 2011a,b, 2012; *Thórarinsson et al.*, 2015; *Trettin*, 1996).

indicates thermal doming that led to the extensive erosion of Upper Cretaceous strata (*Steel and Worsley*, 1984). In contrast, Upper Cretaceous deposits are preserved in the Sverdrup Basin and Northeast Greenland (*Embry and Beauchamp*, 2019; *Hovikoski et al.*, 2018). The Sverdrup Basin, in particular, experienced significant late-stage volcanism, evidenced by thick tholeiitic basalt flows in the Cenomanian Strand Fiord Formation and numerous bentonites in the Kanguk Formation (*Embry and Beauchamp*, 2019). These Upper Cretaceous fills also contain sandstone wedges resulting from continued thermo-tectonic uplift and prograding shoreline systems.

2.5 The HALIP and Environmental Perturbations

LIPs influence climate and are often associated with hyperthermals and mass extinctions throughout the Phanerozoic (*Jones et al.*, 2016; *Bond and Grasby*, 2017; *Smyrak-Sikora et al.*, 2024, Figure 7). There is a strong temporal correlation between LIP activity and oceanic anoxic events (OAEs) in the geological record (e.g., *Percival et al.*, 2021, Figure 8).

However, tying a specific LIP to a specific mass extinction event is challenging when details are considered. Firstly, the magnitude (volume and area), timing (rapid, pulsating or long-lived), nature (extrusive vs intrusive), and location (proximal or distal to the study area) of the magmatism will influence the environmental perturbation (*Jones et al.*, 2016). Similarly, the nature of the host rocks (organic-rich shales, carbonates, siliciclastics, metamorphic basement etc.) will influence what type of gases will be generated during contact metamorphism (*Aarnes et al.*, 2010; *Black et al.*, 2018; *Heimdal et al.*, 2020, 2021; *Svensen et al.*, 2023, 2004). Furthermore, other stress factors affect the fauna and flora prior or during LIP activity. For instance meteorite impacts or plate tectonic reorganizations, will affect the severity of environmental response to large-scale volcanism.

Intrusive igneous complexes (e.g., dykes, sills, saucer-shaped intrusions) are by definition emplaced in the deep to shallow subsurface and initially not in direct contact with the atmosphere. The past decades, however, have highlighted the presence and importance

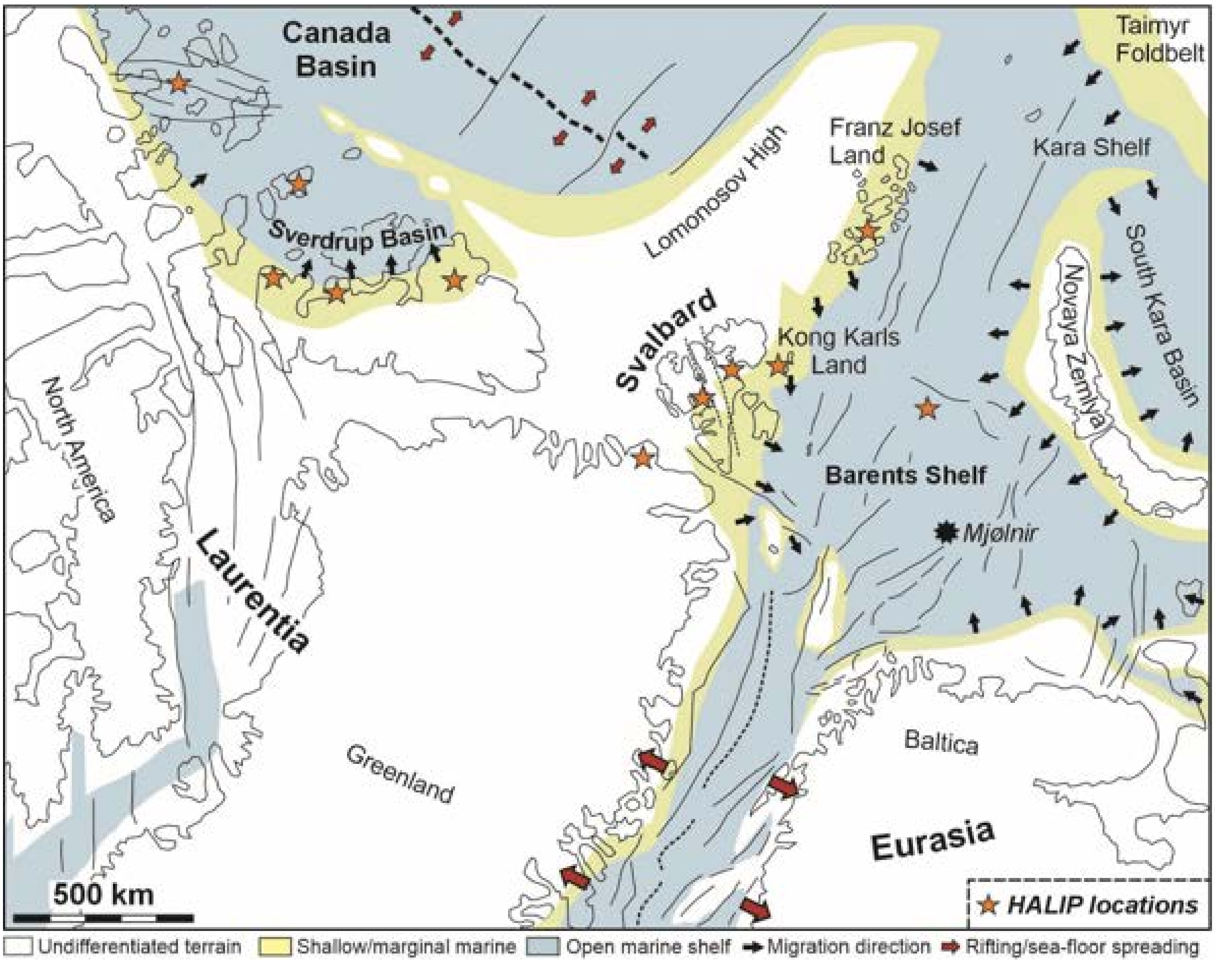

Figure 6 – Circum-Arctic paleogeographic map during the Early Cretaceous, highlighting major sedimentary pathways and key HALIP locations. Figure modified from *Grundvåg et al.* (2017).

of hydrothermal vent complexes in channeling large quantities of greenhouse gases from contact metamorphic aureoles to the atmosphere (*Svensen et al.*, 2004). Such complexes are best mapped using 3D seismic data (e.g., *Magee et al.*, 2014; *Kjoberg et al.*, 2017; *Berndt et al.*, 2023) and have been postulated as a major factor driving the PETM through NAIP volcanism (*Svensen et al.*, 2004; *Frieling et al.*, 2016; *Jones et al.*, 2016; *Berndt et al.*, 2023). Field exposures of hydrothermal vent complexes have been identified in the Karoo Basin of South Africa (*Svensen et al.*, 2008, 2023).

In Svalbard and the rest of the Barents Shelf, potential hydrothermal vent complexes associated with the HALIP have been identified on 2D seismic data (*Polteau et al.*, 2016; *Senger et al.*, 2013) and multibeam bathymetry (*Senger et al.*, 2013, Stop 13). Sills are preferentially emplaced in organic-rich shales, particularly the Middle Triassic Botneheia Formation (*Senger and Galland*, 2022). This enhances the possibility of significant greenhouse gas generation during contact metamorphism.

2.6 Svalbard - an Accessible Part of the HALIP Puzzle

Svalbard is a Norwegian high Arctic archipelago comprising all islands between 15°-35°E and 74°-81°N including the largest island of Spitsbergen (Figure 9). The archipelago is particularly renowned for its nearly continuous post-Caledonian succession recording the interplay of global climate and regional tectonics (*Smyrak-Sikora et al.*, 2024, and references therein). Svalbard also offers many insights into the tectonic evolution of the broader Arctic and North Atlantic systems (e.g., *Harland*, 1997).

In Svalbard, all HALIP rocks are officially classified as the Diabasodden Suite (*Dallmann et al.*, 1999) but referred to as HALIP herein. *Tyrrell and Sandford* (1934) were the first to systematically review the Svalbard dolerites. *Maher* (2001) provided an updated synthesis of the Diabasodden Suite just a few years after the HALIP was officially named (*Tarduno et al.*, 1998). Doleritic sills are the most prevalent manifestations, although dykes occur locally. Time-equivalent extrusives, Aptian plateau lavas are only seen in Kong Karls land and are currently dated ($^{40}Ar/^{39}Ar$) to 126.1 ± 1.7 Ma (Morgan Ganerød, pers. comm. 2020 in *Olaussen et al.*, 2025). *Senger et al.* (2014a) and *Nejbert et al.* (2011) provide comprehensive regional reviews of the Diabasodden Suite, while *Senger and Galland* (2022) focus on the data-rich central Spitsbergen area and the stratigraphic and spatial extent of the igneous rocks.

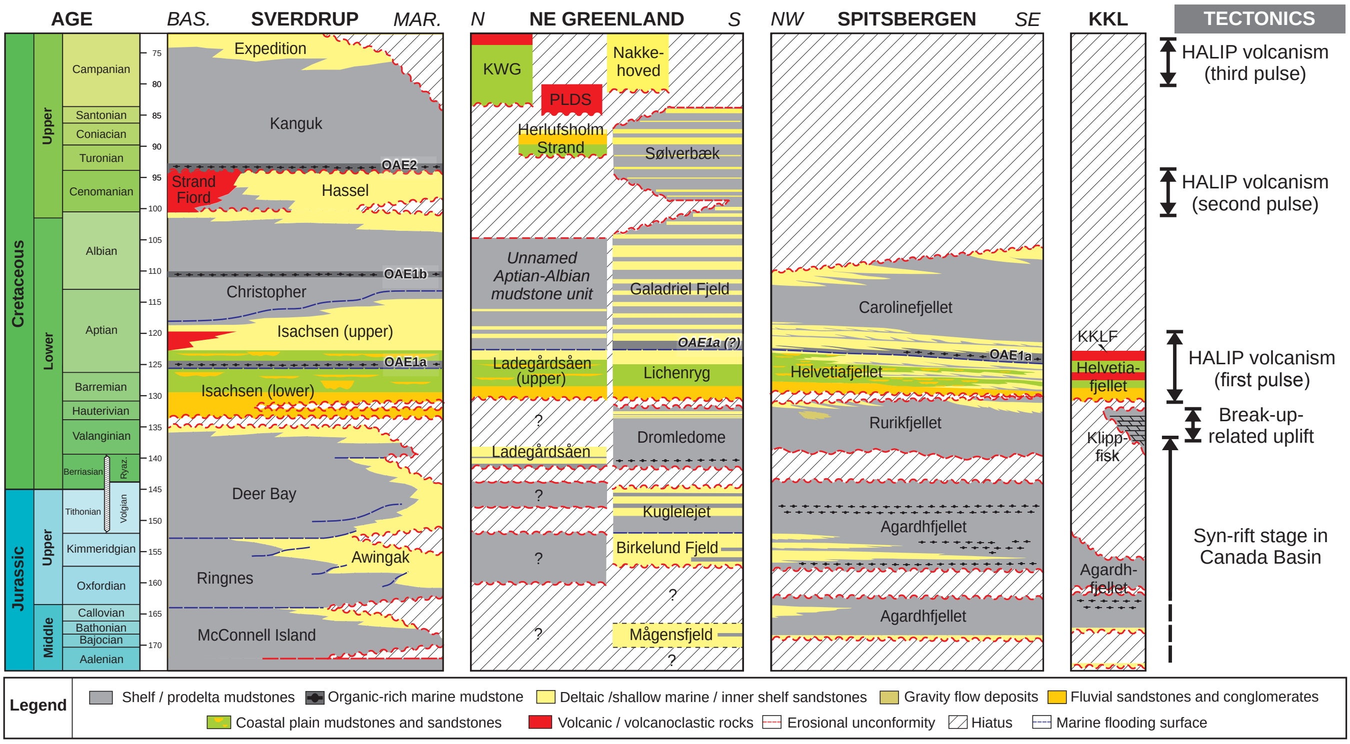

Figure 7 – Circum-Arctic correlation of onshore Cretaceous strata (listed at formation level) exposed in the Sverdrup Basin, Northeast Greenland (outcropping part of the Wandel Sea Basin), Spitsbergen, and the Kong Karls Land (KKL) islands (the latter two representing the exhumed and exposed part of the Barents Shelf basin). Note that the Oceanic Anoxic Event (OAE) 1a has been documented in the lower Aptian of the Sverdrup Basin and on Spitsbergen. On Northeast Greenland, we tentatively place it in the lower mudstone-dominated part of the Galadriel Fjeld Formation. Compiled from *Dypvik et al.* (2002), *Embry and Beauchamp* (2019), *Grundvåg et al.* (2017, 2021), *Hadlari et al.* (2016); *Hadlari* (2024), *Herrle et al.* (2015), *Hovikoski et al.* (2018), *Ineson et al.* (2021), *Jelby et al.* (2025), *Olaussen et al.* (2019), and *Tegner et al.* (2011). Abbreviations: Bas.: basin; Mar: margin; KKL: Kong Karls Land; KKLF: Kong Karls Land lava flows; PLDS: Peary Land dyke swarm; KWG: Kap Washington Group volcanics.

Two major intrusive complexes are identified in Svalbard: 1) Central Isfjorden, including the type locality at Diabasodden, and 2) the Hinlopenstretet to Tusenøyane dolerite belt in eastern Svalbard (Figure 9). Stratigraphically the doleritic sills and dykes are preferentially emplaced in shale-dominated successions in the Middle Triassic, but occur throughout the stratigraphy from basement to the Cretaceous (Figure 10). Exposures of dolerites in the fold-and-thrust belt in western Spitsbergen are identified both in outcrops and in 2D seismic profiles.

Compared to the Canadian Arctic where HALIP exposures are also investigated from a mineral exploration perspective (e.g., *Saumur et al.*, 2022), the Diabasodden Suite has been largely overlooked, even though it represents by far the most easily accessible part of the HALIP. *Senger et al.* (2014a) present a comprehensive synthesis of research on the Svalbard dolerites and argue that a strengthened circum-Arctic perspective is essential for deciphering the evolution of the HALIP as an integrated magmatic system. One of the major research questions is the timing of the HALIP pulse, which in Svalbard only seems to be related to the oldest pulse (*Corfu et al.*, 2013; *Sartell et al.*, 2025). This may be related to the development of the plume head over time or Svalbard's location at the periphery of HALIP magmatism. Another aspect is the regional to local emplacement modes to the peripheral HALIP sites such as Svalbard and the neighbouring Franz Josef Land.

In the past two decades the Diabasodden Suite has been investigated in terms of implications of geochemistry (*Nejbert et al.*, 2011), igneous complex architecture (*Galland et al.*, 2025), storing CO_2 (*Senger et al.*, 2013), contact metamorphism (*Senger et al.*, 2014a), regional spatial and stratigraphic distribution (*Polteau et al.*, 2016; *Senger and Galland*, 2022) and updated geochronology (*Sartell et al.*, 2025).

3 Field Excursion to Isfjorden

In this interactive and partly digital field guide we visit 15 HALIP-related stops in and around Isfjorden (Table 1; Figure 11). The geologically diverse area is (relatively) easily accessible from Longyearbyen and offers a number of tectono-magmatic elements of interest, illustrated on the map and a regional cross-section (Figure 11).

In the east, the field guide area is bounded by the Billefjorden Fault Zone (BFZ), one of a series of N-S trending long-lived lineaments exerting strong control on Svalbard's geological evolution. The BFZ acted as a major shear zone with significant strike-slip movements during the Caledonian orogeny, then > 10 km of reverse offset during the Late Devonian Ellesmerian

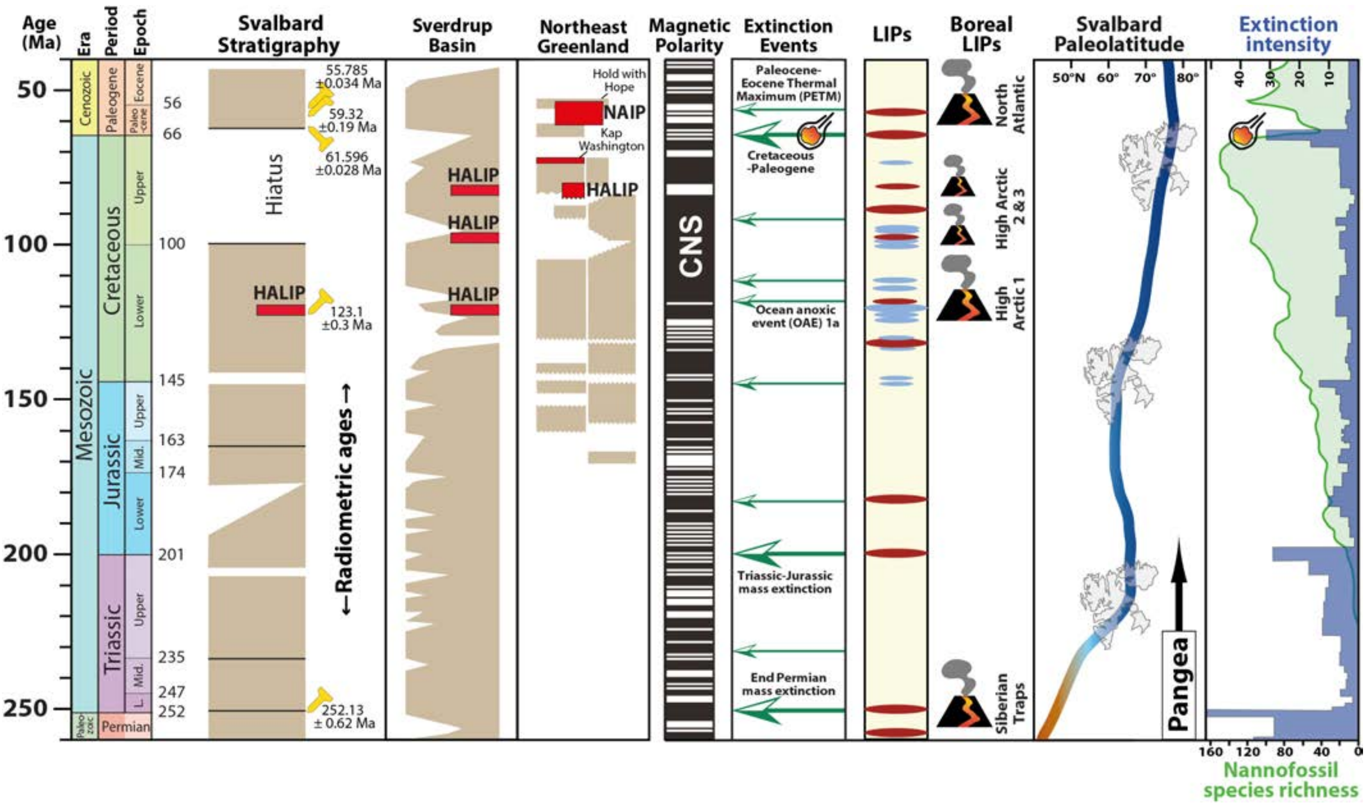

Figure 8 – Overview of key tectonomagmatic and stratigraphic events (*Dypvik et al.*, 2002; *Embry and Beauchamp*, 2019; *Jones et al.*, 2016; *Smyrak-Sikora et al.*, 2024) in the context of global extinction events and significant circum-Arctic LIPs. The right column shows the marine extinction intensity (*Rohde and Muller*, 2005) and the Calcareous nannoplankton evolution and diversity through time (*Bown et al.*, 2004). Red LIPs: continental, blue LIPs: Oceanic. CNS: Cretaceous normal superchron.

deformation, followed by an extensional phase in the middle Carboniferous which led to basin formation and sediment deposition within the Billefjorden Trough half-graben, and finally reactivation during Paleogene transpression/contraction (*Bælum and Braathen*, 2012).

In the west, the excursion area is bounded by the zone of intense deformation related to the West Spitsbergen Fold and Thrust Belt (WSFTB), part of the Eurekan deformation affecting large parts of the Arctic (*Braathen et al.*, 1999; *Bergh et al.*, 1997; *Piepjohn et al.*, 2016). East-west shortening of up to 25 km (*Braathen et al.*, 1999) occurred during the largely transpressional event, with basement-involved thick-skinned deformation in the western part and thin-skinned deformation along three major decollements throughout the field area (*Braathen et al.*, 1999; *Horota et al.*, 2023).

A regional southerly dip of Svalbard's stratigraphy implies that in the southern part of the field guide area Paleogene sediments deposited in the foreland basin of the WSFTB (*Helland-Hansen and Grundvåg*, 2021) cover the underlying Mesozoic-Paleozoic succession. On the northern shores of Isfjorden, the older successions are well exposed. In the inner parts of Nordfjorden Devonian sandstone-dominated successions are present.

3.1 Stop 1: Festningen: Setting the Stratigraphic Scene

The Festningen section in western Spitsbergen is Svalbard's only geotope and an excellent site to introduce us to the regional Paleozoic to Cenozoic stratigraphy (Figure 12). A nearly continuous record from the Carboniferous to the Paleogene is exposed in the ca. 7 km long beach section, near-vertically tilted by the Paleogene tectonics. *Mørk and Grundvåg* (2020) present a comprehensive field guide to the Festningen section. *Senger and Galland* (2022) provide a digital outcrop model of the section, in the context of the regional geology.

Apart from the eight type sections (*Dallmann et al.*, 1999), Festningen also offers an excellent exposure of the Permian-Triassic boundary and the corresponding mass extinction horizon (*Grasby et al.*, 2015; *Bond et al.*, 2015). Ca 15 m above the mass extinction horizon we find a 7 m thick sill emplaced in shale-dominated Lower Triassic strata - the first HALIP rocks we touch on this excursion (Figure 12B). Sill outcrops are also visible in the folded strata in the mountain sides to the south. These sills continue southward at least as far as Wedel Jarlbergs Land.

As an alternative site to Festningen (for instance if a polar bear is also investigating the stratigraphy), Selmaneset on the northern shore of Isfjorden offers the same stratigraphy but with a thinner HALIP sill.

3.2 Stop 2: Colesbukta: Igneous Intrusions in the Subsurface

Colesbukta is a defunct Soviet coal mining settlement located approximately halfway between Festningen and

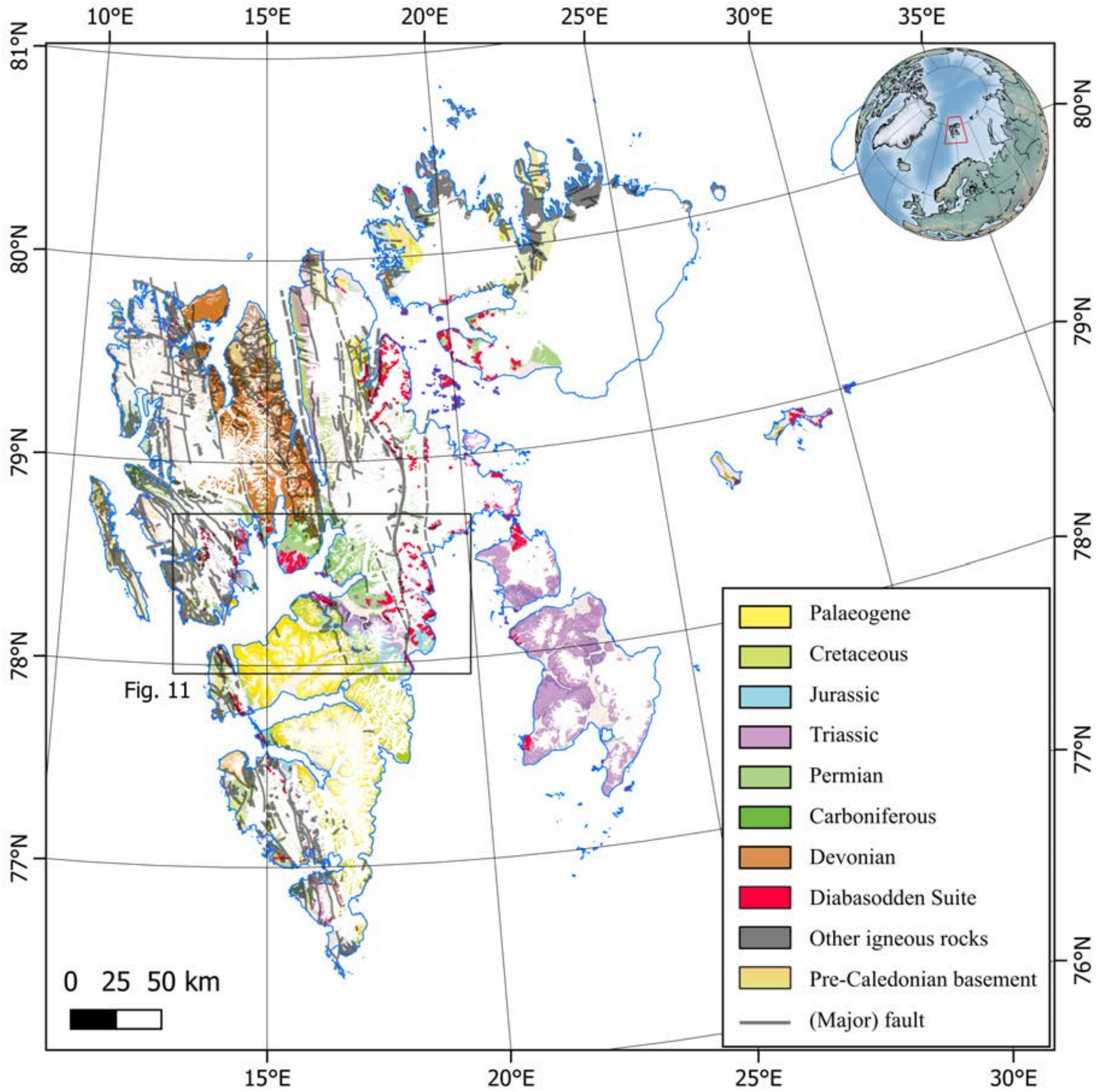

Figure 9 – Geological map of Svalbard (*Dallmann and Norwegian Polar Institute*, 2014), highlighting the extent of the Diabasodden Suite (red). Sill outcrops not shown here also occur along much of the western fold and thrust belt.

Longyearbyen. Tens to hundreds of coal exploration boreholes have been drilled in the vicinity over the past century. These, however, only target the Paleogene succession and are irrelevant for HALIP-related research.

Deep petroleum exploration boreholes facilitate correlation between the outcrops and the subsurface. Eighteen petroleum exploration boreholes were drilled from 1961 to 1994 by a range of Norwegian and international companies through Paleozoic to Cenozoic stratigraphy (*Senger et al.*, 2019). One deep petroleum exploration borehole was drilled in Colesbukta by the Soviet coal mining company Trust Arktikugol in 1974-75 (*Senger et al.*, 2019). The well was drilled through a 43 m thick igneous sill in Lower Triassic strata, at a similar stratigraphic level to that encountered at Festningen 26 km westward (Figure 13). The sill is well imaged on the gamma log (Figures 13 and 14). The resistivity response is strong in the contact metamorphic aureoles (Figure 14), suggesting the presence of conductive pyrite or graphite (as documented in the Neuquen Basin by *Spacapan et al.* (2020). The same response is evident in the Ishøgda borehole, where two sills are emplaced slightly higher up in the stratigraphy (Figure 13). Thinner sills are also reported from the two Vassdalen petroleum exploration boreholes (*Senger and Galland*, 2022) and the fully-cored DH4 scientific borehole (*Senger et al.*, 2014a). Seismic interpretations also suggest the sills extend under the Central Tertiary Basin to the east (*Senger and Galland*, 2022).

Using the base of the Helvetiafjellet Formation as a surface reference level the sills within the Botneheia Formation were emplaced at a depth of 715-1165 m (Figure 13; Senger and Galland, 2022). Compaction of the overburden would have increased this somewhat but the sills were nonetheless emplaced at relatively shallow depths over a large area - while never surfacing as lava flows in the greater Isfjorden area.

Table 1 – Overview of the 15 stops, their overall scientific themes, and key references and relevant data sets.

Stop	Locality	Main theme	Key references, digital outcrop models, photosphere-tours and other resources
1	Festningen	Setting the stratigraphic scene. Introduction to the HALIP with a thin sill just above the Permian-Triassic boundary.	*Mørk and Grundvåg* (2020) *Senger and Galland* (2022) *Betlem and Senger* (2022) https://vrsvalbard.com/the-festningen-section/
2	Colesbukta	Petroleum exploration and subsurface characterization of HALIP sills in boreholes.	*Senger et al.* (2019) *Senger and Galland* (2022)
3	Adventdalen and Deltaneset	Implications of igneous intrusions for CO_2 storage. Contact metamorphism in DH4 aureole.	*Senger et al.* (2013, 2014a) *Ogata et al.* (2014)
4	Diabasodden	Type locality. Onshore-offshore correlation.	*Dallmann et al.* (1999) *Corfu et al.* (2013)
5	Grønsteinfjellet	Igneous complex geometry dykes, sills, transgressive segments	*Malinen* (2024)
6	Botneheia	Sill propagation in organic-rich zones. SvalCLIME project.	*Hagevold* (2019) *Senger and Galland* (2022) https://vrsvalbard.com/svalclime-project/
7	Gåsøyane, Gipshuken and the Billefjorden Fault Zone	Magma-fault interaction in extensional settings. Evidence for HALIP sill in Reindalspasset well further south.	*Odlum et al.* (2019)
8	Skansbukta to Frostisen	Magma propagation in Triassic siliciclastic-dominated successions	*Senger et al.* (2013)
9	Tschermakfjellet	Igneous geometry. Influence of magmatism on petroleum systems.	*Senger et al.* (2017)
10	Blomesletta	3D architecture of a sill. HALIP U-Pb geochronology.	*Galland et al.* (2025) *Sartell et al.* (2025) *Sartell* (2021)
11	Mediumfjellet/WSFTB	Eurekan deformation. HALIP emplacement and subsequent deformation. Tectonic vs thermal fractures.	*Larsen* (2010) *Maher et al.* (2020) *Horota et al.* (2023) https://vrsvalbard.com/west-spitsbergen-fold-and-thrust-belt/
12	Central Isfjorden - geochemistry	Circum-Isfjorden geochemical data.	*Malinen* (2024) *Nejbert et al.* (2011) *Sartell* (2021)
13	Central Isfjorden - mapping intrusions geophysically	Seismic and magnetic characterization. Multibeam mapping of possible hydrothermal vent complex.	*Senger et al.* (2013) *Senger and Galland* (2022)
14	Festningen, Hanaskogdalen and Flyplassveien	The HALIP and influence on sedimentation. Both regional-scale system and volcanic signals within sedimentary record.	*Grundvåg et al.* (2019) *Ineson et al.* (2021)
15	A winter wonderland - visiting HALIP locations on snowmobiles	The HALIP plumbing system and regional stratigraphy.	

In all boreholes except the Reindalspasset borehole the igneous intrusions are found in Triassic shale-dominated successions. In the Reindalspasset borehole a 21 m thick intrusion is emplaced in the sandstone-dominated Ebbadalen Formation, a syn-rift succession within a half-graben east of the BFZ. Interestingly, no HALIP intrusions are present in outcrops within the well-mapped Billefjorden Trough 70 km north of the Reindalspasset borehole. Further south from Isfjorden in Bellsund at Midterhuken a ~20 m thick sill resides within the Kapp Starostin Formation.

3.3 Stop 3: Adventdalen to Deltaneset: Influence of Igneous Intrusions on CO_2 Storage

Our next stop combines both drill cores and corresponding outcrop exposures, in and near Longyearbyen. Due to the regional dip and lack of vegetation, the drilled succession is pristinely exposed at outcrops between Deltaneset and Botneheia 15 km northeast of the CO_2 injection location targeted by the Longyearbyen CO_2 Lab project (Figure 7, Stop 6).

The project's main objective was to determine whether the subsurface is suitable for storing locally produced CO_2, for which 8 boreholes were drilled and fully cored between 2007 and 2013 (*Braathen et al.*, 2012; *Olaussen et al.*, 2019). The project generated a wealth of multidisciplinary data along with the 4.5 km of drill core material, summarized in an open data package that encourages re-use (*Senger et al.*, 2025).

The deepest borehole, DH4, penetrates almost 1 km of Mesozoic stratigraphy and fully cores a 2.28 m thick sill at 950 m depth (Figure 15), i.e., in the lower part of the targeted reservoir. Thin as it is, the sill produces a

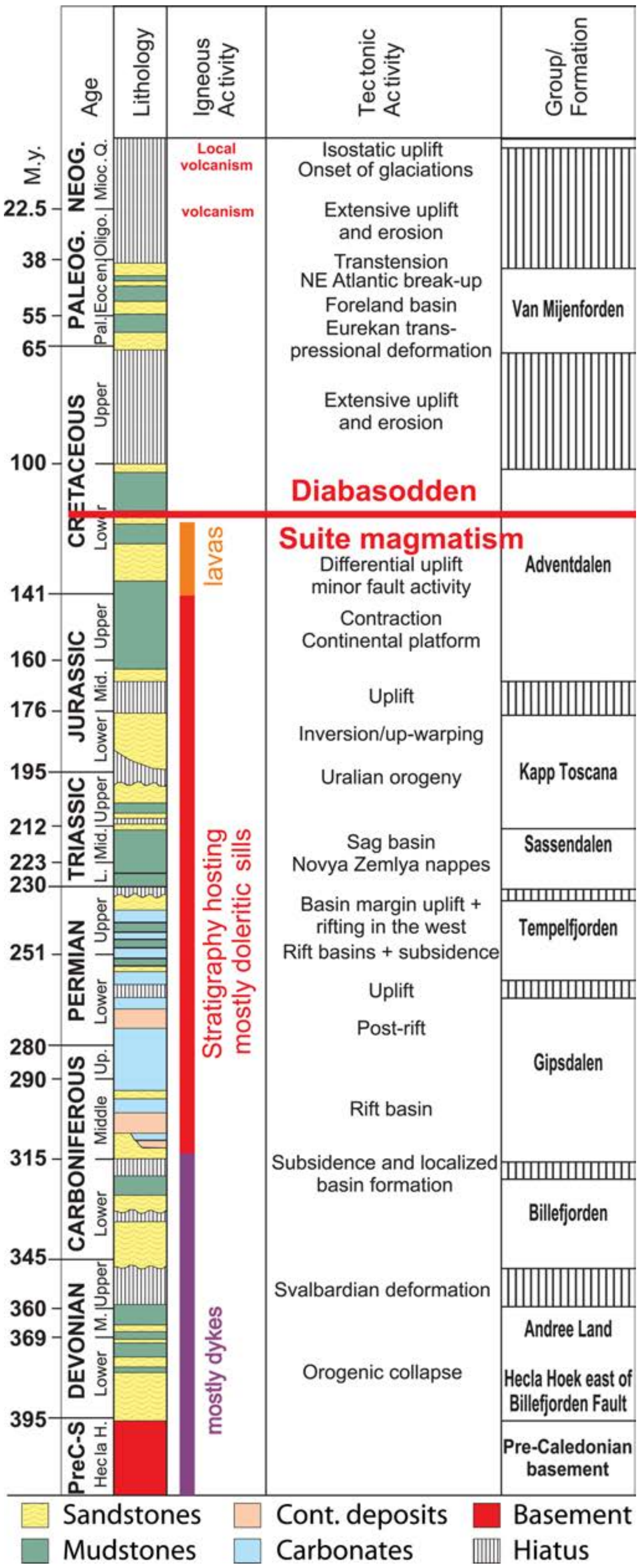

Figure 10 – Stratigraphic column with tectonic elements chart and documented stratigraphy hosting HALIP rocks. Figure modified from *Senger and Galland* (2022).

contact metamorphic aureole corresponding to 160-195% of its thickness (Figure 15B; Senger et al., 2014a). Geochemically, the sill corresponds to the Diabasodden Suite signature (*Senger et al.*, 2014a). Seismic data suggest a thicker (10s of meters thick) sill beneath the drilled interval.

Sills of similar thickness are encountered across the same stratigraphic interval west of Hatten (*Ogata et al.*, 2014; *Senger et al.*, 2014a). A dyke at Botneheia (see also Stop 6) penetrates the entire reservoir succession and extends an unknown distance into the caprock shales. The geometry of the igneous system was investigated in view of the CO_2 lab project by *Senger et al.* (2013), concluding that the igneous intrusions will locally modify the reservoir properties and represent potential baffling zones.

3.4 Stop 4: Diabasodden-Hatten: Visiting the Type Locality of the Diabasodden Suite

Diabasodden is the type locality for the Diabasodden Suite (*Dallmann et al.*, 1999). It consists of a large and thick sill, which in the west merges with the intrusive complex of Hatten. Towards the east, the sill continues through Grønsteinfjellet (Stop 5) all the way to Botneheia (Stop 6).

It is unclear how and from where the magma was emplaced, but the sheer volume and relatively low stratigraphic position implies that Diabasodden-Hatten may represent a regional feeder system that feeds magma as sills to the surroundings. The western margin of Hatten may be a feeder dyke (Figure 16A and 16C), which bathymetric and magnetic data indicates to cross 14 km across all of Isfjorden and connect directly to a ca. 10 m thick dyke exposed at the beach beneath Rotundafjellet (Stop 8).

The ca. 3 km long digital outcrop model of the Hatten-Diabasodden complex (Figure 16E) was generated from 931 drone-based photographs and provides valuable insights into the igneous complex geometry. The sill at Hatten varies in thickness from 40 to 46 m. At Diabasodden itself, the sill is 45 m thick and exemplifies good examples of columnar jointing formed during magma cooling (Figure 16F). The complex represents the most magma-rich part of the Isfjorden area (ca. 0.041 km^3 of magma) and is hypothesised to represent a regional magma feeder system.

Diabasodden is also one of only four places in Svalbard from which reliable U-Pb radiometric ages of the Diabasodden Suite were published, yielding an age of 124.5 ± 0.2 Ma (*Corfu et al.*, 2013; *Sartell et al.*, 2025).

3.5 Stop 5: Grønsteinfjellet: Dykes and Sills

The 309 m high Grønsteinfjellet mountain (Figure 17C) links the Hatten-Diabasodden complex (Stop 4) with the long sill feeding towards Botneheia (Stop 6). The

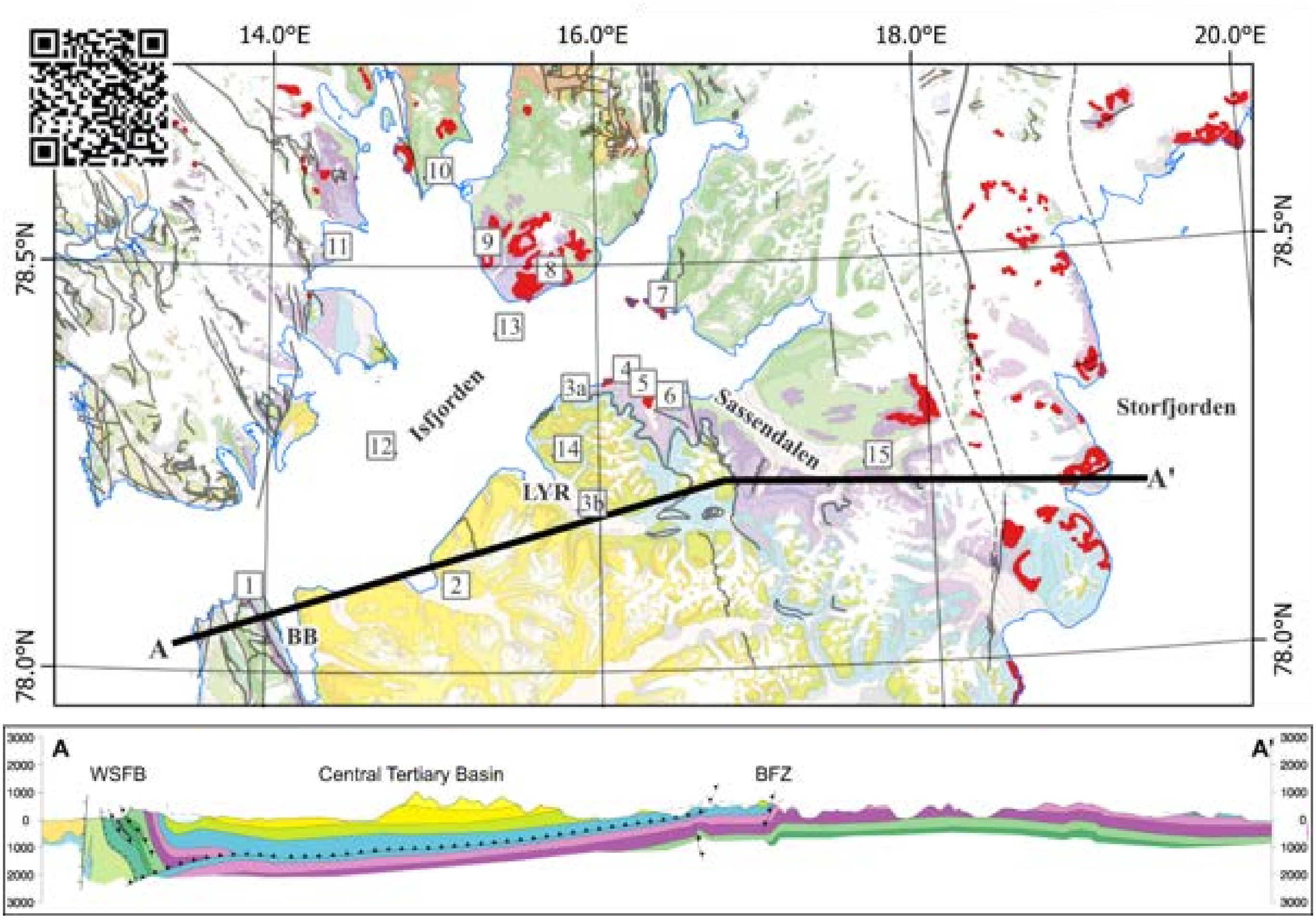

Figure 11 – Geological map and regional cross section across the field area, modified from *Norwegian Polar Institute* (2025), and the 15 investigated field stops (refer to Table 1 for details). LYR = Longyearbyen. WSFB = West Spitsbergen Fold and Thrust Belt. BFZ = Billefjorden Fault Zone. An interactive version of the geological map is available online, accessible via the QR code or directly via: https://geokart.npolar.no/geologi/GeoSvalbard/. A topographic map searchable for all place names is available at toposvalbard.npolar.no.

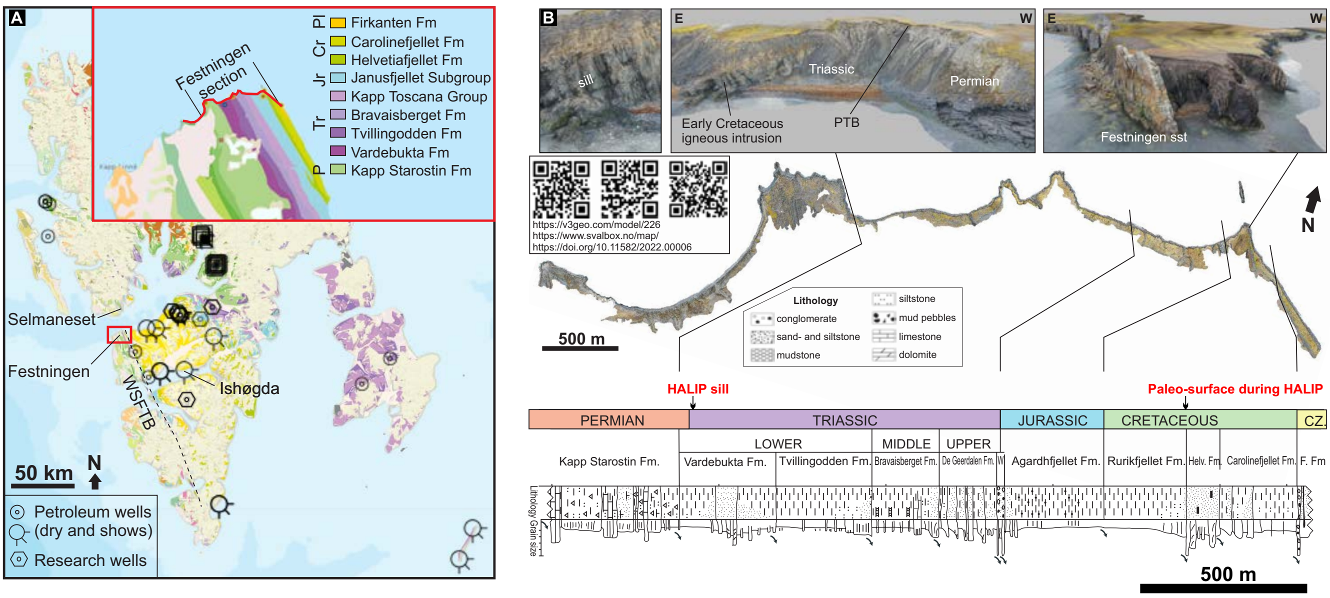

Figure 12 – Location and stratigraphy of the Festningen geotope. A) Location of the Festningen section in western Spitsbergen. B) Digital outcrop model and regional stratigraphy of the Festningen section. A digital tour to the section (https://vrsvalbard.com/the-festningen-section/) and the digital outcrop model itself (https://v3geo.com/model/226) are both available online for viewing and download (*Betlem and Senger*, 2022). Figure modified from *Senger and Galland* (2022).

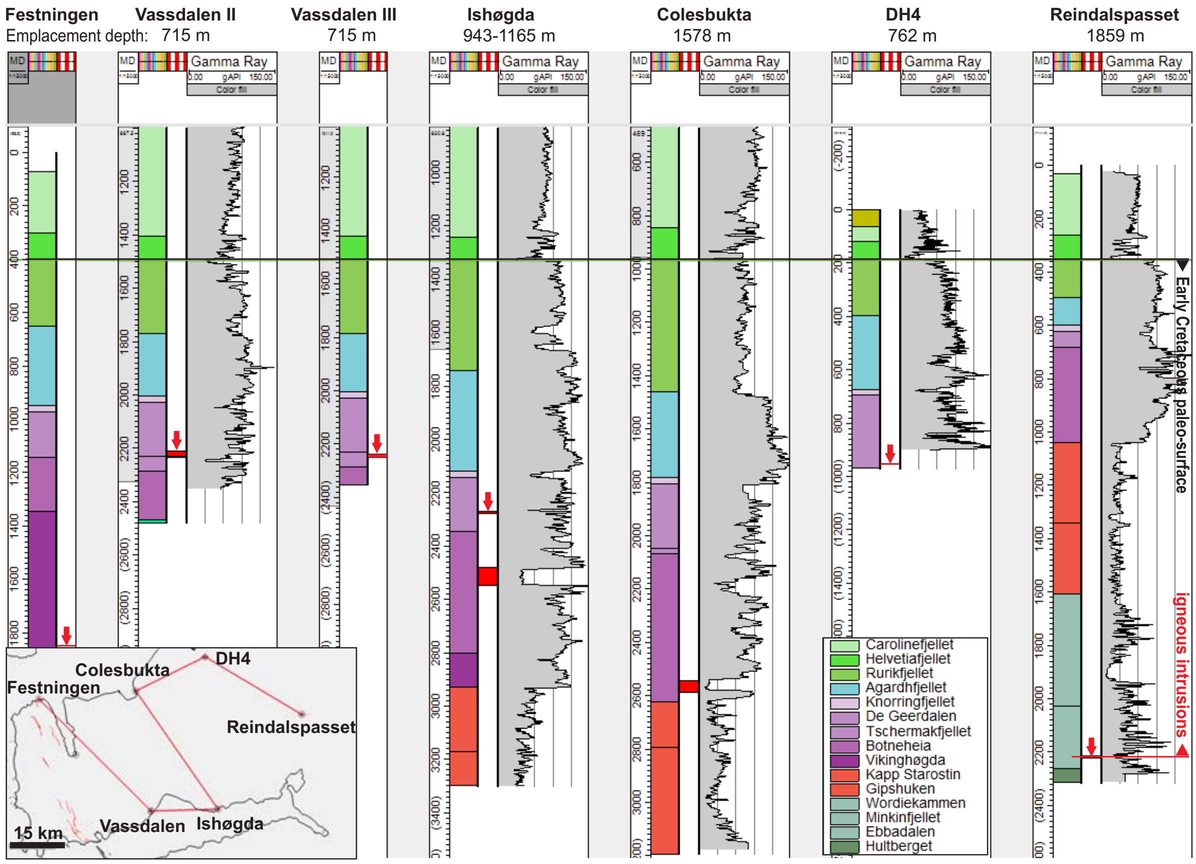

Figure 13 – Synthesis of stratigraphy penetrated by boreholes (and the Festningen section) that encountered HALIP igneous intrusions. The section is flattened at the base of the Helvetiafjellet Formation, representing a proxy for the paleosurface at the time of emplacement during the Early Cretaceous. A zoom-in of the Triassic section in Vassdalen, Ishøgda and Colesbukta is shown in Figure 14. Figure modified from *Senger and Galland* (2022).

mountain provides good examples of both dykes and sills emplaced within Mid-Late Triassic siliciclastic successions. The beach section, which is an ideal starting location for a half-day hike, offers a thin (ca. 1 m) sill and also a rare dyke (Figure 17). The dyke is cut by a thrust fault linked to the WSFTB. Above the beach outcrop the dyke is covered by scree, but following its trend it is obvious that the dyke follows to the top of Grønsteinfjellet where it presumably feeds the sill. The ridges of Grønsteinfjellet, particularly its north-western one, offer good quality outcrops. The south-eastern side is not as well exposed, but from the digital outcrop model (Figure 17B) it is apparent that the sill transgresses to a lower level.

3.6 Stop 6: Botneheia: Contact Metamorphism and Global Climate

The Botneheia mountain offers excellent exposures of sills emplaced in Triassic siliciclastic sediments, particularly its northern slopes (Figure 18). The mountain is the type locality for the Mid-Triassic Botneheia Formation, an organic-rich shale with regional source rock potential (*Wesenlund et al.*, 2022). The HALIP sill intrudes the Botneheia Formation from the west, before transgressing to a higher level within the De Geerdalen Formation. Nonetheless, a thinner offshoot sill continues eastwards within the Botneheia Formation before pinching out towards Flowerdalen (see Figure 11 for location). The top of the Botneheia plateau consists of Wilhelmøya Subgroup strata, the upper reservoir targeted for CO_2 storage (Stop 3). A ca. 4 m thick WNW-ESE oriented dyke cuts the entire reservoir and extends an unknown distance into the overlying caprock of the Agardhfjellet Formation.

Hubred (2006) documents the influence of the 10s-of-meters thick sill at Botneheia on the aureoles, while *Brekke et al.* (2014) expand the study to similar sills in time-equivalent strata in eastern Svalbard. However, detailed aureole studies on outcrops are hampered by scree cover and steep cliffs.

An ongoing international research initiative, SvalCLIME (*Senger et al.*, 2023, https://vrsvalbard.com/svalclime-project/), aims to decipher the relationships of globally significant hyperthermal events with large igneous provinces throughout the Phanerozoic. To better understand the processes occurring when hot magma interacts with organic-rich sediments the SvalCLIME team proposes to drill and fully core three scientific boreholes on Botneheia (Figure 18). Two ca. 200 m deep boreholes are planned in the valleys directly to the west and east of Botneheia to characterize the same stratigraphy with and without the ca. 40 m thick sill. A third borehole will be drilled on top of the plateau to characterize the thinner sill and the upper part of

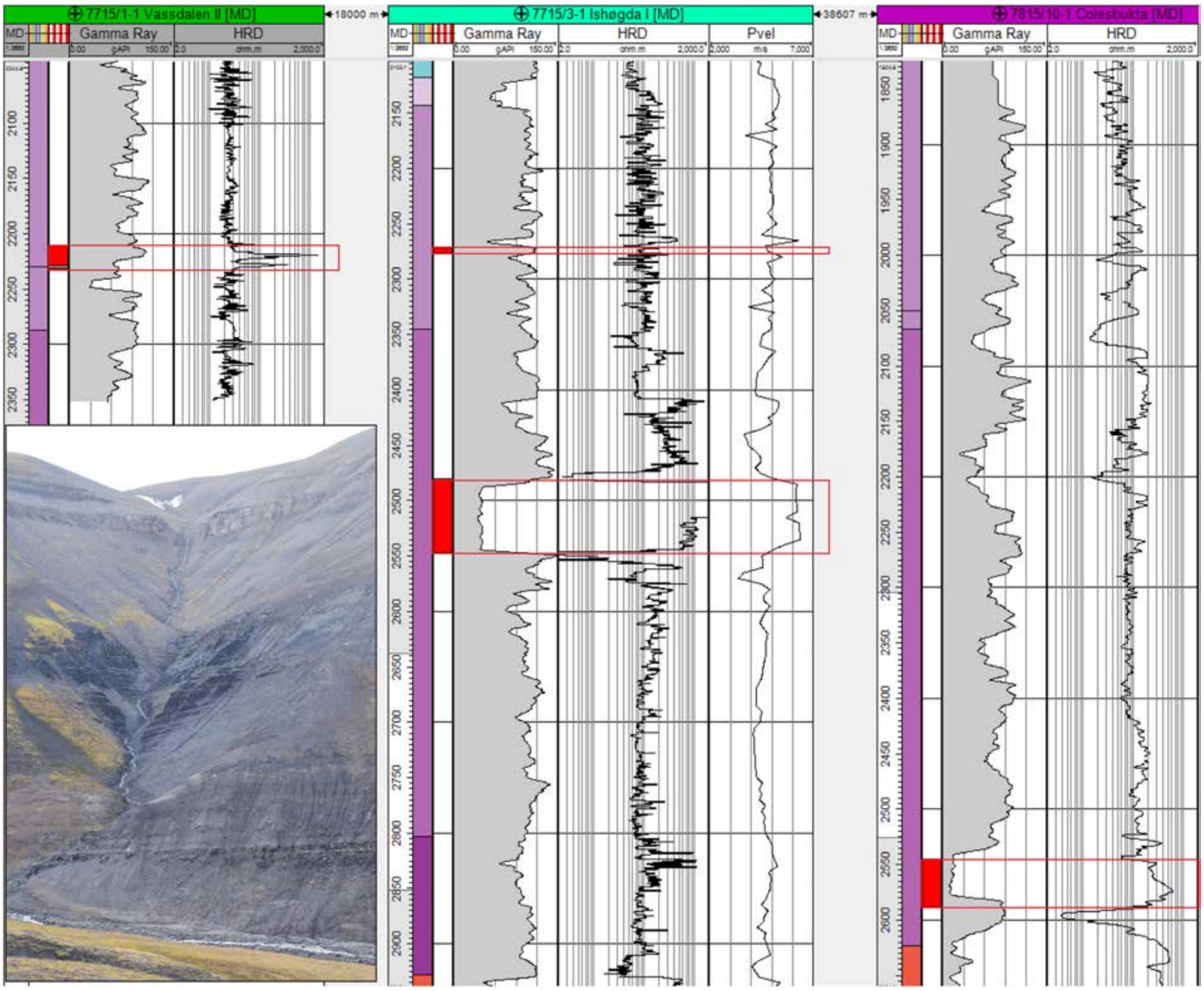

Figure 14 – Wireline and outcrop characterization of sills and their contact metamorphic aureoles within organic-rich shales of the Middle Triassic Botneheia Formation. The outcrop photograph is from southern Tschermakfjellet (see Figure 11 for location). Figure modified from *Senger and Galland* (2022).

the stratigraphy. Additional boreholes will be drilled at Kropotkinfjellet, Nordenskioldfjellet and Platåfjellet to obtain a high-resolution paleoenvironmental and paleoclimate record from the end Permian to the Paleogene (see VFT for further details, https://vrsvalbard.com/svalclime-project/).

3.7 Stop 7: Gåsøyana and Gipshuken: Magma-fault Interaction

The Botneheia plateau is also an excellent excursion during the spring season (March-April), when snowmobiles can be used to drive on top of the plateau and gain impressive vistas of inner Isfjorden (see also Stop 15). Flowerdalen, the valley just east of Botneheia, runs parallel to the Billefjorden Fault Zone. The fault zone is not directly visible here, but becomes prominent on the northern shore of Isfjorden. Here the Billefjorden Fault Zone crosses the Gipshuken mountain, with its prominent fault-propagation fold formed during Paleogene transpression as the Billefjorden Fault Zone was re-activated as a reverse fault.

A petroleum exploration borehole was drilled ca. 45 km south of Gipshuken in Reindalspasset in 1991 targeting a structure associated with the Billefjorden Fault Zone (Figure 19A). The well penetrated an 18 m thick sill in the syn-rift strata (Figure 19B), presumably of HALIP affinity. Interestingly no igneous sills have been reported from the syn-rift strata of the well studied Billefjorden Trough exposed ca. 25 km north of Gipshuken.

HALIP rocks are exclusively exposed on the western side of the fault zone, for instance at Gipsvika (Figure 19C) or the Gåsøyane islands. The islands comprise only dolerites and are absolutely worth a visit, especially to observe the regular cooling joints. *Maher et al.* (2020) systematically mapped such fracture patterns in dolerites throughout Svalbard and argued that the regional stress regime also influences the direction of the cooling joints.

The Billefjorden Fault Zone (and several other N-S oriented long-lived lineaments) was a major weakness zone during the emplacement of the HALIP. A working hypothesis is that magma utilised the fault zone during emplacement. While further work remains to understand magma-fault interactions in Svalbard, *Odlum et al.* (2019) has already identified enhanced hydrothermal fluid circulation within the Billefjorden Fault Zone at precisely the time of HALIP emplacement.

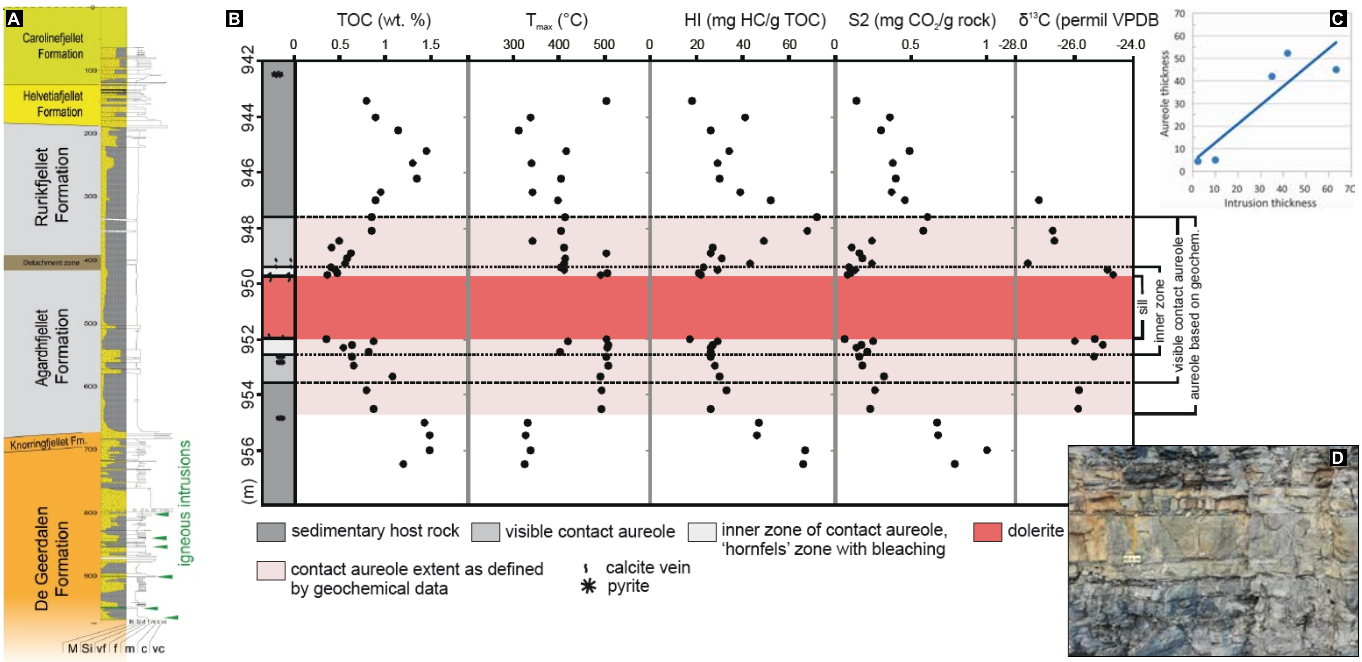

Figure 15 – A) Reservoir-caprock-overburden succession in the DH4 borehole, highlighting the presence of thin igneous intrusions at several intervals. B) Detailed study of the contact metamorphic aureole of the 2.28 m thick intrusion at 950 m depth. For details refer to *Senger et al.* (2014b). C) Correlation between intrusion and contact aureole thickness for five intrusions in boreholes in Svalbard. D) Thin sill at an outcrop beneath Grønsteinfjellet (Stop 5), in a similar stratigraphic setting as in the DH4 borehole.

3.8 Stop 8: Svenskehuset-Frostisen-Rotundafjellet: Influence of Stratigraphy on Magma Emplacement

The southern tip of Dickson Land offers some of the most impressive HALIP exposures in the field area. The area can be explored both in summer and spring, but is fairly remote and some of the inland localities require long walks from the coastline. As is obvious from the geological map (Figure 20A), the igneous intrusions are most prevalent in Triassic siliciclastic host rocks. In southern Dickson Land intrusions are largely manifested as relatively homogeneous tabular sills. Single sills often span several mountainsides and in general the igneous complex is less structurally complex on the northern shore of Isfjorden than in the south (*Senger et al.*, 2013).

One important site absolutely worth visiting is the beach beneath Rotundafjellet, where a ca. 8 m thick dyke is exposed. The onshore dyke corresponds directly with a magnetic high anomaly in Isfjorden that links Rotundafjellet to Hatten (Stop 4). The dyke is also partly exposed in the scree slopes at Rotundafjellet, and most likely feeds the mountain-capping sill.

The cultural heritage site of Svenskehuset with its strong history (*Aasebø and Kjaer*, 2009) is certainly worth visiting while in the area. In addition, there are two sills exposed above the location of the cabin. While the upper sill emplaced in Botneheia Formation does not exhibit good outcrop quality and is therefore of relatively little significance, there is an interesting yet not very well studied exposure of a few meter thick inclined sheet/sill, which has also been captured as a digital outcrop model. No work has been published from this locality to date, but the sills show distinct internal deformation and veins (Figure 20D). Samples collected from these up to several cm-wide veins show distinct "interlayers" of calcite and pyrite as well as up to cm-scale macro-pores filled with unspecified organic matter, releasing distinct hydrocarbon smell upon breaking. Geological implications of this site are considerable, but it seems possible that it presents an example of inclined sills as an upward fluid pathway through low-permeability formations, possibly under hydrothermal conditions.

3.9 Stop 9: Tschermakfjellet: Igneous Geometries and Influence on Petroleum Systems

The Tschermakfjellet mountain on the south-western corner of Dickson Land deserves its own stop. The characteristic cup-shaped intrusion is best appreciated from a boat or airplane at some distance (Figure 21A). As at Botneheia (Stop 6), the sill is emplaced in both the Botneheia and De Geerdalen formations. The Botneheia Formation (e.g., *Wesenlund et al.*, 2022) is a major regional source rock across the entire Barents Shelf, while the De Geerdalen Formation is an important reservoir rock targeted by the Longyearbyen CO_2 lab project (Stop 3; *Braathen et al.*, 2012).

Igneous intrusions have both positive and negative impacts on the petroleum system (as reviewed by *Senger et al.* (2017); Figure 21B, C). The Tschermakfjellet geometry nicely illustrates how intrusive complexes may segment and compartmentalize a reservoir, and locally overmature a source rock, thus negatively influencing

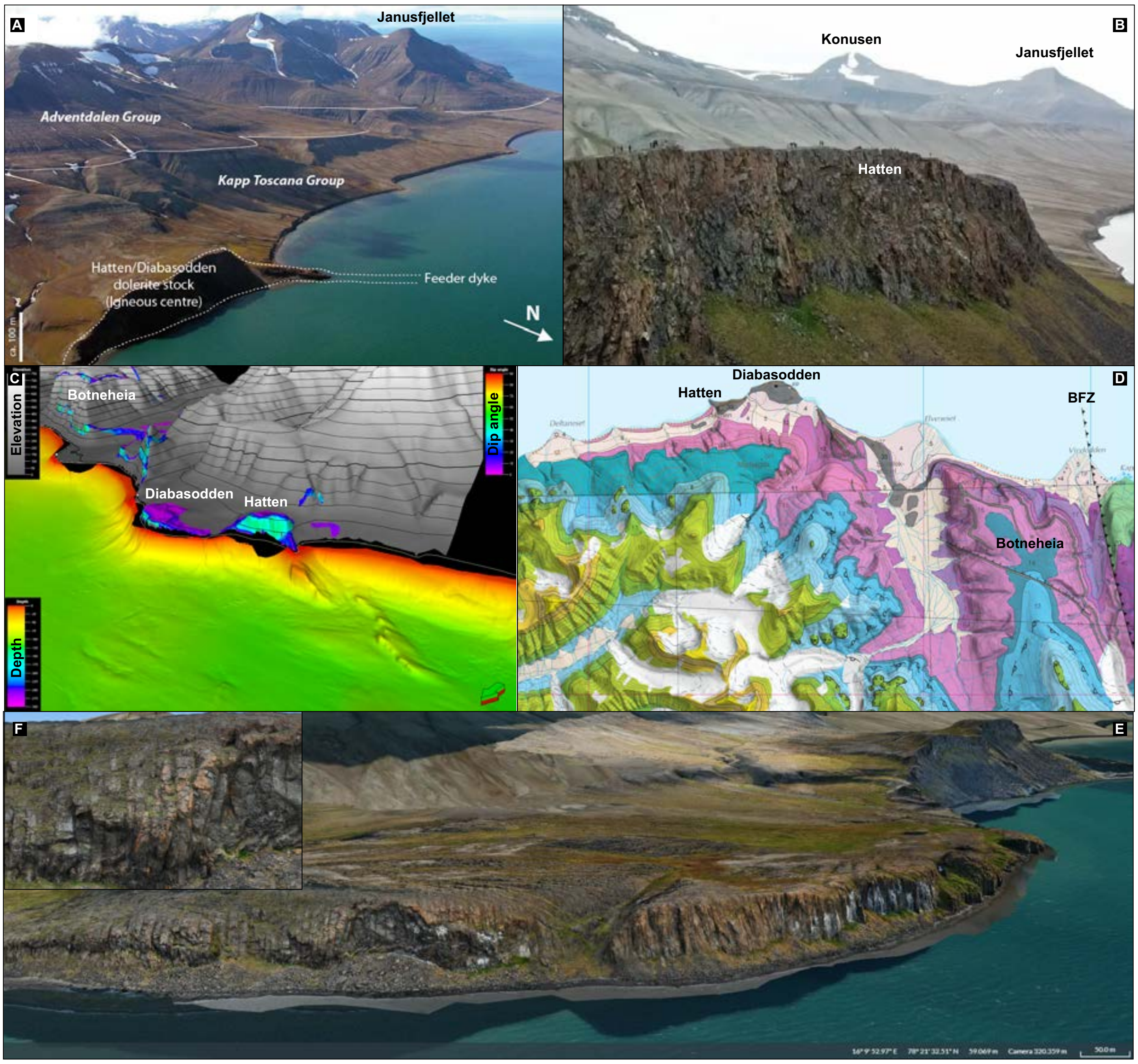

Figure 16 – Diabasodden and Hatten area. A) Helicopter overview picture of Hatten, looking westward towards Janusfjellet. Photo by Winfried Dallmann. B) Drone image of Hatten, while students and teachers of the Arctic Tectonics and Volcanism course (*Senger et al.*, 2024) walk on top of the intrusive complex. Photo by Owen Anfinson. C) Integration of onshore and offshore terrain data, with the HALIP intrusions highlighted in colour. Note the continuation of the Hatten feeder dyke offshore. D) Geological map of the Deltaneset to Vindodden area, from geokart.npolar.no. E) Digital outcrop model of the Diabasodden-Hatten complex. F) Zoom-in of columnar jointing illustrated by the model. The model is available in context for interactive web viewing at https://vrsvalbard.com/ag-214-vfgs-the-high-arctic-large-igneous-province-halip/

the petroleum system. On the other hand, regionally immature source rocks may be brought into the oil or gas window by enhanced regional heat flow due to magmatism and thus benefit the petroleum system. Structural traps such as faults may be breached by magma propagating along the fault, but igneous rocks may also form traps or even reservoirs (Figure 21).

3.10 Stop 10: Blomesletta/James I Land: 3D Sill Geometries

West of Dickson Land, the HALIP intrusions are predominantly emplaced in stratigraphically older Permian carbonate-evaporite-dominated successions. The N-S trending Blomesletta Fault offset some of the stratigraphy and intruded sills, but is not easily visible in the field (Figure 22). A large dolerite sill, however, is well exposed on the peaks of the mountains like Kapitol as well as along cliffs related to the plateau in the south east of James I Land, at Stjerthøgda and Vengeberget (Figure 22C). *Galland et al.* (2025) constrain the 3D architecture of the main sill body based on field observations and analyses of digital outcrop models, documenting the stratigraphic control on sill morphology.

The 3-dimensional mapping indicates that the sill comprises several sub-horizontal segments emplaced at distinct stratigraphic levels. The morphologies of the sill segments differ depending on the stratigraphic level they are emplaced at. The sill segments emplaced along the stratigraphic contact between the Gipshuken Formation and the Kapp Starostin Formation, which is marked by a competent, fossil-rich

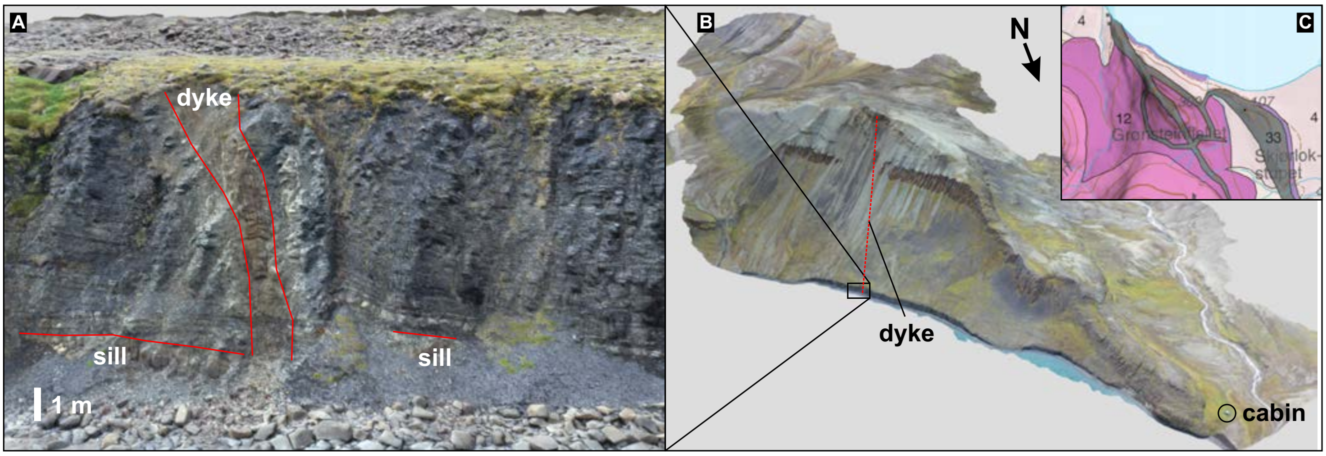

Figure 17 – A) Outcrop-scale (*Rodes et al.*, 2024a) and B) mountain-scale (*Rodes et al.*, 2024a) digital outcrop models of the Grønsteinfjellet mountain, illustrating the sill-dyke architecture. For interactive viewing of the digital outcrop models visit https://sketchfab.com/models/7185d44b49d74a9daad35f438d52cf2a/embed?autostart=1&ui_inspector=0.

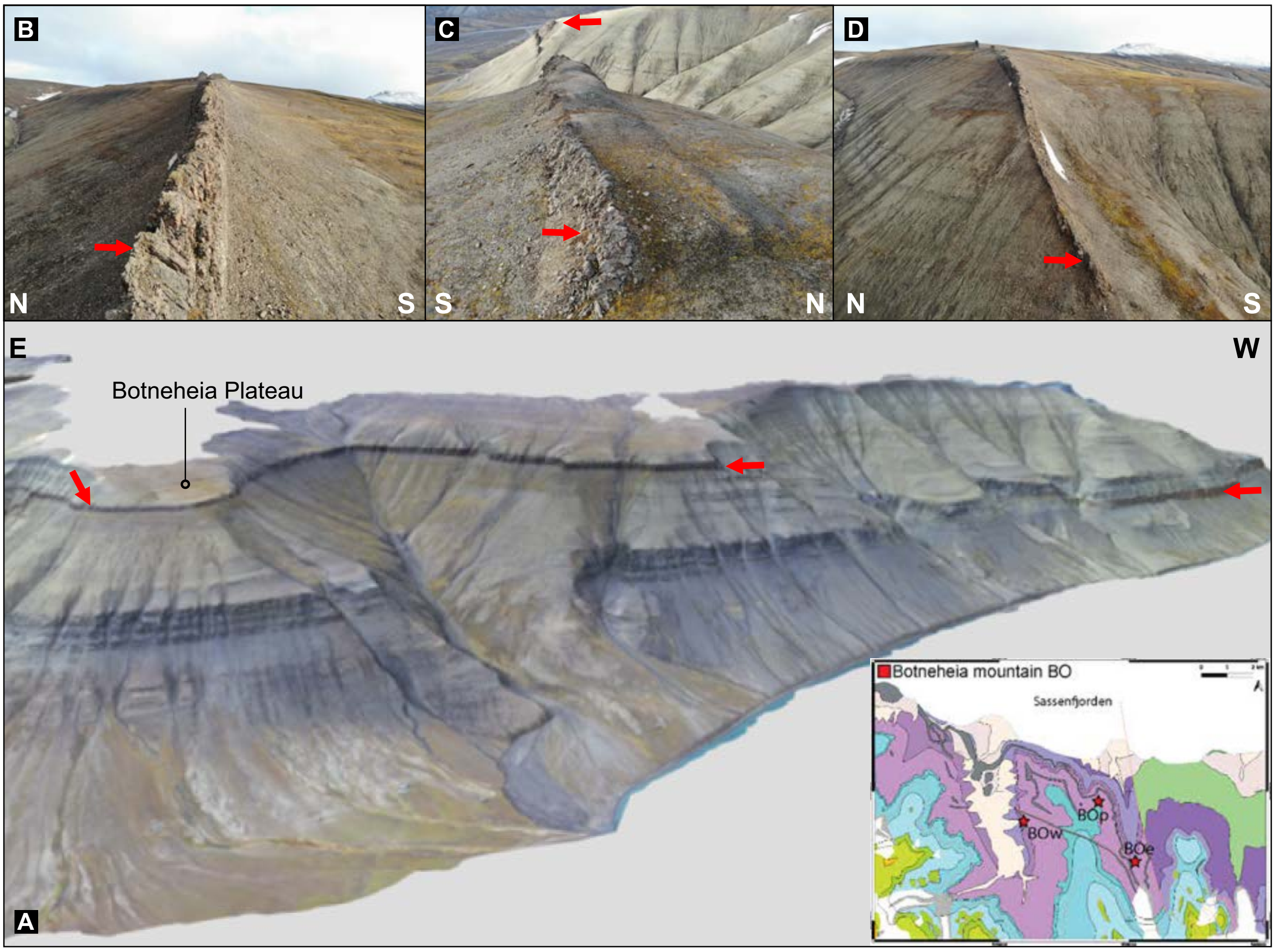

Figure 18 – A) Screenshot of a digital outcrop model of the Botneheia mountain (*Rodes et al.*, 2024b). The full interactive model is available at https://sketchfab.com/3d-models/botneheia-0897fb5a22d8436facf738c0d35b3921 Botneheia offers numerous styles of igneous intrusions, dominated by an eastward-propagating sill that transgresses from the Botneheia Formation to the De Geerdalen Formation. The entire plateau is dissected by a ca. 5 m thick dyke. The inset map shows the locations of three planned scientific boreholes targeted by the SvalCLIME project *Senger et al.* (2023). B) to D) Drone images of the dyke cutting across Botneheia.

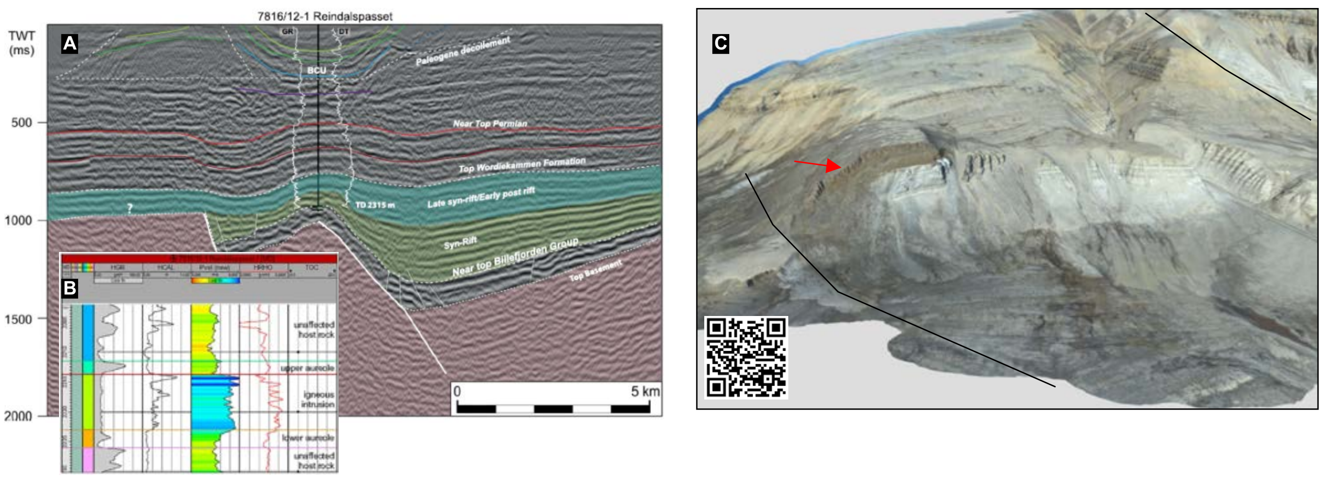

Figure 19 – Magma-fault interaction. A) Seismic line across the Reindalspasset borehole, illustrating the penetrated stratigraphy and the geometry of the Pennsylvanian half graben. B) Wireline log signature of an igneous sill in the syn-rift sandstone-dominated strata. C) Digital outcrop model of Gipshuken (*Smyrak-Sikora et al.*, 2024), highlighting the HALIP sill (red arrow) and the position of two fault strands of the Billefjorden Fault Zone (black arrows). The model can be examined interactively by following the QR code (https://zenodo.org/records/12624872; www.svalbox.no/map).

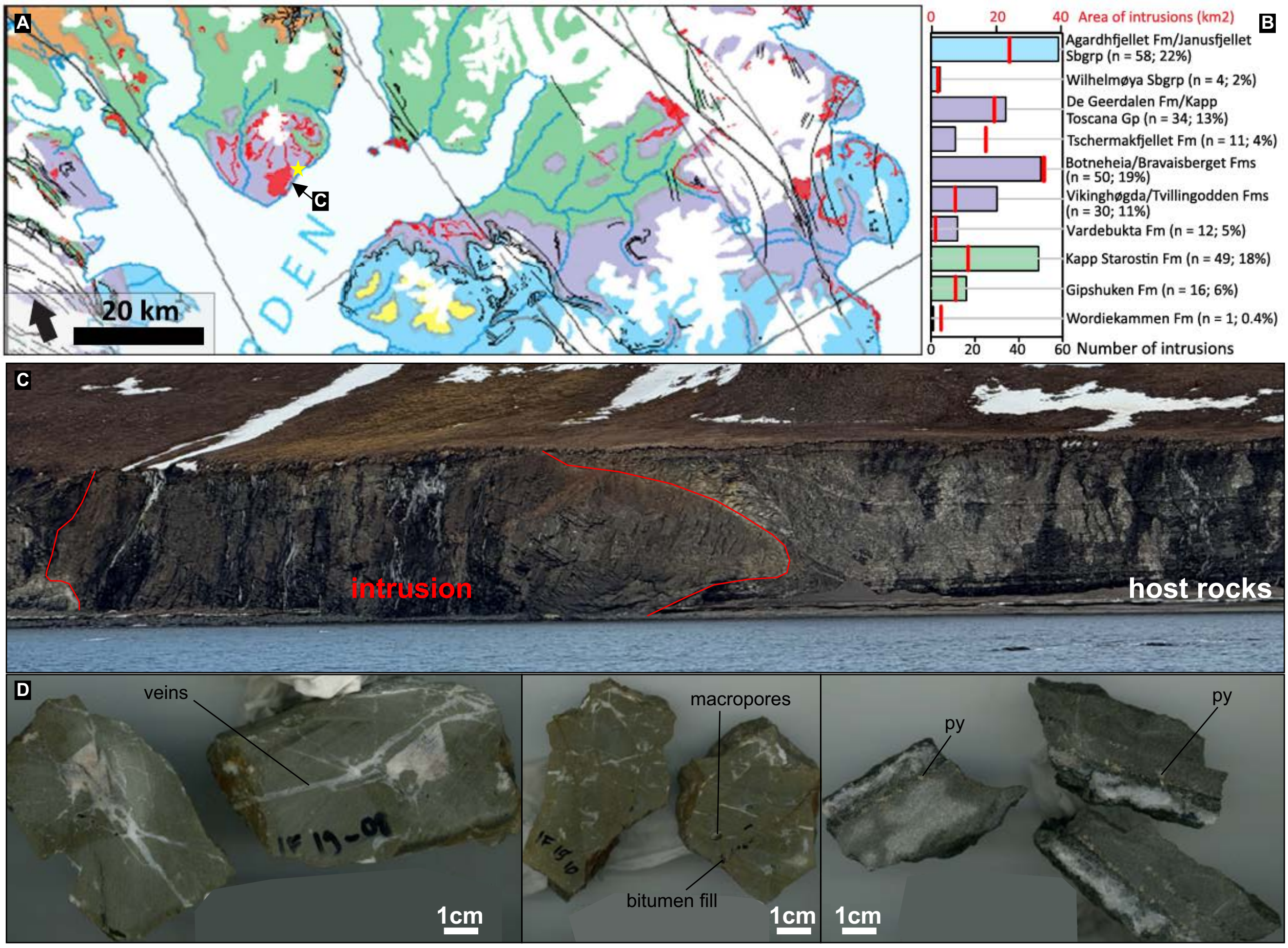

Figure 20 – Igneous intrusions exposed in southern Dickson Land. A) Geological map of central-eastern Spitsbergen highlighting the extent of the Diabasodden Suite (red) in the context of the regional stratigraphy. Note the extensive intrusions in the siliciclastic-dominated Triassic host rocks of southern Dickson Land. B) Number (bars) and mean area (red lines) of individual mapped intrusions as identified from the regional geological map. Figure elements from *Senger and Galland* (2022). C) Example of an unmapped igneous intrusion on the coastline of southern Dickson Land. D) Cut samples from a dolerite sheet on the slopes above Svenskehuset (yellow star in A). Note the hydrothermal venting, bitumen material within the sill and extensive pyrite occurrence in the units.

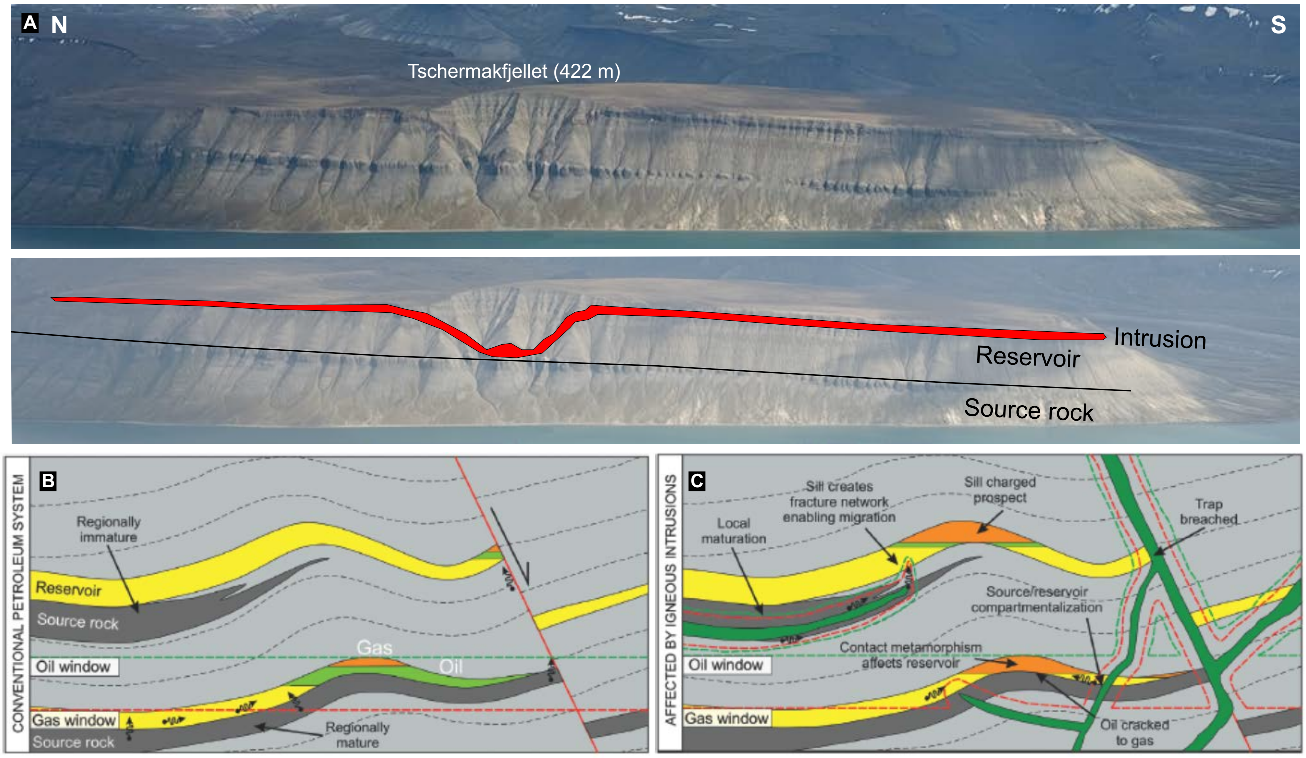

Figure 21 – A) Petroleum system elements in the context of the Tschermakfjellet mountain. Photograph taken on 7 Aug 2025 from the Longyearbyen-Ny Ålesund plane. B) Schematic illustration of a conventional petroleum system unaffected by igneous intrusions. C) Schematic illustration of how igneous intrusions may impact the various petroleum system elements, including charge, migration, reservoir, trap and seal. B) and C) are modified from *Senger et al.* (2017).

carbonate layer (the Vøringen Member), are straight and strata-concordant. Conversely, the segments emplaced within the Gipshuken and Kapp Starostin formations, which appear less heterogeneous than the Vøringen Member, are more irregular and exhibit locally discordant contacts (Figure 22B, insets).

Field observations also show that the segments emplaced at different stratigraphic levels are connected by steeply dipping steps, which formed through shearing/dilations of the host rocks between the tips of the sill segments. Along these steps, the host rocks layers are offset, giving the impression that the steps are emplaced along faults. However, there is no visible faulting through the strata below and above the steps, showing that the observed offset accommodated only the thickening of the sill segments.

The strike of the steeply dipping steps is dominantly NW/SE. In addition, thickness measurements of the segments conducted on the DOMs show systematic thinning of the sill towards the SE. These data suggest that the sill in James I Land was fed from the NW.

3.11 Stop 11: Mediumfjellet and the WSFTB: Deformed Intrusions and Tectonic and Thermal Fracturing in Intrusions

The western part of central Spitsbergen is dominated by Eurekan deformation manifested as the West Spitsbergen Fold and Thrust Belt. The north-western coast of Isfjorden provides some of the most spectacular structural features in the field area. Mediumfjellet, in particular, is an excellent example of multiple imbricate stacks thrust on top of each other during the deformation.

The HALIP magmatism pre-dates the Eurekan deformation and sills and dykes have been deformed together with their host rocks, including at Festningen (Stop 1). Initial studies in the area focussed on the Eurekan deformation and the resulting structural styles (*Bergh et al.*, 1997). Furthermore, the complex geometry was used as input to seismic modelling studies that compared the imaging of the structures at Mediumfjellet with those along Isfjorden to the south (*Johansen et al.*, 1994).

Many of the outcrops on the coastal stretch of Oscar II Land have been digitized. Mediumfjellet itself was initially modelled using helicopter-lidar (*Larsen*, 2010); https://v3geo.com/viewer/#/142), and more recently using drone-based SfM photogrammetry (*Rodes et al.*, 2023). *Horota et al.* (2023) provide a thematic digital data package on the WSFTB, including relevant digital outcrop models, an online virtual field trip (https://vrsvalbard.com/west-spitsbergen-fold-and-thrust-belt/) and an overview of the regional significance of this deformation event.

Fracturing of the HALIP sills themselves may be related to tectonism (pre- or post-emplacement), emplacement and thermal contraction. A number of

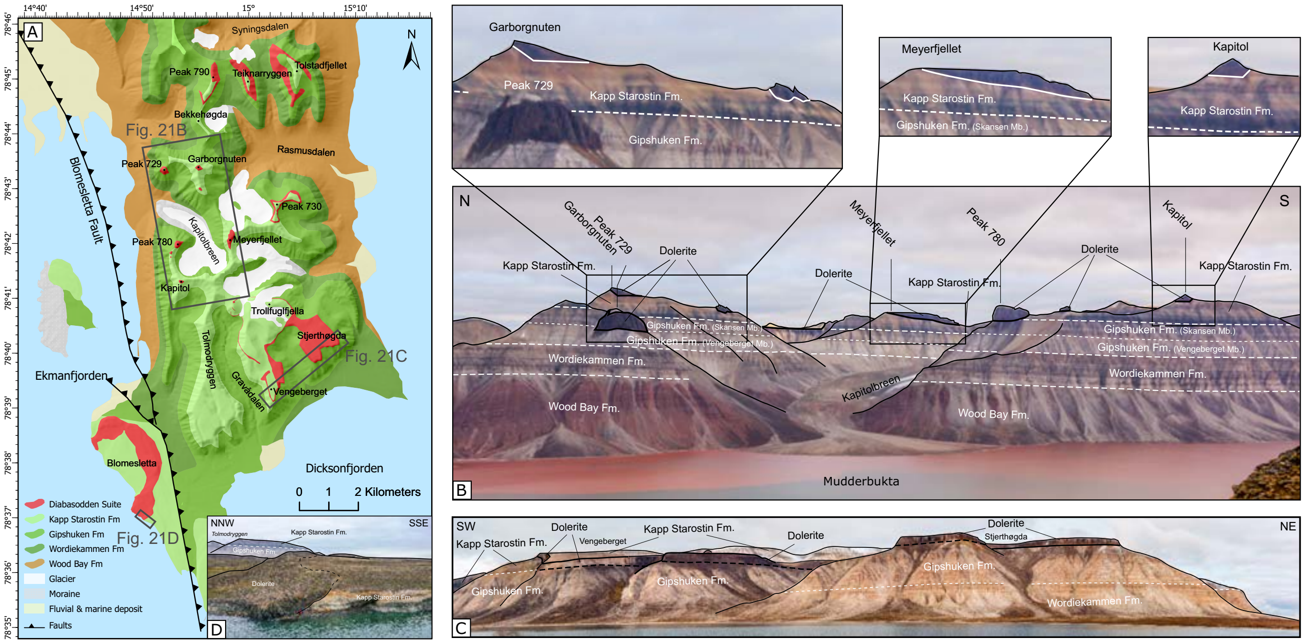

Figure 22 – Examples of sills emplaced in carbonate-dominated successions between Ekmanfjorden and Dicksonfjorden. A) Geological map of the Dicksonfjorden-Ekmanfjorden area illustrating the extent and stratigraphic position of the HALIP intrusions. B) Examples of the HALIP intrusions in different parts of the stratigraphy as seen from Mudderbukta in Ekmanfjorden. C) The south-eastern part of the study area, dominated by dolerite sills capping the topography of Vengeberget and Stjerthøgda. D) Lower contact aureole at Blomesletta. Figure elements from *Galland et al.* (2025).

studies have looked at the fractures in the sills and dykes in both Isfjorden and beyond (*Maher et al.*, 2020). The identified fractures are likely some mix of emplacement-related deformation mechanisms, tectonics and cooling. Distinguishing thermal discontinuities (i.e., cooling joints) from tectonic or emplacement-related ones is challenging but can be done by considering their orientations with respect to regional stress fields, or direct evidence of tectonism (e.g., slickensides). Striated surfaces adorned with chlorite are common in the diabase at Mediumfjellet and likely resulted from the Eurekan deformation. Calcite and pyrite vein networks are also relatively common within the intrusions as well as the surrounding host rock. *Maher et al.* (2020) identify fracture trends in sills throughout Svalbard and conclude that the predominant E-W and N-S trends of the cooling joints is likely related to regional stress during the Early Cretaceous.

3.12 Stop 12: Geochemical and Petrological Signature of the Diabasodden Suite

Whole-rock geochemical data from the Isfjorden area is available from 52 samples collected at Festningen, James I Land (Ekmanfjorden), Kapp Thordsen, Gåsøyane, Hyperittfossen, Botneheia, and Grønsteinfjellet (Figure 24; *Malinen*, 2024; *Nejbert et al.*, 2011; *Sartell*, 2021). The Diabasodden Suite in this region is characterized as tholeiitic basalts, with MgO contents ranging from ca. 2.85 to 6.3 wt%, SiO_2 contents from 44.5 to 51.2 wt%, FeOtot 11.2 to 17.8 wt%, and TiO_2 from 2.4 to 5.3 wt%. Ni content decreases with decreasing MgO content, indicative of olivine fractionation (*Malinen*, 2024; *Nejbert et al.*, 2011; *Sartell*, 2021). This trend is clearest for the samples from James I Land and Festningen, while there is a smaller decrease in Ni contents with decreasing MgO content for samples from Hyperittfossen, Botneheia, and Grønsteinfjellet (Figure 24B). The highest as well as the lowest TiO_2 contents from the available Isfjorden dataset are from James I Land, and these samples are also slightly higher in SiO_2 than other Isfjorden samples (Figure 24C). Negative Eu anomalies can be interpreted to be a result of plagioclase fractionation. The trace element ratio Tb/Yb normalized to primitive mantle (*Sun and McDonough*, 1989) can be used as a proxy of the depth of partial melting (*Wang et al.*, 2002). For the majority of samples from the Isfjorden dolerites, the Tb/YbN ratio is higher than 1.8, which suggests deeper partial melting below the garnet-spinel transition line (*Nejbert et al.*, 2011; *Sartell*, 2021). This transition occurs at around 85 to 75 km, which is the minimum pressure at which garnet is stable (*Wang et al.*, 2002). This indicates that partial melting related to the magma emplaced in Isfjorden occurred at depths below this transition zone, in the garnet stability field.

Petrographically, the dolerites from Isfjorden primarily consist of plagioclase, clinopyroxene, and Fe-Ti oxides, with occasional olivine present. Plagioclase is mainly labradorite and bytownite, and occurs commonly as phenocrysts and smaller grains in the groundmass. Clinopyroxene is often augite, present in the ground mass (*Malinen*, 2024; *Sartell*, 2021). Fe-Ti oxides are mainly Ti-magnetite and ilmenite, up to 5 mm in size, and are typically found as needles or stubby crystals (*Nejbert et al.*, 2011).

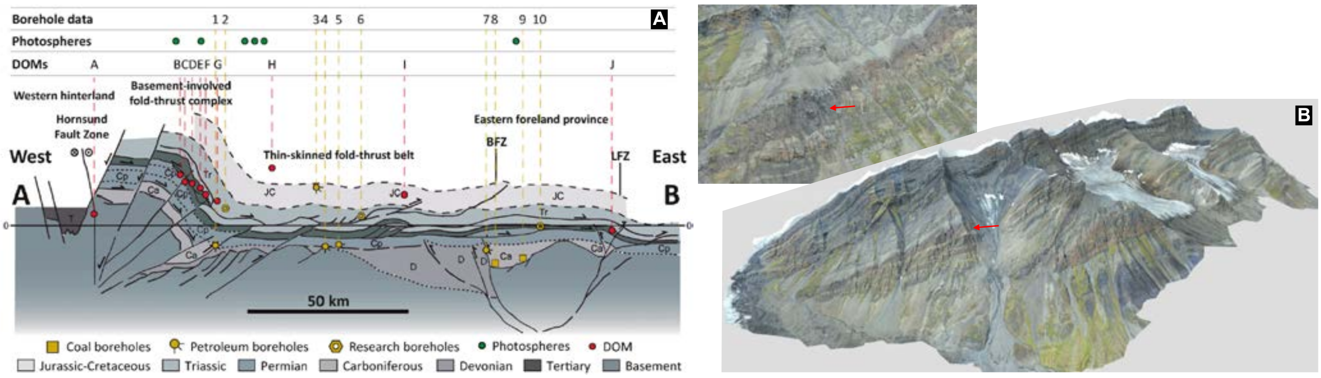

Figure 23 – Structural overview of the West Spitsbergen Fold and Thrust Belt (WSFTB), a largely compressional event occurring during the Paleogene following the emplacement of the HALIP sills (*Braathen et al.*, 1999; *Piepjohn et al.*, 2016). A) Regional east-west cross-section highlighting the geometry of the WSFTB and relevant data sets (figure modified from *Horota et al.*, 2023). B) Photogrammetric digital outcrop model of the Mediumfjellet mountain with a zoom-in on the deformed HALIP sill. The digital outcrop model is freely available online (*Rodes et al.*, 2023).

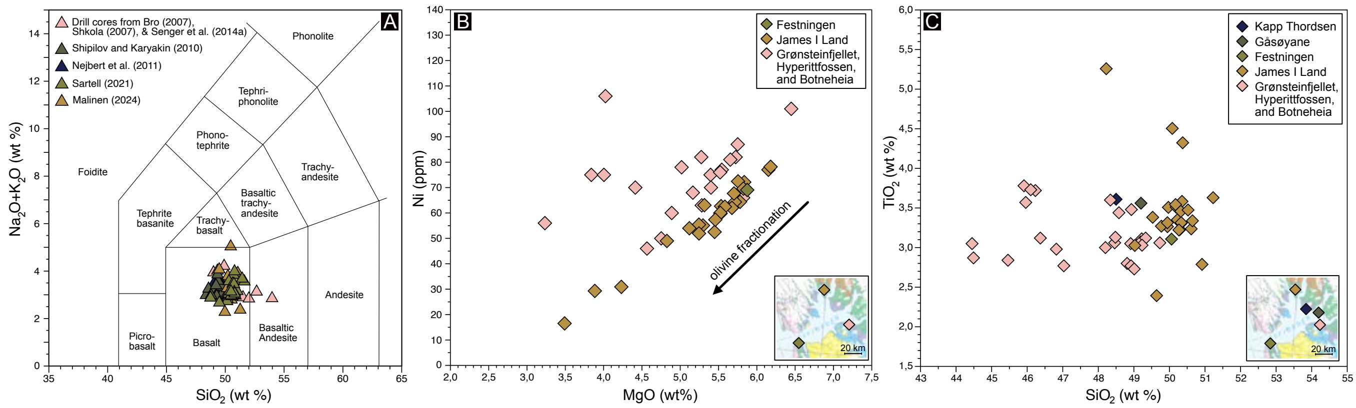

Figure 24 – Geochemical signatures of the Diabasodden Suite intrusions in Isfjorden. A) Normalized total alkali versus silica discrimination plot based on *Le Bas et al.* (1986). B) Whole-rock geochemical MgO (wt%) and Ni (ppm) contents from Festningen, James I Land, Grønsteinfjellet, Hyperittfossen, and Botneheia. Map showing sample locations is modified from (*Dallmann*, 2015). Geochemical data are from *Malinen* (2024) and *Sartell* (2021). C) Whole-rock geochemical SiO_2 (wt%) and TiO_2 (wt%) contents from Kapp Thordsen, Gåsøyane, Festningen, James I Land, Grønsteinfjellet, Hyperittfossen, and Botneheia. Map showing sample locations is modified from *Dallmann* (2015). Geochemical data are from *Malinen* (2024), *Nejbert et al.* (2011), and *Sartell* (2021).

3.13 Stop 13: Central Isfjorden: Imaging HALIP with Multi-physical and Multi-scale Geophysics

Not all HALIP locations are as easily observable. When traveling across the fjord between the various stops in central Isfjorden, one passes over a large submarine igneous complex that is equivalent in extent to what can be observed onshore. This is best seen through the integration of various geophysical data sets, including a dense network of 2D seismic and high-resolution multibeam bathymetry, and other field data acquired in the marine part of the field area.

Magnetic data are available both regionally from aerial campaigns (*Olesen et al.*, 2010) and ship-based magnetic data acquired as part of the Svalex 2D seismic acquisition campaigns (*Senger et al.*, 2013). In addition, helicopter-based magnetic data were recently acquired and utilised in forward modelling of regional profiles across parts of Nordenskiöld Land (*Ammerlaan et al.*, 2025). Due to the contrasting magnetic susceptibility properties of HALIP compared to their sedimentary host rocks, magnetic data is an excellent tool for resolving subsurface igneous intrusions (*Minakov et al.*, 2012). Strong regional and local magnetic anomalies (Figure 25) are present north of Deltaneset, connecting the outcropping intrusions at Diabasodden (Isfjorden's southern shore) with those exposed on the northern shorelines. Zooming in, a circular positive relief feature is documented 4 km south-east of Kapp Thordsen (Figure 25E). The feature is less magnetic than its surroundings and has been tentatively interpreted as a hydrothermal vent complex by *Senger et al.* (2013). The integration of the accessible onshore outcrops furthermore facilitates direct onshore-offshore correlation and has been instrumental in the mapping of geometries and geospatial characterisation of the igneous complex in the field area (*Senger et al.*, 2013; *Senger and Galland*, 2022).

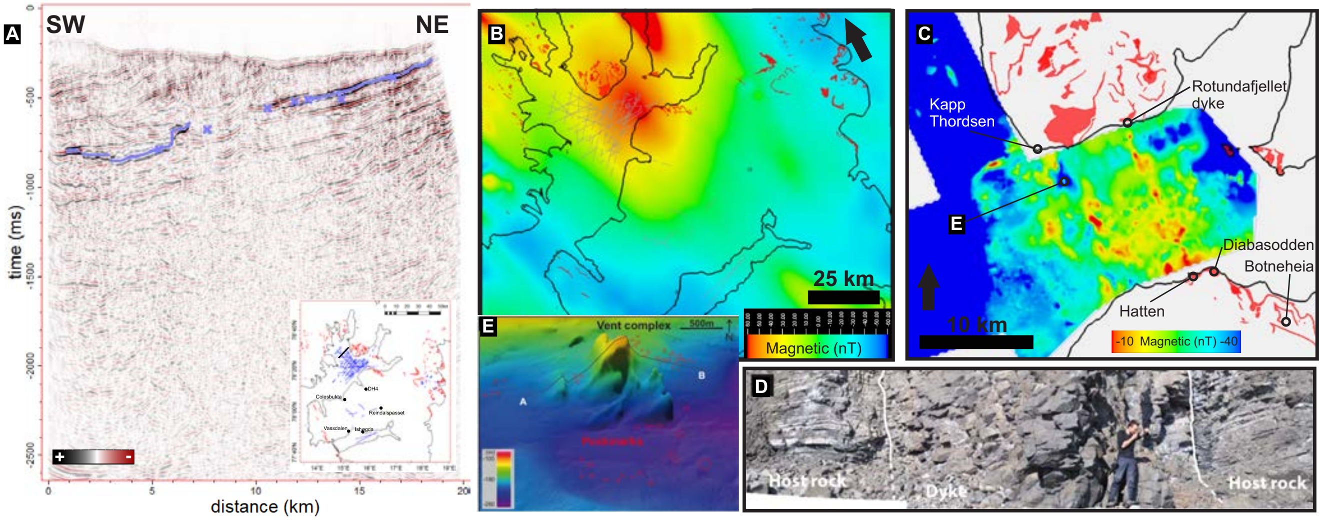

Figure 25 – Geophysical signatures of the HALIP in Isfjorden itself. A) Example of a seismic profile in Nordfjorden, with an interpreted intrusion. Note also the regional dip of the basin. The inset map illustrates all mapped igneous intrusions on seismic (blue) and onshore (red). B) Regional magnetic grid over central Spitsbergen. C) Ship-based magnetic data with higher resolution in inner Isfjorden. Note the linear positive NNW-SSE oriented anomaly linking Rotundafjellet to Hatten. D) Picture of the onshore exposure of this lineament, a ca 10 m thick HALIP dyke beneath Rotundafjellet. E) Positive relief circular structure on multibeam bathymetric data south-east of Kapp Thordsen, tentatively interpreted as a hydrothermal vent complex. Figure elements from *Senger and Galland* (2022, A, B, C, D) and *Senger et al.* (2013, E).

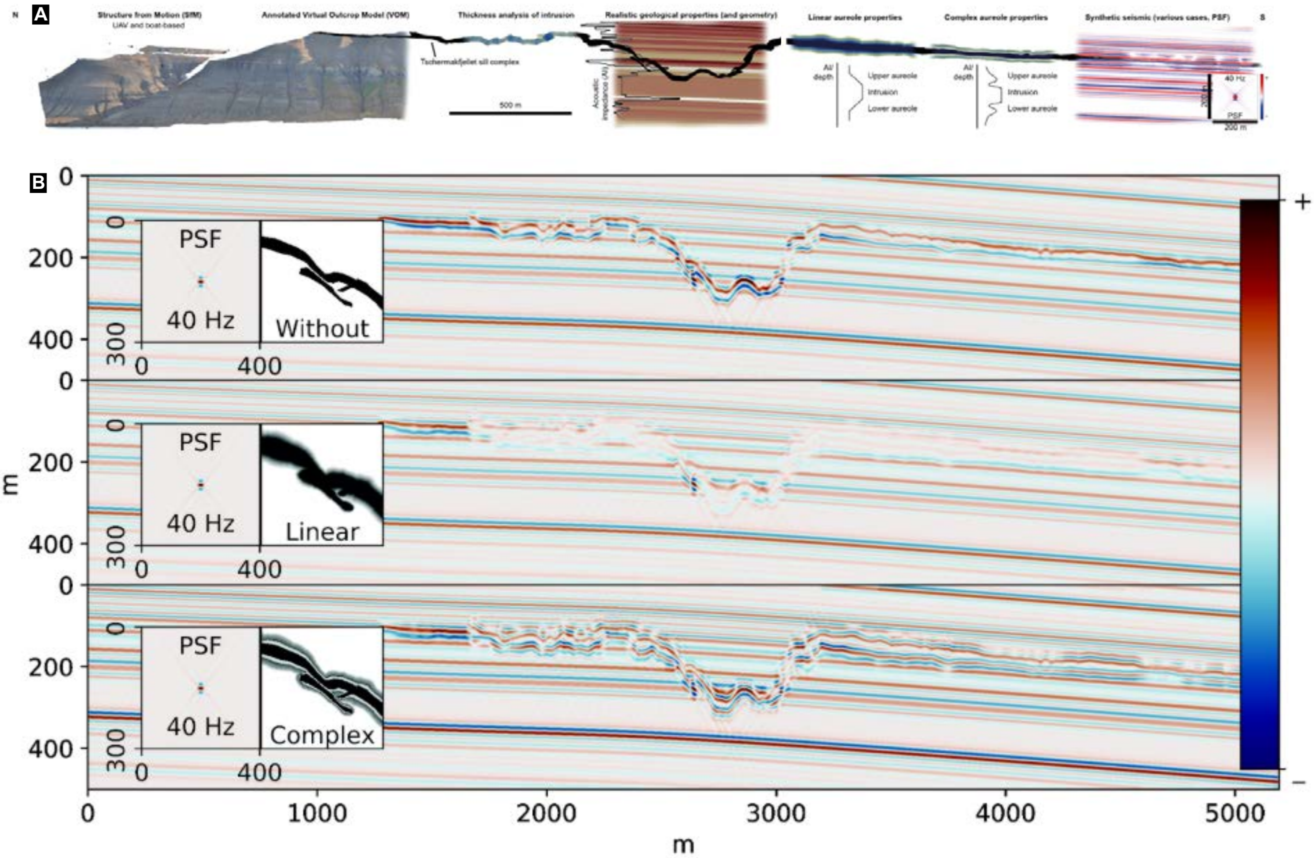

Figure 26 – A) Digital outcrop-based forward modelling allows for the creation of well-constrained synthetic references that aid the identification of intrusions through their seismic responses. The schematic (adapted from *Betlem et al.*, 2020) shown here illustrates the workflow from outcrop digitalisation, facilitating geospatial analysis, to integration with borehole derived petrophysical data, to model the acoustic response of both linear and more complex contact aureole properties. B) Synthetic seismic models of Tschermakfjellet without and with aureoles included in the geological models.

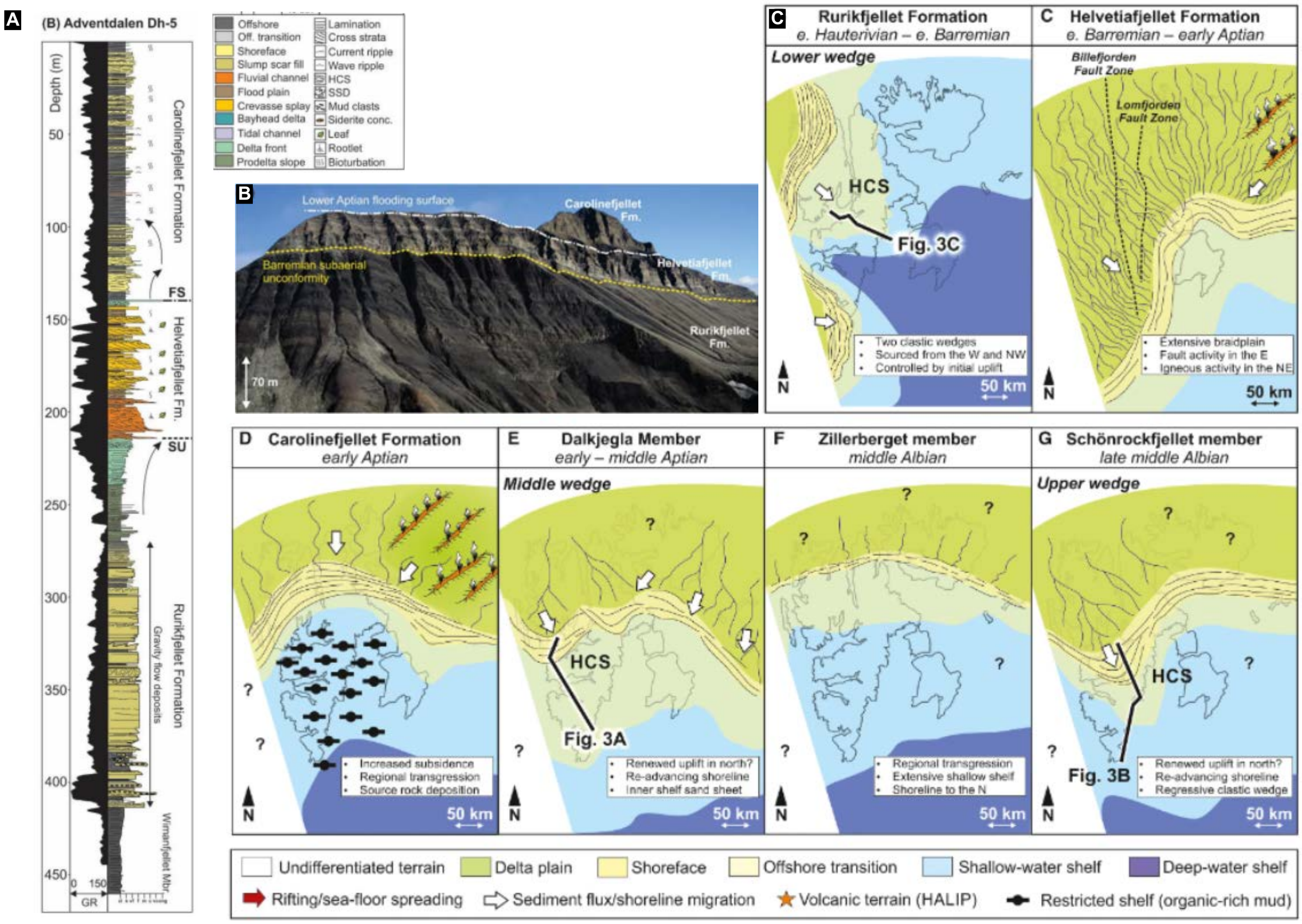

Figure 27 – Sedimentology and paleogeography of the Lower Cretaceous succession in Svalbard. A) Sedimentary log of the succession in the DH5 borehole in Adventdalen. B) Outcrop section of the succession. C) Series of regional paleogeographic reconstructions illustrating the development of a northerly sediment source and the influence of HALIP magmatism. Figure elements compiled from *Grundvåg and Olaussen* (2017); *Grundvåg et al.* (2019, 2021).

Seismic forward modelling of key outcrops provides additional confidence in seismic mapping of igneous bodies. Figure 26 illustrates a forward model of the Tschermakfjellet intrusion (Stop 9). Populated with realistic seismic attributes derived from nearby boreholes, the modelled seismic response is an important aid for the identification of igneous bodies from Svalbard's legacy seismic data, as it provides a reference library of possible geophysical responses (*Rabbel et al.*, 2018).

3.14 Stop 14: Flyplassveien and CO_2 Lab Cores: Regional to Local Sedimentary Response to HALIP Magmatism

The Upper Jurassic to Lower Cretaceous sedimentary succession in Svalbard (Figure 27) is nearly continuous and records multiple evidence of HALIP-influenced sedimentation. One of the most prominent features is the lithologically sharp, erosional unconformity at the base of the Helvetiafjellet Formation, which formed due to thermal uplift and southward tilting of the entire Svalbard Platform, likely related to the oldest HALIP pulse in Svalbard. Ash layers (i.e., bentonites) of Barremian ages, directly tied to HALIP activity, were encountered in several research boreholes in Adventdalen and dated radiometrically to ca. 123 Ma (*Corfu et al.*, 2013; *Midtkandal et al.*, 2016). These ages have subsequently been used to constrain the Aptian-Albian boundary interval on the global geological timescale (*Zhang et al.*, 2021).

A significant amount of plagioclase feldspar and mafic volcanic lithics are found in the Aptian part of the Carolinefjellet Formation, giving it a very characteristic red-brown color (*Edwards*, 1979; *Maher et al.*, 2004). The excellent outcrop along the road between the airport and Longyearbyen displays numerous storm beds with scoured bases, pinch-and-swell geometries, and hummocky cross stratification, indicating deposition on a storm-dominated, shallow shelf (*Grundvåg et al.*, 2021). A rich trace fossil assemblage typical of open marine, storm-swept shelf conditions has also been reported from this outcrop section (Leszczyński et al., 2023). Based on paleogeographic reconstructions, as well as the lack of HALIP extrusives in the Isfjorden area, the source area for the shelf sands was likely to the north, outside the outcrop window (*Grundvåg and Olaussen*, 2017). There is a distinct

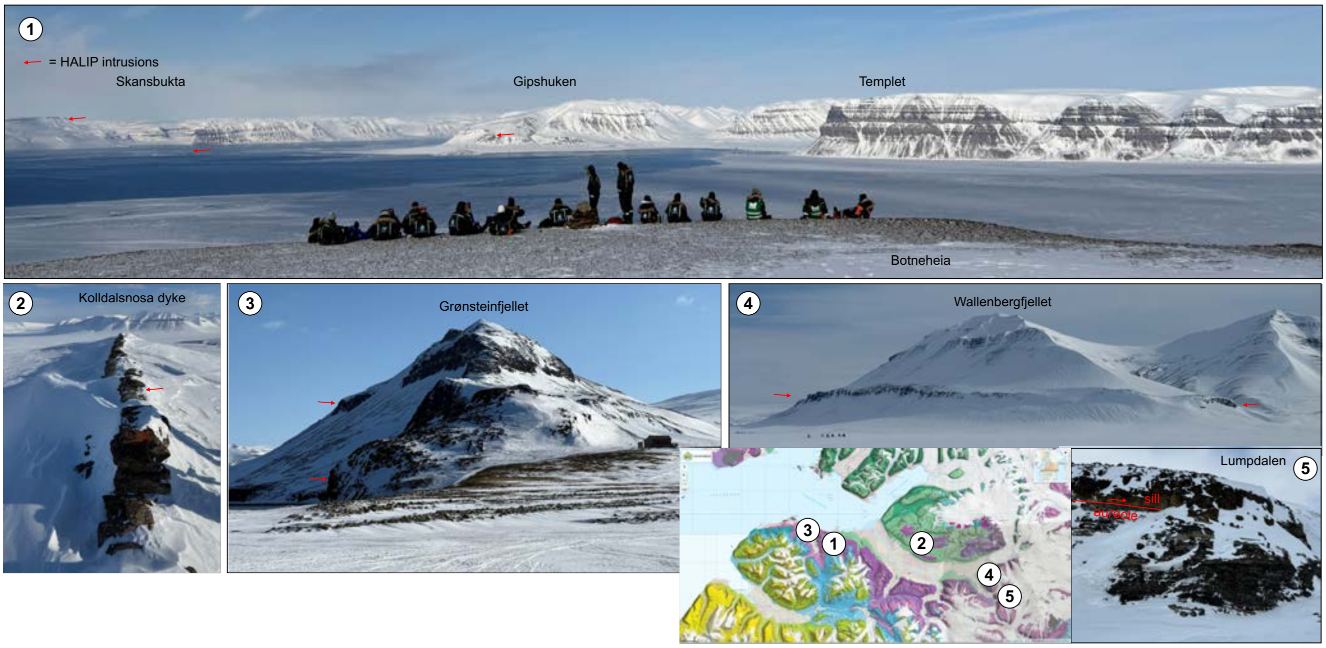

Figure 28 – Photographs of HALIP-relevant field sites to the greater Sassendalen area east of Longyearbyen in April 2025. The HALIP dolerites are highlighted with red arrows. All sites are accessible during day trips on snowmobile from Longyearbyen.

color difference between sandstones in the Helvetiafjellet and Carolinefjellet formations in Central Spitsbergen, reflecting a drastic change in composition from more mature, quartz-dominated sands to a significant increase in lithic and plagioclase-bearing sands (*Maher et al.*, 2004). The Helvetiafjellet Formation fluvial system mainly drained exposed basement terrain and Paleozoic to Mesozoic strata to the north and northwest, which lacked HALIP extrusives. Only with significant time did HALIP detritus arrive in the Isfjorden area via west- to southwest-directed longshore drift, along the ENE-SWS-oriented paleo-shoreline (*Maher et al.*, 2004; *Grundvåg et al.*, 2019, 2021). In eastern Spitsbergen, the compositional change between the two units appears more transitional, with plagioclase-rich sandstones gradually becoming more abundant upwards in the Helvetiafjellet Formation (*Edwards*, 1979). This may reflect proximity to an exposed HALIP sediment source further to the NE, which promoted sediment mixing. Exposed HALIP extrusives are only found on Kong Karls Land (*Olaussen et al.*, 2019), thus supporting this notion.

3.15 Stop 15: A Winter Wonderland - Visiting HALIP Exposures on Snowmobiles

The spring field season from March to early May facilitates access to some HALIP exposures using snowmobiles. The steep dolerite cliffs are often, contrary to the sedimentary host rocks, not snow-covered and their large-scale geometries can be appreciated (Figure 28). Some of the stops (e.g., Diabasodden, Grønsteinfjellet, Botneheia) may be visited during this season. In addition, snowmobiles allow good access to the HALIP exposures in Sassendalen and towards the east coast of Spitsbergen.

A dyke emplaced in the Permian strata is accessible at Kolldalsnosa (Figure 28). In the inner part of Sassendalen, the Wallenbergfjellet mountain offers a sill emplaced at the vicinity of the Permian-Triassic boundary, climbing upwards in the stratigraphy towards the east (Figure 28). Its lower aureole is well exposed in Lumpdalen (Figure 28), even in late winter conditions.

3.16 Synthesis of the (Virtual) Field Trip

During this field trip we visited 15 locations in and around Isfjorden, enlightening us about the HALIP from a wide range of perspectives and themes (Table 1; Figure 29). Collectively they showcase the HALIP as an onshore-offshore igneous province with research significance well beyond Isfjorden.

4 Further Exploration with Digital Geoscientific Data

Over the past decade, UNIS has compiled, digitized and spatially integrated a lot of geoscientific data in the Svalbox database (*Senger et al.*, 2020). In parallel, we have used drones to digitize a growing number of outcrops using photogrammetry, and share these openly through the Svalbox portal (www.svalbox.no/map; *Betlem et al.*, 2023). Drones are also used to acquire aerial photospheres, collectively providing thematic excursions and virtual field trips on the UNIS-managed VR Svalbard online platform (www.vrsvalbard.com; *Horota et al.*, 2023).

This effort has been largely driven by education challenges at UNIS, where geosciences are taught year-round even in strongly seasonal conditions (i.e., polar night, snow cover, harsh conditions; *Senger*

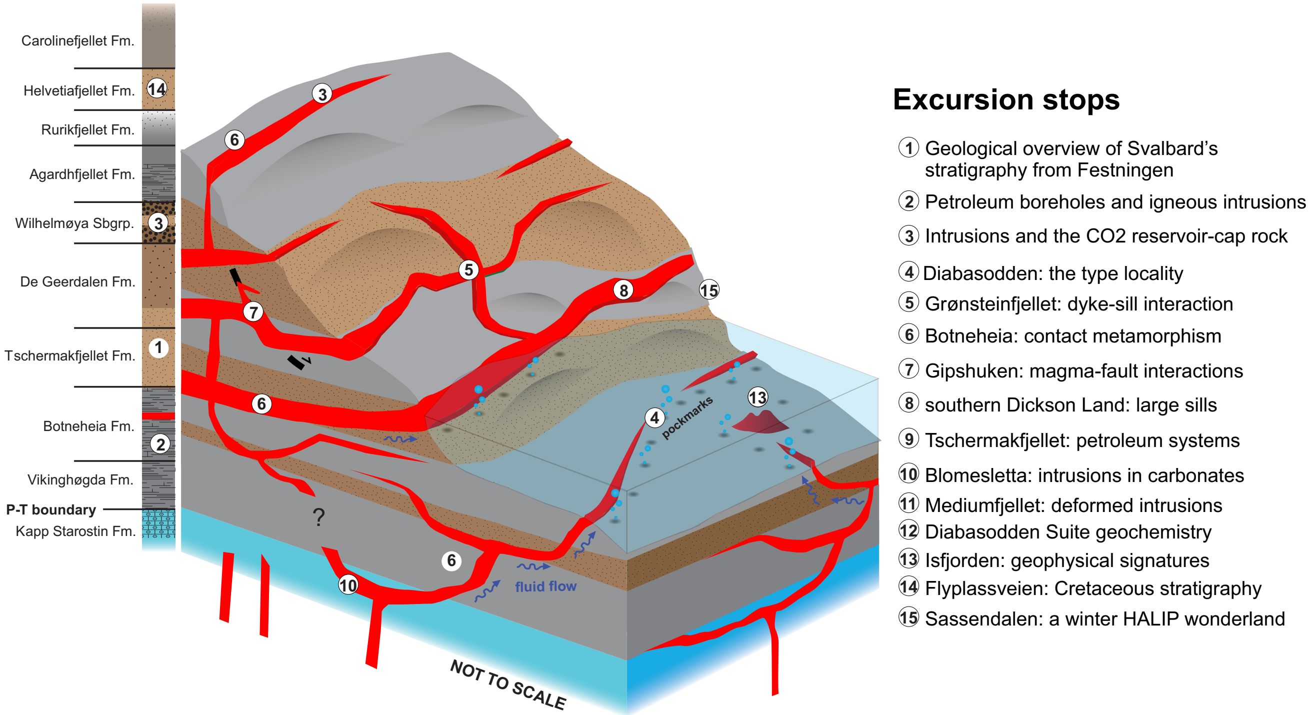

Figure 29 – Synthesis of the visited stops in the context of a schematic representation of the igneous complex in the Isfjorden field area. Figure updated from *Senger et al.* (2013).

et al., 2020, 2021). As more and more data sets became integrated in the Svalbox project, we have started to compile thematic data packages to facilitate geoscientific learning. *Horota et al.* (2023) presents a data package related to the Eurekan deformation in western Spitsbergen. *Senger et al.* (2024) compile and discuss a data package on Arctic Tectonics and Volcanism used for teaching at a UNIS graduate course.

5 Knowledge and Data Gaps

We hope that this field guide will stimulate further research on the HALIP in Svalbard and beyond. *Senger et al.* (2024) and *Senger and Galland* (2022) both identified a number of knowledge and data gaps and avenues for further research, which we refine here and illustrate in Figure 30:

Contact metamorphism in host rocks of various lithologies needs to be quantified to assess the potential for greenhouse gas generation during magma emplacement. Furthermore, systematic exploration to identify potential hydrothermal vent complex connecting the intruded magma with the atmosphere is required.

Structural and stratigraphic characterization of age-equivalent lava flows on Kong Karls Land and Early Cretaceous sedimentary strata to constrain the Early Cretaceous paleo-environment.

Regionally and locally the heterogeneous host rock composition and pre-existing weakness zones (i.e., fault zones) will likely control magma propagation. But more inter-disciplinary research combining numerical and analogue modelling with field studies is needed to decipher these processes.

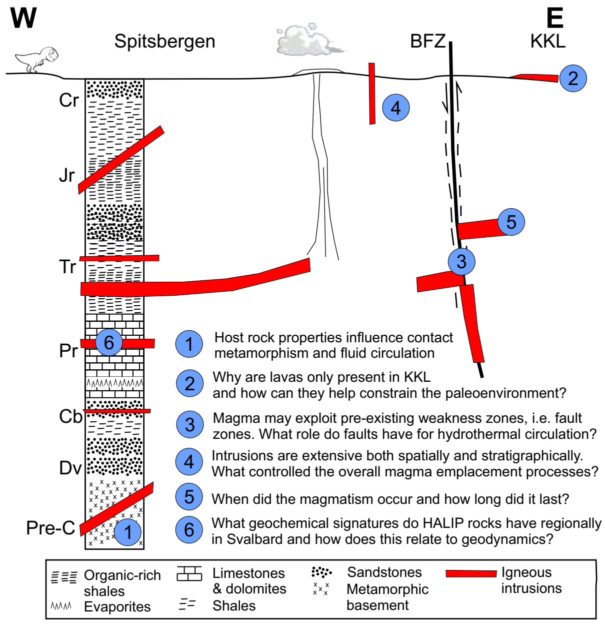

Figure 30 – Cartoon illustrating the identified knowledge gaps with respect to HALIP in Svalbard, updated from *Senger and Galland* (2022).

Characterizing circum-Arctic, regional and local magma emplacement pathways and mechanisms. At the circum-Arctic scale, magma has likely propagated through a giant dyke swarm centered on the Alpha

Figure 31 – Polar bears on the Diabasodden Suite dolerites on Barentsøya, August 2024.

Ridge, but sills may also be responsible for feeding magma to the more peripheral parts of the HALIP including Svalbard. The mechanics of sill-dominated versus dike-dominated emplacement are worth further consideration and have implications for the research avenue 1 presented above. On a regional scale, magma emplacement appears to be shallower towards the east, culminating with the lava flows on Kong Karls Land.

Constraining the timing and duration of circum-Arctic HALIP magmatism. Too few robust (i.e., U/Pb) radiometric ages are available from Svalbard. On the positive side, systematic age determinations are currently ongoing, based also on samples from eastern Svalbard.

Systematic geochemical studies at several levels (individual sills, igneous complexes and a regional approach also incorporating Lu-Hf isotopic characterization) is required to understand the magma chamber evolution, melting depths and emplacement modes.

6 Further Reading

Table 2 provides an overview of thematically summarized key literature on the HALIP in Svalbard.

7 Practical Considerations: Fieldwork in Isfjorden

While Isfjorden is relatively easily accessible compared to other High Arctic locations, each excursion beyond Longyearbyen's city limits should be planned like an expedition. There are no roads to any HALIP localities and the field area has several site-specific challenges including steep and partly unstable cliffs, potentially harsh and rapidly changing weather conditions, lack of infrastructure and the presence of polar bears (Figure 31). The summer season (late June to early September) is optimal for visiting the described sites. Some sites (e.g., Botneheia, Coloradoplatå, Diabasodden) are also accessible on snow-covered ground in the spring (March-April) using snowmobiles. While all sites (except stop 15) are accessible as (long) day trips from Longyearbyen using boats, chartering a vessel/sailboat with an option for overnight stays is optimal. Tenting, while in theory permitted, is not recommended in the greater Isfjorden area due to the increasing presence of polar bears and importance of mitigating even potential conflict situations.

Stop 15 is designed to be undertaken during the spring season using snowmobiles. Snowmobiles (and guides) may be rented from a number of tourism companies, or organised as a research and education campaign through The University Centre in Svalbard (UNIS).

UNIS has been organizing research-based field courses at BSc to PhD level for over 30 years, and provides valuable advice and extensive safety courses for conducting fieldwork in and around Isfjorden in both summer and spring. A MSc/PhD course at UNIS ("Arctic Tectonics and Volcanism"; *Senger et al.*, 2024) regularly visits some of the described HALIP sites.

Some of the sites (e.g., parts of Festningen, Grønsteinfjellet, Blomesletta contact) are located

Table 2 – Summary of key literature on the Svalbard dolerites.

Overall theme	Comment	Reference
Reviews and formal definition	First review of the Svalbard dolerites	*Tyrrell and Sandford* (1934)
	Formal definition of Diabasodden Suite	*Dallmann et al.* (1999)
	Synthesis of Svalbard dolerites in the context of the HALIP	*Maher* (2001)
	Regional geochemical study and discussion of the Svalbard dolerites	*Nejbert et al.* (2011)
	Most recent review of the Diabasodden Suite	*Senger et al.* (2014b)
	Related postgraduate course on Arctic tectonics and volcanism	*Senger et al.* (2024)
	Characterization of sills and spatial extent	*Senger and Galland* (2022)
Geochronology	U-Pb age determinations from Linnevatnet, Diabasodden and Adventdalen	*Corfu et al.* (2013)
	U-Pb age determination from Ekmanfjorden	*Sartell et al.* (2025)
Igneous complexes and their geometries	Integrated mapping of the igneous complex in central Spitsbergen in the context of CO_2 storage	*Senger et al.* (2013)
	Field and digital mapping of a 3D sill in Ekmanfjorden	*Galland et al.* (2025)
	Crustal structure and dyke emplacement	*Minakov et al.* (2018)
	Intrusions offshore eastern Svalbard	*Minakov et al.* (2012)
	Intrusion mapping on Barents Shelf	*Grogan et al.* (2000)
Contact metamorphism	Aureole characterization at Botneheia	*Hubred* (2006)
	Thermal imprints at Edgeøya	*Brekke et al.* (2014)
	Characterization of a 2.28 m thin sill fully cored in the DH4 borehole	*Senger et al.* (2014b)
Cretaceous stratigraphy and paleoclimate/ paleoenvironments	Regional sedimentology of Early Cretaceous succession	*Grundvåg et al.* (2017)
	Regional sedimentology of Early Cretaceous succession	*Grundvåg et al.* (2019)
	Regional sedimentology of Early Cretaceous succession	*Midtkandal et al.* (2016)
	Paleogeography and sediment provenance	*Sømme et al.* (2018)
Key circum-Arctic HALIP-related papers	Geodynamic modelling of multiple pulses	*Heyn et al.* (2024)
	Geochronology and geochemistry	*Dockman et al.* (2025)
	Sverdrup focus; 3 pulses	*Dockman et al.* (2018)

directly at the coastline and careful planning is required with respect to the tides.

Most research in Svalbard requires a permit and notification of travel from the Governor of Svalbard, and all research must be registered in the Research in Svalbard database (www.researchinsvalbard.no). Further practical information on conducting fieldwork in Svalbard is provided by the Svalbard Science Forum (https://www.forskningsradet.no/en/svalbard-science-forum/) and Svalbard Integrated Arctic Earth Observing System (https://sios-svalbard.org/Logistics).

8 Optional Additional Reading

8.1 Cretaceous Stratigraphy and Circum-Arctic Correlations - Uplift and Sedimentation Patterns During the HALIP

8.1.1 Cause and Timing of HALIP-related Uplift

The emplacement of a LIP is usually associated with regional-scale thermal uplift (e.g., *He et al.*, 2003; *Saunders et al.*, 2007), although subsidence may also occur if lithospheric heterogeneities are properly accounted for (*Burov et al.*, 2007). In the Arctic, the first HALIP pulse was associated with large-scale uplift and a major shift in sedimentation patterns, for instance in the Sverdrup Basin (*Tullius et al.*, 2014; *Hadlari*, 2024), the Wandel Sea Basin of Northeast Greenland (*Ineson et al.*, 2021), and the Barents Shelf, including Svalbard (e.g., *Grundvåg and Olaussen*, 2017; *Midtkandal et al.*, 2020a, Figure 6). However, the exact timing, magnitude, extent and processes controlling this uplift remains poorly constrained. The opening of the Canada Basin (within the Amerasia Basin) may have played a significant role. This basin is thought to have been initiated by continental rifting in the Jurassic, followed by seafloor spreading in the Early Cretaceous (*Grantz et al.*, 2011). Based on magnetic anomalies and plate tectonic modelling, various age estimates have been proposed for the oceanic crust in the Canada Basin, spanning from approximately 142 Ma to 120 Ma (e.g., *Grantz et al.*, 2011; *Shephard et al.*, 2013; *Døssing et al.*, 2020). Recent models, however, favor a relatively short-lived period of seafloor spreading beginning in the Hauterivian and continuing into the early Aptian (at ca. 127–120 Ma) (*Døssing et al.*, 2020; *Hutchinson et al.*, 2025). This time frame overlaps with the age for the first HALIP pulse on Svalbard (at ca. 123 Ma) (*Corfu et al.*, 2013; *Senger et al.*, 2014a) and other Arctic regions (at ca. 122 Ma; Figure 4). A major Hauterivian (132.6 ± 0.6 to 125.77 Ma) break-up unconformity has been documented along the conjugate margins of Alaska and Arctic Canada (*Molenaar*, 1983; *Embry and Beauchamp*, 2019). In Northeast Greenland, biostratigraphy indicates the presence of a late Hauterivian–early Barremian hiatus in the northern part of the outcrop belt, expanding southward to a late Valanginian–early Barremian hiatus (*Hovikoski et al.*, 2018; *Ineson et al.*, 2021). In contrast, central and southern Spitsbergen exhibits a prominent uplift-related unconformity of early Barremian (?) age at the base of the Barremian–Aptian Helvetiafjellet Formation (*Grundvåg et al.*, 2017; *Śliwińska et al.*, 2020). This unconformity expands in magnitude east towards the islands of Kong Karls Land to an Early Kimmeridgian-Valanginian hiatus (*Smelror et al.*, 2018). Northern Svalbard, including the northernmost region of Spitsbergen, appears to have served as a sediment source area onwards from the Jurassic–Early Cretaceous. This terrain likely defined the northern margin of the basin, characterized by a sparse and fragmented record of post-Devonian strata, with no preserved Lower Cretaceous deposits (*Dörr et al.*, 2012).

8.1.2 Evidence of Diachronous Uplift and Sedimentary Response

The age variation of the uplift unconformity within the various Lower Cretaceous basin fill successions across the Arctic (Figures 6 and 7) reflects supra-regional differences in the rate and magnitude of uplift and exhumation. This variability may have been influenced by differential movements along structural lineaments, denudation and isostatic uplift, as well as doming associated with the formation of igneous centers during continental break-up and HALIP emplacement. Together, these processes resulted in diachronous erosion and sedimentary responses to the break-up. The Barremian age of the unconformity recorded in central to southern Spitsbergen is puzzling, as it suggests a delayed sedimentary response compared to that observed in adjacent Arctic basin fills. This may have been caused by the gradual southward tilting of the entire Svalbard Platform, culminating in uplift and exposure of the entire region during the Barremian. Nonetheless, in all the basins, the unconformities are typically succeeded by fluvio-deltaic to estuarine sandstone-rich successions (*Tullius et al.*, 2014; *Grundvåg et al.*, 2017, 2019; *Hovikoski et al.*, 2018; *Olaussen et al.*, 2019; *Embry and Beauchamp*, 2019; *Ineson et al.*, 2021; *Hadlari*, 2024), indicating that increased subsidence rates coupled with high sediment influx followed the uplift. Interestingly, shallow to moderately deep shelf conditions were established across the entire region in post-early/middle Aptian times, possibly in response to rising eustatic sea level coupled with thermally-driven subsidence in the aftermath of the HALIP (*Embry and Beauchamp*, 2019; *Grundvåg et al.*, 2021; *Ineson et al.*, 2021; *Hadlari*, 2024).

8.1.3 Pre-HALIP Tectono-sedimentary Evolution

On Svalbard, the Middle Jurassic to Lower Cretaceous succession is assigned to the Adventdalen Group (*Dallmann et al.*, 1999). Several clastic wedges are present in the succession. Embedded in the otherwise mudstone-dominated Middle Jurassic to lowermost Cretaceous (Bathonian–Berriasian) Agardhfjellet Formation, a fine-grained, intensely bioturbated, sandstone-rich unit of inferred distal delta front to prodelta origin is present (*Koevoets et al.*, 2019). This unit, of Kimmeridgian–Volgian age, thickens to the northwest and may represent an early sedimentary response to basin margin uplift, perhaps related to rifting in the incipient Canada Basin. A similar unit, albeit dominated by sandstone, is present in Northeast Greenland (i.e., the Birkelund Fjeld Formation) (*Hovikoski et al.*, 2018; *Ineson et al.*, 2021), possibly representing a proximal expression of the same clastic wedge. A comparable development is reported in the Sverdrup Basin, where a series of shallow marine sandstone wedges, assigned to the Oxfordian–Kimmeridgian Awingak Formation, extend from the basin margin northwest towards the basin center (*Hadlari et al.*, 2016; *Embry and Beauchamp*, 2019).

In the Valanginian–lowermost Barremian Rurikfjellet Formation, a pronounced, large-scale coarsening upward trend is evident, particularly in the upper, Hauterivian part of the Formation, where a series of vertically stacked sandstone-rich units are present (*Jelby et al.*, 2020; *Grundvåg et al.*, 2021; *Jelby et al.*, 2025). This storm-influenced, shallow marine to deltaic clastic wedge thins markedly towards the east and southeast, and pinches out south towards central Spitsbergen (*Jelby et al.*, 2025). In southern Spitsbergen, a thicker and significantly coarser-grained clastic wedge, also of shallow marine to deltaic affinity occur (*Grundvåg et al.*, 2017; *Grundvåg and Olaussen*, 2017). Together, these two clastic wedges represent laterally coeval, basinward-prograding depositional systems that developed in response to renewed basin margin uplift (*Jelby et al.*, 2025). Time- and facies-equivalent strata is poorly preserved in Northeast Greenland due to the regional uplift unconformity, albeit, thin, storm-reworked sandstones are present in the upper part of the Valanginian–Hauterivian Dromledome Formation (*Hovikoski et al.*, 2018; *Ineson et al.*, 2021). A Valangian, shallow marine clastic wedge is present in the Sverdrup Basin, there assigned to the lowermost part of the Isachsen Formation (*Hadlari et al.*, 2016; *Hadlari*, 2024; *Embry and Beauchamp*, 2019). This unit, which is truncated by the Hauterivian break-up unconformity, reflects shoreline regression caused by an early phase of basin margin uplift (*Embry and Beauchamp*, 2019).

8.1.4 Regional Sedimentation Patterns During the Main HALIP Pulse

On Svalbard, the Barremian–Aptian Helvetiafjellet Formation unconformably overlies the Rurikfjellet Formation. This fluvio-deltaic unit, characterized by a basal sandstone sheet of braided stream origin, represents a direct sedimentary response to HALIP activity. A notable shift from quartz arenites in the lower part of the formation—generally sourced from the west to northwest—to volcanic arenites in the upper part, sourced from the east to northeast, reflects the influx of HALIP-related volcanic sediments (*Edwards*, 1979; *Maher*, 2001; *Maher et al.*, 2004). Further evidence of HALIP influence includes a bentonite layer in the upper part of the formation, dated to 123.1 ± 0.3 Ma (*Corfu et al.*, 2013; *Midtkandal et al.*, 2016), numerous dolerite intrusions (*Senger et al.*, 2014a; *Polteau et al.*, 2016), and Aptian basaltic plateau lavas interbedded with alluvial plain, volcanoclastic sandstones and pyroclastics in the Helvetiafjellet Formation on Kong Karls Land (*Olaussen et al.*, 2019). Additionally, the Oceanic Anoxic Event (OAE) 1a, associated with LIP emplacement during the early Aptian, is recorded in an organic-rich marine mudstone unit that blankets the fluvio-deltaic deposits of the Helvetiafjellet Formation (*Midtkandal et al.*, 2016; *Vickers et al.*, 2016; *Grundvåg et al.*, 2019). This regionally extensive transgressive mudstone unit also marks the basal boundary of the overlying lower Aptian–middle Albian Carolinefjellet Formation (*Midtkandal et al.*, 2016; *Grundvåg et al.*, 2017). The Carolinefjellet Formation, exceeding 1 km in thickness, comprises intercalated sandstone-rich and mudstone-dominated units of shallow marine to shelfal origin (*Grundvåg et al.*, 2019, 2021; *Leszczyński et al.*, 2023). The presence of significant volcanic detritus within the sandstone units indicates continued sediment supply from exposed HALIP terrain located to the east and northeast of Spitsbergen (*Maher et al.*, 2004). The early Cretaceous uplift event is associated with SSE-prograding Barremian intrashelf platform lobes in the west-central Barents Sea (*Faleide et al.*, 2019; *Midtkandal et al.*, 2020b,a) and prograding reflections in the eastern Barents Sea (*Polteau et al.*, 2016).

Comparable stratigraphic developments are documented in both Northeast Greenland and the Sverdrup Basin, reflecting contemporaneous uplift events followed by transgression and basin-margin drowning. In Northeast Greenland, fluvio-deltaic deposits of the coeval Ladegårds and Lichenryg formations, both of Barremian–Aptian age, transitions upward into shallow marine and shelf deposits of the Aptian–Albian Galadriel Fjeld Formation (*Dypvik et al.*, 2002; *Hovikoski et al.*, 2018; *Ineson et al.*, 2021). Similarly, in the Sverdrup Basin, the Barremian–Aptian Isachsen Formation displays a two-fold stratigraphic architecture, with a lower section of braided stream origin overlain by marginal marine deposits. These are separated by an organic-rich marine mudstone unit of early Aptian age, which notably records the OAE 1a (*Tullius et al.*, 2014; *Hadlari et al.*, 2016; *Herrle et al.*, 2015; *Embry and Beauchamp*, 2019). The Isachsen Formation is transitionally overlain by a thick shelfal sequence of the Aptian–Albian Christopher Formation (*Herrle et al.*, 2015; *Embry and Beauchamp*, 2019; *Hadlari*, 2024). Volcanogenic rocks are present in both the Isachsen and Christopher formations in the Sverdrup Basin, recording six discrete intervals of magmatism ranging from approximately 130 Ma to 101 Ma (*Evenchick et al.*, 2015). Thus, volcanism began earlier and occurred more frequently in the Sverdrup Basin than in other HALIP-influenced basins such as Svalbard.

8.1.5 Uplift and Sedimentation Patterns During Later HALIP Pulses

On Spitsbergen, the presence of a low-angle unconformity spanning the upper Albian to lowermost

Paleocene, which is associated with >1 km of erosion, may reflect thermal doming during the youngest HALIP pulses (*Maher*, 2001). Consequently, Upper Cretaceous strata are missing from the whole of Svalbard, albeit reworked palynomorphs in the Paleocene succession of southern Spitsbergen suggest that an Upper Cretaceous succession may have been present prior to post-Albian regional uplift and erosion (*Smelror and Larssen*, 2016). In contrast, Upper Cretaceous strata are present in Northeast Greenland and the Sverdrup Basin, generally recording deposition in shelf and offshore environments (*Hovikoski et al.*, 2018; *Embry and Beauchamp*, 2019). The Sverdrup Basin was significantly influenced by late stage HALIP volcanism during the Late Cretaceous. This is evidenced by the presence of thick tholeiitic basalt flows within the Cenomanian Strand Fiord Formation, as well as an abundance of bentonites in the upper Cenomanian–Campanian Kanguk Formation (*Evenchick et al.*, 2015; *Herrle et al.*, 2015; *Davis et al.*, 2017). Furthermore, the Upper Cretaceous part of the basin fill contains several sandstone wedges of shallow marine to shelfal origin, which likely represent basinward-prograding shoreline systems formed in response to thermo-tectonic uplift (*Embry and Beauchamp*, 2019).

8.2 Paleomagnetism

Paleomagnetism is a key tool for reconstructing the paleogeographic position of the HALIP magmatic suite. Early Cretaceous dolerite sills and dikes on Svalbard were extensively studied paleomagnetically from the late 1960s to the 1980s, including work in Isfjorden (*Krumsiek and Nagel*, 1968; *Spall*, 1968), Hornsund (*Vincenz et al.*, 1981), the eastern coast of Spitsbergen (*Briseid and Halvorsen*, 1974; *Vincenz et al.*, 1981), and the Hinlopen Strait (*Halvorsen*, 1989). These studies provided insights into natural remanent magnetization (NRM) and its carriers, with some paleopoles aligning with the Late Mesozoic apparent polar wander Path (APWP) of Baltica (*Halvorsen*, 1989), suggesting long-term stability of the northeastern Eurasian Plate, while others deviated from the reference path *Vincenz et al.* (1981, 1984). A major limitation of earlier work is the lack of precise age control: only a part of paleomagnetic sites were dated using K-Ar, which yielded minimum crystallization ages. As a result, it remains uncertain whether directional dispersion reflects intrusions of different ages or tectonic rotations. On western Spitsbergen, secondary magnetization associated with the Eurekan orogen is common and often overprints primary signals (*Vincenz et al.*, 1981). Moreover, mafic rocks present additional challenges due to rapid crystallization and the limited averaging of secular geomagnetic variations. Overall, there is still no modern, comprehensive study of the HALIP dolerites of Svalbard that integrates advanced paleomagnetic and rock-magnetic techniques with high-precision U-Pb geochronology of baddeleyite and zircon, framed within contemporary paleogeographic models of the Arctic.

9 Summary

We have provided a field guide and relevant scientific background to 15 sites of relevance for HALIP exposures in and around Isfjorden, Svalbard. Collectively the sites represent the broad range of HALIP-focussed studies in the area over the past two decades, spanning from applied research (e.g., CO_2 storage), fundamental research (e.g., igneous complex extent and characterization) to research of circum-Arctic relevance (e.g., timing and duration of HALIP magmatism and linkage to global anoxic events). Ample knowledge and data gaps remain, for what promises to be an exciting several decades research on HALIP in Svalbard and beyond.

Acknowledgements

We sincerely thank all our geoscience colleagues and students who have explored the described HALIP sites with us over the years, including Tereza Mosočiová, Lauri Malinen, Lilith Kuckero, Elise Lindell, Karen Mair, Tobias Schmiedel and the countless UNIS students and field assistants. UNIS logistics and the Czech Arctic Research Station facilitated accessing the described sites. UNIS sincerely appreciates the academic licenses for Petrel, Blueback Toolbox and SeisRoX provided by Schlumberger, Cegal and NORSAR, respectively. Finally, we sincerely appreciate the constructive feedback provided by an anonymous reviewer and Enrico Tavarnelli and the editorial handling by journal editors Chiara Montomoli and Graeme Eagles.

Funding for HALIP research at UNIS has been a mixture of networking funds (from the University of Arctic and a Svalbard Strategic Grant from the Svalbard Science Forum), Arctic Field Grants (from the Research Council of Norway), international cooperation projects (NOR-R-AM and NOR-R-AM2, from the Research Council of Norway, RCN) and UNIS in-kind contributions. The University of Helsinki and the Vilho, Yrjö and Kalle Väisälä Fund of the Finnish Academy of Science and Letters funded a PhD position for Anna Sartell focussed on the HALIP on Svalbard. Carmen Gaina and Grace Shephard acknowledge support from the RCN through its Centers of Excellence funding scheme for Centre for Planetary Habitability, Project Number 332523, the NOR-R-AM2 project 309477, the DYPOLE project 325984, and Young Research Talent scheme for POLARIS— Evolution of the Arctic in Deep Time, Project Number 326238. Sverre Planke and Morgan Jones are supported by the RCN through its PETROMAKS program, project number 336293 (PALMAR). Peter Betlem acknowledges basic funding to NGI from The Research Council of Norway.

Author contributions

Kim Senger – Conceptualization, Writing - Original Draft, Writing - Review & Editing, Visualization, Project administration, Funding acquisition
Fenna Ammerlaan - Writing - Review & Editing

Peter Betlem - Writing - Review & Editing, Visualization
Carmen Gaina – Writing - Original Draft, Writing - Review & Editing, Visualization, Funding acquisition
Olivier Galland – Writing - Review & Editing, Visualization, Funding acquisition
Sten-Andreas Grundvåg – Writing - Original Draft, Writing - Review & Editing, Visualization, Funding acquisition
Rafael Horota - Writing - Review & Editing
Hans Jørgen Kjøll - Writing - Review & Editing
Morgan T. Jones - Writing - Review & Editing
Denise Kulhanek - Writing - Review & Editing
Harmon Maher - Writing - Review & Editing
Krzysztof Michalski - Writing - Original Draft, Funding acquisition
Kei Ogata - Writing - Review & Editing, Visualization
Snorre Olaussen - Writing - Review & Editing, Funding acquisition
Sverre Planke - Writing - Review & Editing
Ole Rabbel - Writing - Review & Editing
Nil Rodes - Writing - Review & Editing
Anna M. R. Sartell - Writing - Original Draft, Writing - Review & Editing, Visualization, Funding acquisition
Grace E. Shephard - Writing - Original Draft, Writing - Review & Editing, Funding acquisition
Aleksandra Smyrak-Sikora - Writing - Review & Editing
Christian Tegner - Writing - Original Draft, Writing - Review & Editing, Visualization

Data availability

This article has relied on using thematic data packages and a selection of digital outrcrop models provided through the Svalbox database.
Thematic data packages:
Senger, K. & Shephard, G. (2023). Arctic Tectonics and Volcanism: a multi-scale, multidisciplinary educational approach (Petrel and GPlates data package) [Dataset]. Zenodo. doi:10.5281/zenodo.10259590.
Senger, K., Ammerlaan, F. & SVALGEOL team. (2024). Geology of Svalbard: Deep-time and Deep-Earth (Digital Appendix to SESS Report Chapter SVALGEOL). Zenodo. doi:10.5281/zenodo.14019367.
Digital outcrop models
Betlem, P., and K. Senger (2022), Svalbox-DOM_2020-0001_Festningen, doi:10.11582/2022.00006.
Rodes, N., A. M. R. Sartell, J. Whattam, E. Lindell, and Svalbox Team (2023), Svalbox-DOM_2023-0023, doi:10.5281/ZENODO.8311422.
Rodes, N., T. Mosociova, A. M. R. Sartell, K. Senger, and Svalbox Team (2024a), Svalbox-DOM_2022-0005, doi:10.5281/ZENODO.11191036.
Rodes, N., K. Senger, T. Mosočiová, A. M. Sartell, and Svalbox Team (2024b), Svalbox-DOM_2022-0027, doi:10.5281/ZENODO.12699304.

Competing interests

The authors declare no competing interests.

Peer review

This publication was peer-reviewed by Enrico Tavarnelli and an annymous reviewer. The full peer-review report can be found here: Review Report.

Copyright notice

References

Aarnes, I., H. Svensen, J. A. D. Connolly, and Y. Y. Podladchikov (2010), How contact metamorphism can trigger global climate changes: Modeling gas generation around igneous sills in sedimentary basins, *Geochimica et cosmochimica acta*, *74*(24), 7179–7195, https://doi.org/10.1016/j.gca.2010.09.011.

Aasebø, U., and K. G. Kjaer (2009), Lead poisoning as possible cause of deaths at the Swedish House at Kapp Thordsen, Spitsbergen, winter 1872-3, *BMJ (Clinical Research Ed.)*, *339*(dec04 1), b5038, https://doi.org/10.1136/bmj.b5038.

Ammerlaan, F., M.-A. Dumais, A. Smyrak-Sikora, A. Ruppel, and K. Senger (2025), Crustal heterogeneity onshore Spitsbergen: Data integration and forward modeling of potential field data, *Geochemistry, Geophysics, Geosystems: G(3)*, *26*(12), https://doi.org/10.1029/2025gc012355.

Amundsen, H. E., A. Evdokimov, V. D. Dibner, and A. Andresen (1998), Geochemistry and petrogenetic significance of Mesozoic magmatism on Franz Josef Land, Northeastern Barents Sea, *In: Solheim, A. , Musatov, E. , Heintz, N. (eds) Geological aspects of Franz Josef Land and the northernmost Barents Sea*, *151*, 105–120.

Andersen, B. O., P. Knudsen, S. Kenyon, and S. Holmes (2014), Global and arctic marine gravity field from recent satellite altimetry (DTU13), in *Proceedings 76th EAGE Conference and Exhibition 2014*, vol. 2014, p. 1–5, EAGE Publications BV, Netherlands, https://doi.org/10.3997/2214-4609.20140897.

Bergh, S. G., A. Braathen, and A. Andresen (1997), Interaction of basement-involved and thin-skinned tectonism in the Tertiary fold-thrust belt of central Spitsbergen, Svalbard, *AAPG Bulletin*, *81*(4), 637–661, https://doi.org/10.1306/522b43f7-1727-11d7-8645000102c1865d.

Berndt, C., S. Planke, C. A. Alvarez Zarikian, J. Frieling, M. T. Jones, J. M. Millett, H. Brinkhuis, S. Bünz, H. H. Svensen, J. Longman, R. P. Scherer, J. Karstens, B. Manton, M. Nelissen, B. Reed, J. I. Faleide, R. S. Huismans, A. Agarwal, G. D. M. Andrews, P. Betlem, J. Bhattacharya, S. Chatterjee, M. Christopoulou, V. J. Clementi, E. C. Ferré, I. Y. Filina, P. Guo, D. T. Harper, S. Lambart, G. Mohn, R. Nakaoka, C. Tegner, N. Varela, M. Wang, W. Xu, and S. L. Yager (2023), Shallow-water hydrothermal venting linked to the Palaeocene–Eocene Thermal Maximum, *Nature Geoscience*, *16*(9), 803–809, https://doi.org/10.1038/s41561-023-01246-8.

Betlem, P., and K. Senger (2022), Svalbox-DOM_2020-0001_Festningen, https://doi.org/10.11582/2022.00006.

Betlem, P., O. Rabbel, I. Lecomte, and K. Senger (2020), Seismic modelling of virtual outcrops: Application of rock physics beyond the borehole, in *Fifth EAGE Workshop on Rock Physics*, European Association of Geoscientists & Engineers, https://doi.org/10.3997/2214-4609.2020603039.

Betlem, P., N. Rodés, T. Birchall, A. Dahlin, A. Smyrak-Sikora, and K. Senger (2023), Svalbox Digital Model Database: A geoscientific window into the High Arctic, *Geosphere*, *19*(6), 1640–1666, https://doi.org/10.1130/ges02606.1.

Black, B. A., R. R. Neely, J.-F. Lamarque, L. T. Elkins-Tanton, J. T. Kiehl, C. A. Shields, M. J. Mills, and C. Bardeen (2018), Systemic swings in end-Permian climate from Siberian Traps carbon and sulfur outgassing, *Nature Geoscience*, *11*(12), 949–954, https://doi.org/10.1038/s41561-018-0261-y.

Bond, D. P. G., and S. E. Grasby (2017), On the causes of mass extinctions, *Palaeogeography, Palaeoclimatology, Palaeoecology*, *478*, 3–29, https://doi.org/10.1016/j.palaeo.2016.11.005.

Bond, D. P. G., P. B. Wignall, M. M. Joachimski, Y. Sun, I. Savov, S. E. Grasby, B. Beauchamp, and D. P. G. Blomeier (2015), An abrupt extinction in the Middle Permian (Capitanian) of the Boreal Realm (Spitsbergen) and its link to anoxia and acidification, *Geological Society of America Bulletin*, *127*(9-10), 1411–1421, https://doi.org/10.1130/b31216.1.

Bown, P. R., J. A. Lees, and J. R. Young (2004), Calcareous nannoplankton evolution and diversity through time, in *Coccolithophores*, edited by H. R. Thierstein and J. R. Young, pp. 481–508, Springer Berlin Heidelberg, Berlin, Heidelberg, https://doi.org/10.1007/978-3-662-06278-4_18.

Braathen, A., S. G. Bergh, and J. Maher (1999), Application of a critical wedge taper model to the Tertiary transpressional fold-thrust belt on Spitsbergen, Svalbard, *Geological Society of America Bulletin*, *111*(10), 1468–1485.

Braathen, A., K. Bælum, H. H. Christiansen, T. Dahl, O. Eiken, H. Elvebakk, F. Hansen, T. H. Hanssen, M. Jochmann, T. A. Johansen, H. Johnsen, L. Larsen, T. Lie, J. Mertes, A. Mørk, M. B. Mørk, W. J. Nemec, S. Olaussen, V. Oye, K. Rød, G. O. Titlestad, J. Tveranger, and K. Vagle (2012), Longyearbyen CO2 lab of Svalbard, Norway – first assessment of the sedimentary succession for CO2 storage, *Norwegian Journal of Geology*, *92*(4), 353–376.

Brekke, T., K. Krajewski, and J. Hubred (2014), Organic geochemistry and petrography of thermally altered sections of the Middle Triassic Botneheia Formation on south-western Edgeøya, Svalbard, *Norwegian Petroleum Directorate Bulletin*, *11*, 111–128, https://doi.org/https://www.npd.no/globalassets/1-npd/publikasjoner/npd-bulletins/npd-bulletin-11-2015.pdf.

Briseid, E., and E. Halvorsen (1974), Primary magnetic remanence dolerite sill from northeast Spitsbergen, *Physics of the Earth and Planetary Interiors*, *9*(1), 45–50.

Brown, P. E., I. Parsons, and S. M. Becker (1987), Peralkaline volcanicity in the Arctic Basin—the Kap Washington Volcanics, petrology and palaeotectonics, *Journal of the Geological Society*, *144*(5), 707–715, https://doi.org/10.1144/gsjgs.144.5.0707.

Bryan, S. E., and R. E. Ernst (2008), Revised definition of Large Igneous Provinces (LIPs), *Earth-Science Reviews*, *86*(1-4), 175–202, https://doi.org/10.1016/j.earscirev.2007.08.008.

Burov, E., L. Guillou-Frottier, E. d'Acremont, L. Le Pourhiet, and S. Cloetingh (2007), Plume head–lithosphere interactions near intra-continental plate boundaries, *Tectonophysics*, *434*(1-4), 15–38, https://doi.org/10.1016/j.tecto.2007.01.002.

Bælum, K., and A. Braathen (2012), Along-strike changes in fault array and rift basin geometry of the Carboniferous Billefjorden Trough, Svalbard, Norway, *Tectonophysics*, *546-547*, 38–55, https://doi.org/10.1016/j.tecto.2012.04.009.

Bédard, J. H., B.-M. Saumur, M.-C. Williamson, C. Tegner, V. R. Troll, F. M. Deegan, C. A. Evenchick, S. E. Grasby, and K. Dewing (2020), Geochemical database of Cretaceous High Arctic Large Igneous Province magmatic rocks, Arctic Canada, *Tech. Rep. Open File, 8759, 7*, Geological Survey of Canada.

Bédard, J. H., B. M. Saumur, C. Tegner, V. R. Troll, F. M. Deegan, C. A. Evenchick, S. E. Grasby, and K. Dewing (2021a), Geochemical systematics of high arctic large igneous province continental tholeiites from Canada—evidence for progressive crustal contamination in the plumbing system, *Journal of Petrology*, *62*(9), egab041, https://doi.org/10.1093/petrology/egab041.

Bédard, J. H., V. R. Troll, F. M. Deegan, C. Tegner, B. M. Saumur, C. A. Evenchick, S. E. Grasby, and K. Dewing (2021b), High arctic large igneous province alkaline rocks in Canada: Evidence for multiple mantle components, *Journal of Petrology*, *62*(9), egab042, https://doi.org/10.1093/petrology/egab042.

Chernykh, A., V. Glebovsky, M. Zykov, and M. Korneva (2018), New insights into tectonics and evolution of the Amerasia Basin, *Journal of Geodynamics*, *119*, 167–182, https://doi.org/10.1016/j.jog.2018.02.010.

Chian, D., H. R. Jackson, D. R. Hutchinson, J. W. Shimeld, G. N. Oakey, N. Lebedeva-Ivanova, Q. Li, R. W. Saltus, and D. C. Mosher (2016), Distribution of crustal types in Canada Basin, Arctic Ocean, *Tectonophysics*, *691*, 8–30, https://doi.org/10.1016/j.tecto.2016.01.038.

Coakley, B., K. Brumley, N. Lebedeva-Ivanova, and D. Mosher (2016), Exploring the geology of the central Arctic Ocean; understanding the basin features in place and time, *Journal of the Geological Society*, *173*(6), 967–987, https://doi.org/10.1144/jgs2016-082.

Corfu, F., S. Polteau, S. Planke, J. I. Faleide, H. Svensen, A. Zayoncheck, and N. Stolbov (2013), U–Pb geochronology of Cretaceous magmatism on Svalbard and Franz Josef Land, Barents Sea Large Igneous Province, *Geological Magazine*, *150*(6), 1127–1135, https://doi.org/10.1017/s0016756813000162.

Dallmann, W., and Norwegian Polar Institute (2014), Geological map of Svalbard (1:750000), https://doi.org/10.21334/NPOLAR.2014.09DBE7B2.

Dallmann, W. K. (2015), *Geoscience atlas of Svalbard*, Norsk polarinstituttt, Norway.

Dallmann, W. K., H. Dypvik, J. G. Gjelberg, W. B. Harland, E. P. Johannessen, H. B. Keilen, G. B. Larssen, Lønøy, P. S. Midbøe, Mørk, J. Nagy, I. Nilsson, Nøttvedt, S. Olaussen, T. M. Pcelina, R. J. Steel, and D. Worsley (1999), Lithostratigraphic Lexicon Svalbard: Review recommendations nomenclature use, *Norsk Polarinstitutt*.

Dam, G., M. Larsen, and M. Sønderholm (1998), Sedimentary response to mantle plumes: Implications from Paleocene onshore successions, West and East Greenland, *Geology*, *26*(3), 207, https://doi.org/10.1130/0091-7613(1998)026<0207:srtmpi>2.3.co;2.

Davis, W. J., C. J. Schröder-Adams, J. M. Galloway, J. O. Herrle, and A. T. Pugh (2017), U–Pb geochronology of bentonites from the Upper Cretaceous Kanguk Formation, Sverdrup Basin, Arctic Canada: constraints on sedimentation rates, biostratigraphic correlations and the late magmatic history of the High Arctic Large Igneous Province, *Geological Magazine*, *154*(4), 757–776, https://doi.org/10.1017/s0016756816000376.

Deegan, F. M., V. Pease, I. G. Nobre Silva, J. H. Bédard, and G. Morris (2023), Age and geochemistry of high Arctic large igneous province tholeiitic magmatism in NW Axel Heiberg Island, Canada, *Geochemistry, Geophysics, Geosystems: G(3)*, *24*(11), e2023GC011,083, https://doi.org/10.1029/2023gc011083.

Dockman, D. M., D. G. Pearson, L. M. Heaman, S. A. Gibson, and C. Sarkar (2018), Timing and origin of magmatism in the Sverdrup Basin, Northern Canada—Implications for lithospheric evolution in the High Arctic Large Igneous Province (HALIP), *Tectonophysics*, *742-743*, 50–65, https://doi.org/10.1016/j.tecto.2018.05.010.

Dockman, D. M., T. Hadlari, D. G. Pearson, L. M. Heaman, C. Sarkar, and K. Dewing (2025), U-Pb geochronology and Lu-Hf isotopic characterization of the Canadian high arctic large igneous province (HALIP): Comparison to oceanic plateau magmatism, *Geochemistry, Geophysics, Geosystems: G(3)*, *26*(2), e2024GC011,762, https://doi.org/10.1029/2024gc011762.

Dostal, J., and A. MacRae (2018), Cretaceous basalts of the High Arctic large igneous province at Axel Heiberg Island (Canada): Volcanic stratigraphy, geodynamic setting, and origin, *Geological Journal*, *53*(6), 2918–2934, https://doi.org/10.1002/gj.3132.

Dypvik, H., E. Håkansson, and C. Heinberg (2002), Jurassic and Cretaceous palaeogeography and stratigraphic comparisons in the North Greenland-Svalbard region, *Polar Research*, *21*(1), 91–108, https://doi.org/10.3402/polar.v21i1.6476.

Dörr, N., F. Lisker, P. D. Clift, A. Carter, D. G. Gee, A. M. Tebenkov, and C. Spiegel (2012), Late Mesozoic–Cenozoic exhumation history of northern Svalbard and its regional significance: Constraints from apatite fission track analysis, *Tectonophysics*, *514-517*, 81–92, https://doi.org/10.1016/j.tecto.2011.10.007.

Døssing, A., H. R. Jackson, J. Matzka, I. Einarsson, T. M. Rasmussen, A. V. Olesen, and J. M. Brozena (2013), On the origin of the Amerasia Basin and the High Arctic Large Igneous Province—Results of new aeromagnetic data, *Earth and Planetary Science Letters*, *363*, 219–230, https://doi.org/10.1016/j.epsl.2012.12.013.

Døssing, A., C. Gaina, and J. M. Brozena (2017), Building and breaking a large igneous province: An example from the High Arctic: Building and Breaking a LIP, *Geophysical Research Letters*, *44*(12), 6011–6019, https://doi.org/10.1002/2016gl072420.

Døssing, A., C. Gaina, H. R. Jackson, and O. B. Andersen (2020), Cretaceous ocean formation in the High Arctic, *Earth and Planetary Science Letters*, *551*(116552), 116,552, https://doi.org/10.1016/j.epsl.2020.116552.

Edwards, M. B. (1979), Sandstone in lower Cretaceous helvetiafjellet formation, Svalbard: Bearing on reservoir potential of Barents Shelf, *AAPG Bulletin*, *63*(12), 2193–2203, https://doi.org/10.1306/2f918905-16ce-11d7-8645000102c1865d.

Embry, A., and B. Beauchamp (2019), Sverdrup Basin, in *The Sedimentary Basins of the United States and Canada*, edited by A. D. Miall, pp. 559–592, Elsevier, https://doi.org/10.1016/b978-0-444-63895-3.00014-0.

Ernst, R. E., and S. M. Jowitt (2013), Large Igneous Provinces (LIPs) and Metallogeny, in *Tectonics, Metallogeny, and Discovery*, edited by M. Colpron, T. Bissig, B. G. Rusk, and J. F. H. Thompson, pp. 17–51, Society of Economic Geologists, https://doi.org/10.5382/sp.17.02.

Ernst, R. E., and N. Youbi (2017), How Large Igneous Provinces affect global climate, sometimes cause mass extinctions, and represent natural markers in the geological record, *Palaeogeography, Palaeoclimatology, Palaeoecology*, *478*, 30–52, https://doi.org/10.1016/j.palaeo.2017.03.014.

Estrada, S. (2000), Basaltic dykes in the Kap Washington and frigg fjord areas (north Greenland), *Polarforschung*, *68*, 19–23, https://doi.org/10.2312/POLARFORSCHUNG.68.19.

Estrada, S. (2015), Geochemical and Sr–Nd isotope variations within Cretaceous continental flood-basalt suites of the Canadian High Arctic, with a focus on the Hassel Formation basalts of northeast Ellesmere Island, *International Journal of Earth Sciences*, *104*(8), 1981–2005, https://doi.org/10.1007/s00531-014-1066-x.

Estrada, S., and F. Henjes-Kunst (2004), Volcanism in the Canadian High Arctic related to the opening of the Arctic Ocean, *Zeitschrift der Deutschen Geologischen Gesellschaft*, *154*(4), 579–603, https://doi.org/10.1127/zdgg/154/2004/579.

Estrada, S., and K. Piepjohn (2019), Early Cretaceous magmatism and post-Early Cretaceous deformation on

Ellef Ringnes Island, Canadian High Arctic, related to the formation of the Arctic Ocean, in *Circum-Arctic Structural Events: Tectonic Evolution of the Arctic Margins and Trans-Arctic Links with Adjacent Orogens*, vol. 541, pp. 303–323, Geological Society of America, https://doi.org/10.1130/2018.2541(15).

Estrada, S., A. Höhndorf, and F. Henjes-Kunst (2001), Cretaceous/tertiary volcanism in north Greenland: The Kap Washington group, *Polarforschung*, *69*, 17–23, https://doi.org/10.2312/polarforschung.69.17.

Estrada, S., K. Piepjohn, F. Henjes-Kunst, and W. Gosen (2006), Geology, magmatism and structural evolution of the Yelverton bay area, northern Ellesmere island, arctic Canada, *Polarforschung*, *73*, 59–75.

Estrada, S., F. Henjes-Kunst, F. Melcher, and F. Tessensohn (2010), Paleocene alkaline volcanism in the Nares Strait region: evidence from volcanic pebbles, *International Journal of Earth Sciences*, *99*(4), 863–890, https://doi.org/10.1007/s00531-009-0432-6.

Estrada, S., D. Damaske, F. Henjes-Kunst, B. Schreckenberger, G. N. Oakey, K. Piepjohn, K. Eckelmann, and U. Linnemann (2016), Multistage Cretaceous magmatism in the northern coastal region of Ellesmere Island and its relation to the formation of Alpha Ridge – evidence from aeromagnetic, geochemical and geochronological data, *Norwegian Journal of Geology*, *96*(2), 65–95, https://doi.org/10.17850/njg96-2-03.

Evenchick, C. A., W. J. Davis, J. H. Bédard, N. Hayward, and R. M. Friedman (2015), Evidence for protracted High Arctic large igneous province magmatism in the central Sverdrup Basin from stratigraphy, geochronology, and paleodepths of saucer-shaped sills, *Geological Society of America Bulletin*, *127*(9-10), 1366–1390, https://doi.org/10.1130/b31190.1.

Evenchick, C. A., J. M. Galloway, B. M. Saumur, and W. J. Davis (2019), A revised stratigraphic framework for Cretaceous sedimentary and igneous rocks at Mokka Fiord, Axel Heiberg Island, Nunavut, with implications for the Cretaceous Normal Superchron, *Canadian Journal of Earth Sciences*, *56*(2), 158–174, https://doi.org/10.1139/cjes-2018-0129.

Faleide, T. S., I. Midtkandal, S. Planke, R. Corseri, J. I. Faleide, C. S. Serck, and J. P. Nystuen (2019), Characterisation and development of Early Cretaceous shelf platform deposition and faulting in the Hoop area, southwestern Barents Sea—constrained by high-resolution seismic data, *Norwegian Journal of Geology*, *99*(3), 1–20, https://doi.org/10.17850/njg99-3-7.

Frieling, J., H. H. Svensen, S. Planke, M. J. Cramwinckel, H. Selnes, and A. Sluijs (2016), Thermogenic methane release as a cause for the long duration of the PETM, *Proceedings of the National Academy of Sciences of the United States of America*, *113*(43), 12,059–12,064, https://doi.org/10.1073/pnas.1603348113.

Funck, T., H. R. Jackson, and J. Shimeld (2011), The crustal structure of the Alpha Ridge at the transition to the Canadian Polar Margin: Results from a seismic refraction experiment, *Journal of Geophysical Research*, *116*(B12), https://doi.org/10.1029/2011jb008411.

Gaina, C., S. C. Werner, R. Saltus, S. Maus, and the CAMP-GM GROUP (2011), Chapter 3 Circum-Arctic mapping project: new magnetic and gravity anomaly maps of the Arctic, *Geological Society London Memoirs*, *35*(1), 39–48, https://doi.org/10.1144/m35.3.

Gaina, C., M. Jakobsson, E. O. Straume, M.-L. Timmermans, K. Boggild, S. Bünz, V. Schlindwein, and A. Døssing (2025), Arctic Ocean bathymetry and its connections to tectonics, oceanography and climate, *Nature Reviews. Earth & Environment*, *6*(3), 211–227, https://doi.org/10.1038/s43017-025-00647-0.

Galland, O., A. M. R. Sartell, R. K. Horota, H. J. Kjøll, J. J. S. Runge, I. Midtkandal, and K. Senger (2025), Stratigraphic influence on emplacement and 3-dimensional structure of a large mafic sill in sedimentary strata, *Basin Research*, *37*(4), https://doi.org/10.1111/bre.70047.

Galloway, J. M., R. A. Fensome, G. T. Swindles, T. Hadlari, J. Fath, C. Schröder-Adams, J. O. Herrle, and A. Pugh (2022), Exploring the role of High Arctic Large Igneous Province volcanism on Early Cretaceous Arctic forests, *Cretaceous Research*, *129*(105022), 105,022, https://doi.org/10.1016/j.cretres.2021.105022.

Glebovsky, V. Y., V. D. Kaminsky, A. N. Minakov, S. A. Merkur'ev, V. A. Childers, and J. M. Brozena (2006), Formation of the Eurasia Basin in the Arctic Ocean as inferred from geohistorical analysis of the anomalous magnetic field, *Geotectonics*, *40*(4), 263–281, https://doi.org/10.1134/s0016852106040029.

Grantz, A., D. L. Clark, R. L. Phillips, S. P. Srivastava, C. D. Blome, L. B. Gray, H. Haga, B. L. Mamet, D. J. McIntyre, D. H. McNeil, M. B. Mickey, M. W. Mullen, B. I. Murchey, C. A. Ross, C. H. Stevens, N. J. Silberling, J. H. Wall, and D. A. Willard (1998), Phanerozoic stratigraphy of Northwind Ridge, magnetic anomalies in the Canada basin, and the geometry and timing of rifting in the Amerasia basin, Arctic Ocean, *Geological Society of America Bulletin*, *110*(6), 801–820, https://doi.org/10.1130/0016-7606(1998)110<0801:psonrm>2.3.co;2.

Grantz, A., P. E. Hart, and V. A. Childers (2011), Chapter 50 Geology and tectonic development of the Amerasia and Canada Basins, Arctic Ocean, *Geological Society London Memoirs*, *35*(1), 771–799, https://doi.org/10.1144/m35.50.

Grasby, S. E., B. Beauchamp, D. P. G. Bond, P. Wignall, C. Talavera, J. M. Galloway, K. Piepjohn, L. Reinhardt, and D. Blomeier (2015), Progressive environmental deterioration in northwestern Pangea leading to the latest Permian extinction, *Geological Society of America Bulletin*, *127*(9-10), 1331–1347, https://doi.org/10.1130/b31197.1.

Grogan, P., K. Nyberg, B. Fotland, R. Myklebust, S. Dahlgren, and F. Riis (2000), Cretaceous Magmatism South and East ofSvalbard: Evidence from Seismic Reflection and Magnetic Data, *Polarforschung*, *68*, 25–34.

Grundvåg, S.-A., and S. Olaussen (2017), Sedimentology of the Lower Cretaceous at Kikutodden and Keilhaufjellet, southern Spitsbergen: implications for an onshore–offshore link, *Polar Research*, *36*(1), 1302,124, https://doi.org/10.1080/17518369.2017.1302124.

Grundvåg, S.-A., D. Marin, B. Kairanov, K. K. Śliwińska, H. Nøhr-Hansen, M. E. Jelby, A. Escalona, and S. Olaussen (2017), The Lower Cretaceous succession of the northwestern Barents Shelf: Onshore and offshore correlations, *Marine and Petroleum Geology*, *86*, 834–857, https://doi.org/10.1016/j.marpetgeo.2017.06.036.

Grundvåg, S.-A., M. E. Jelby, K. K. Sliwinska, H. Nøhr-Hansen, T. Aadland, S. E. Sandvik, I. Tennvassås, T. Engen, and S. Olaussen (2019), Sedimentology and palynology of the Lower Cretaceous succession of central Spitsbergen: integration of subsurface and outcrop data, *Norwegian Journal of Geology*, *99*(2), 247–277, https://doi.org/10.17850/njg006.

Grundvåg, S.-A., M. E. Jelby, S. Olaussen, and K. K. Śliwińska (2021), The role of shelf morphology on storm-bed variability and stratigraphic architecture, Lower Cretaceous, Svalbard, *Sedimentology*, *68*(1), 196–237, https://doi.org/10.1111/sed.12791.

Hadlari, T. (2024), Rift to post-rift tectonostratigraphy of the Sverdrup Basin in relation to onset of the High Arctic Large Igneous Province (HALIP) in the early Cretaceous, arctic Canada, *Geochemistry, Geophysics, Geosystems: G(3)*, *25*(7), e2023GC011,411, https://doi.org/10.1029/2023gc011411.

Hadlari, T., D. Midwinter, J. M. Galloway, K. Dewing, and A. M. Durbano (2016), Mesozoic rift to post-rift tectonostratigraphy of the Sverdrup Basin, Canadian Arctic, *Marine and Petroleum Geology*, *76*, 148–158, https://doi.org/10.1016/j.marpetgeo.2016.05.008.

Hagevold, S. (2019), From outcrop to synthetic seismic: 2D and 3D modelling of igneous intrusions at Botneheia, central Spitsbergen, Master's thesis, University of Bergen, Bergen, Norway.

Halvorsen, E. (1989), A paleomagnetic pole position of Late Jurassic/Early Cretaceous dolerites from Hinlopenstretet, Svalbard, and its tectonic implications, *Earth and Planetary Science Letters*, *94*(3-4), 398–408, https://doi.org/10.1016/0012-821x(89)90156-8.

Harland, W. B. (1997), *The Geology Of Svalbard*, vol. 17, Geological Society, Bath, England.

He, B., Y.-G. Xu, S.-L. Chung, L. Xiao, and Y. Wang (2003), Sedimentary evidence for a rapid, kilometer-scale crustal doming prior to the eruption of the Emeishan flood basalts, *Earth and Planetary Science Letters*, *213*(3-4), 391–405, https://doi.org/10.1016/s0012-821x(03)00323-6.

Heimdal, T. H., M. T. Jones, and H. H. Svensen (2020), Thermogenic carbon release from the Central Atlantic magmatic province caused major end-Triassic carbon cycle perturbations, *Proceedings of the National Academy of Sciences of the United States of America*, *117*(22), 11,968–11,974, https://doi.org/10.1073/pnas.2000095117.

Heimdal, T. H., Y. Godderis, M. T. Jones, and H. H. Svensen (2021), Assessing the importance of thermogenic degassing from the Karoo Large Igneous Province (LIP) in driving Toarcian carbon cycle perturbations, *Nature Communications*, *12*(1), 6221, https://doi.org/10.1038/s41467-021-26467-6.

Helland-Hansen, W., and S.-A. Grundvåg (2021), The Svalbard Eocene-Oligocene (?) Central Basin succession: Sedimentation patterns and controls, *Basin Research*, *33*(1), 729–753, https://doi.org/10.1111/bre.12492.

Herrle, J. O., C. J. Schröder-Adams, W. Davis, A. T. Pugh, J. M. Galloway, and J. Fath (2015), Mid-Cretaceous High Arctic stratigraphy, climate, and Oceanic Anoxic Events, *Geology*, *43*(5), 403–406, https://doi.org/10.1130/g36439.1.

Heyn, B. H., G. E. Shephard, and C. P. Conrad (2024), Prolonged multi-phase magmatism due to plume-lithosphere interaction as applied to the High Arctic Large Igneous Province, *Geochemistry, Geophysics, Geosystems: G(3)*, *25*(6), e2023GC011,380, https://doi.org/10.1029/2023gc011380.

Horota, R. K., K. Senger, N. Rodes, P. Betlem, A. Smyrak-Sikora, M. O. Jonassen, D. Kramer, and A. Braathen (2023), West Spitsbergen fold and thrust belt: A digital educational data package for teaching structural geology, *Journal of Structural Geology*, *167*(104781), 104,781, https://doi.org/10.1016/j.jsg.2022.104781.

Hovikoski, J., G. K. Pedersen, P. Alsen, K. Svennevig, H. N. Hansen, E. Sheldon, K. Dybkjær, J. B. Koefoed, M. Bjerager, J. Ineson, B. W. Lauridsen, and S. Piasecki (2018), The Jurassic–Cretaceous lithostratigraphy of Kilen, Kronprins Christian Land, eastern North Greenland, *Bulletin of the Geological Society of Denmark*, *66*, 61–112, https://doi.org/10.37570/bgsd-2018-66-04.

Hubred, J. H. (2006), Thermal Effects of Basaltic Sill Emplacement in Source Rocks on Maturation and Hydrocarbon Generation, Master's thesis, University of Oslo, Oslo, Norway.

Hutchinson, D. R., H. R. Jackson, D. W. Houseknecht, Q. Li, J. W. Shimeld, D. C. Mosher, D. Chian, R. W. Saltus, and G. N. Oakey (2017), Significance of northeast-trending features in Canada Basin, arctic ocean: Canada basin northeast-trending features, *Geochemistry, Geophysics, Geosystems: G(3)*, *18*(11), 4156–4178, https://doi.org/10.1002/2017gc007099.

Hutchinson, D. R., D. W. Houseknecht, and D. C. Mosher (2025), Canada Basin Tectono-Sedimentary Element, arctic ocean, *Geological Society London Memoirs*, *57*(1), 1016–1028, https://doi.org/10.1144/m57-2022-49.

Ineson, J. R., J. Hovikoski, E. Sheldon, S. Piasecki, P. Alsen, M. B. W. Fyhn, M. Bjerager, K. Dybkjær, P. Guarnieri, B. W. Lauridsen, H. Nøhr-Hansen, G. K. Pedersen, K. Svennevig, J. Therkelsen, R. Weibel, and J. A. Bojesen-Koefoed (2021), Regional impact of Early Cretaceous tectono-magmatic uplift in the Arctic: Implications of new data from eastern North Greenland, *Terra nova*, *33*(3), 284–292, https://doi.org/10.1111/ter.12514.

Jelby, M. E., S.-A. Grundvåg, W. Helland-Hansen, S. Olaussen, and L. Stemmerik (2020), Tempestite facies variability and storm-depositional processes across a wide ramp: Towards a polygenetic model for hummocky cross-stratification, *Sedimentology*, *67*(2), 742–781, https://doi.org/10.1111/sed.12671.

Jelby, M. E., S.-A. Grundvåg, K. K. Śliwińska, P. Alsen, M. L. Vickers, S. Olaussen, and L. Stemmerik (2025), Lower Cretaceous holostratigraphy in Svalbard: the Arctic key piece of the Boreal basin puzzle, *Geological Society Special Publication*, *545*(1), 325–371, https://doi.org/10.1144/sp545-2023-177.

Johansen, S. E., S. Kibsgaard, A. Andresen, T. Henningsen, and J. R. Granli (1994), Seismic modeling of a strongly emergent thrust front, West Spitsbergen fold belt, Svalbard, *AAPG Bulletin*, *78*(7), 1018–1027, https://doi.org/10.1306/a25fe419-171b-11d7-8645000102c1865d.

Jones, M. T., D. A. Jerram, H. H. Svensen, and C. Grove (2016), The effects of large igneous provinces on the global carbon and sulphur cycles, *Palaeogeography, Palaeoclimatology, Palaeoecology*, *441*, 4–21, https://doi.org/10.1016/j.palaeo.2015.06.042.

Jowitt, S. M., M.-C. Williamson, and R. E. Ernst (2014), Geochemistry of the 130 to 80 ma Canadian high arctic large igneous province (HALIP) event and implications for Ni-cu-PGE prospectivity, *Economic Geology and the Bulletin of the Society of Economic Geologists*, *109*(2), 281–307, https://doi.org/10.2113/econgeo.109.2.281.

Kingsbury, C. G., R. E. Ernst, B. L. Cousens, and M.-C. Williamson (2016), The High Arctic LIP in Canada: Trace element and Sm–Nd isotopic evidence for the role of mantle heterogeneity and crustal assimilation, *Norwegian Journal of Geology*, *96*(2), 97–117, https://doi.org/10.17850/njg96-2-02.

Kingsbury, C. G., S. L. Kamo, R. E. Ernst, U. Söderlund, and B. L. Cousens (2018), U-Pb geochronology of the plumbing system associated with the Late Cretaceous Strand Fiord Formation, Axel Heiberg Island, Canada: part of the 130-90 Ma High Arctic large igneous province, *Journal of Geodynamics*, *118*, 106–117, https://doi.org/10.1016/j.jog.2017.11.001.

Kjoberg, S., T. Schmiedel, S. Planke, H. H. Svensen, J. M. Millett, D. A. Jerram, O. Galland, I. Lecomte, N. Schofield, O. T. Haug, and A. Helsem (2017), 3D structure and formation of hydrothermal vent complexes at the Paleocene-Eocene transition, the Møre Basin, mid-Norwegian margin, *Interpretation*, *5*(3), SK65–SK81, https://doi.org/10.1190/int-2016-0159.1.

Koevoets, M. J., O. Hammer, S. Olaussen, K. Senger, and M. Smelror (2019), Integrating subsurface and outcrop data of the Middle Jurassic to Lower Cretaceous Agardhfjellet Formation in central Spitsbergen, *Norwegian Journal of Geology*, https://doi.org/10.17850/njg98-4-01.

Kontak, D. J., S. M. Jensen, J. Dostal, D. A. Archibald, and T. K. Kyser (2001), Cretaceous mafic dyke swarm, Peary land, northernmost Greenland: Geochronology and petrology, *The Canadian Mineralogist*, *39*(4), 997–1020, https://doi.org/10.2113/gscanmin.39.4.997.

Korago, E. A., A. N. Evdokimov, and N. M. Stolbov (2010), Late Mesozoic and Cenozoic magmatism of the north-western Eurasian continental margin, *Transaction of All-Russia Research Institute for geology and mineral resources of the World ocean*, *215*, 1–174.

Krumsiek, K., and E. M. Nagel (1968), Record palaeomagnetic measurements some igneous rocks from Isfjorden region, in *Norsk Polarinstitutt Årbok*, pp. 76–83, Norsk polarinstitutt, Spitsbergen, Norway.

Larsen, T. (2010), Fractured carbonates Mediumfjellet thrust-stack Tertiary fold-and-thrust belt Spitsbergen, Master's thesis, University of Tromsø, Tromsø, Norway.

Le Bas, M. J. L., R. W. L. Le Maitre, A. Streckeisen, B. Zanettin, and IUGS Subcommission on the Systematics of Igneous Rocks (1986), A chemical classification of volcanic rocks based on the total alkali-silica diagram, *Journal of Petrology*, *27*(3), 745–750, https://doi.org/10.1093/petrology/27.3.745.

Leszczyński, S., M. J. Warchoł, and W. Nemec (2023), Sedimentary deposits and bioturbation in an Early Cretaceous subarctic stormy greenhouse shelf environment, *Environmental Earth Sciences*, *82*(7), https://doi.org/10.1007/s12665-023-10841-2.

Magee, C., C. A.-L. Jackson, and N. Schofield (2014), Diachronous sub-volcanic intrusion along deep-water margins: insights from the Irish Rockall Basin, *Basin Research*, *26*(1), 85–105, https://doi.org/10.1111/bre.12044.

Maher, H., K. Senger, A. Braathen, M. J. Mulrooney, A. Smyrak-Sikora, P. T. Osmundsen, and K. Ogata (2020), Mesozoic-Cenozoic regional stress field evolution in Svalbard, *Tectonics*, *39*(4), https://doi.org/10.1029/2018tc005461.

Maher, H. D., T. Hays, R. Shuster, and J. Mutrux (2004), Petrography of lower cretaceous sandstones on Spitsbergen, *Polar Research*, *23*(2), 147–165, https://doi.org/10.1111/j.1751-8369.2004.tb00005.x.

Maher, H. D., Jr (2001), Manifestations of the cretaceous high arctic large igneous province in Svalbard, *The Journal of Geology*, *109*(1), 91–104, https://doi.org/10.1086/317960.

Malinen, L. (2024), The magmatic evolution of igneous intrusions in Grønsteinfjellet-Botneheia, Svalbard, Ph.D. thesis, University of Helsinki, Helsinki, Finland.

Midtkandal, I., H. H. Svensen, S. Planke, F. Corfu, S. Polteau, T. H. Torsvik, J. I. Faleide, S.-A. Grundvåg, H. Selnes, W. Kürschner, and S. Olaussen (2016), The Aptian (Early Cretaceous) oceanic anoxic event (OAE1a) in Svalbard, Barents Sea, and the absolute age of the Barremian-Aptian boundary, *Palaeogeography, Palaeoclimatology, Palaeoecology*, *463*, 126–135, https://doi.org/10.1016/j.palaeo.2016.09.023.

Midtkandal, I., J. I. Faleide, T. S. Faleide, C. S. Serck, S. Planke, R. Corseri, M. Dimitriou, and J. P. Nystuen (2020a), Lower Cretaceous Barents Sea strata: epicontinental basin configuration, timing, correlation and depositional dynamics, *Geological Magazine*, *157*(3), 458–476, https://doi.org/10.1017/s0016756819000918.

Midtkandal, I., T. S. Faleide, J. I. Faleide, S. Planke, I. Anell, and J. P. Nystuen (2020b), Nested intrashelf platform clinoforms—Evidence of shelf platform growth exemplified by Lower Cretaceous strata in the Barents Sea, *Basin Research*, *32*(2), 216–223, https://doi.org/10.1111/bre.12377.

Miller, E. L., K. E. Meisling, V. V. Akinin, K. Brumley, B. J. Coakley, E. S. Gottlieb, C. W. Hoiland, T. M. O'Brien, A. Soboleva, and J. Toro (2018), Circum-Arctic Lithosphere Evolution (CALE) Transect C: displacement of the Arctic Alaska–Chukotka microplate towards the Pacific during opening of the Amerasia Basin of the Arctic, *Geological Society Special Publication*, *460*(1), 57–120, https://doi.org/10.1144/sp460.9.

Minakov, A., R. Mjelde, J. I. Faleide, E. R. Flueh, A. Dannowski, and H. Keers (2012), Mafic intrusions east of Svalbard imaged by active-source seismic tomography, *Tectonophysics*, *518-521*, 106–118, https://doi.org/10.1016/j.tecto.2011.11.015.

Minakov, A., V. Yarushina, J. I. Faleide, N. Krupnova, T. Sakoulina, N. Dergunov, and V. Glebovsky (2018), Dyke emplacement and crustal structure within a continental large igneous province, northern Barents Sea, *Geological Society Special Publication*, *460*(1), 371–395, https://doi.org/10.1144/sp460.4.

Molenaar, C. (1983), Depositional relations of Cretaceous and lower Tertiary rocks, northeastern Alaska, *AAPG Bulletin*, *67*, 1066–1080, https://doi.org/10.1306/03B5B6FF-16D1-11D7-8645000102C1865D.

Mukasa, S. B., A. Andronikov, K. Brumley, L. A. Mayer, and A. Armstrong (2020), Basalts from the Chukchi borderland: 40 Ar/ 39 Ar ages and geochemistry of submarine intraplate lavas dredged from the western arctic ocean, *Journal of Geophysical Research. Solid Earth*, *125*(7), https://doi.org/10.1029/2019jb017604.

Mørk, A., and S.-A. Grundvåg (2020), Festningen - A 300-million-year journey through shoreline exposures of the Carboniferous and Mesozoic in 7 kilometers, *Tech. rep.*, Geological Society of Norway (NGF).

Naber, T. V., S. E. Grasby, J. P. Cuthbertson, N. Rayner, and C. Tegner (2020), New constraints on the age, geochemistry, and environmental impact of High Arctic Large Igneous Province magmatism: Tracing the extension of the Alpha Ridge onto Ellesmere Island, Canada, *Geological Society of America Bulletin*, *133*(7-8), 1695–1711, https://doi.org/10.1130/b35792.1.

Nejbert, K., K. P. Krajewski, E. Dubinska, and Z. Pécskay (2011), Dolerites of Svalbard, north-west Barents Sea Shelf: age, tectonic setting and significance for geotectonic interpretation of the High-Arctic Large Igneous Province, *Polar Research*, *30*(1), 7306, https://doi.org/10.3402/polar.v30i0.7306.

Nikishin, A. M., C. Gaina, E. I. Petrov, N. A. Malyshev, and S. I. Freiman (2018), Eurasia Basin and Gakkel Ridge, Arctic Ocean: Crustal asymmetry, ultra-slow spreading and continental rifting revealed by new seismic data, *Tectonophysics*, *746*, 64–82, https://doi.org/10.1016/j.tecto.2017.09.006.

Nikishin, A. M., G. R. Foulger, V. V. Akinin, E. A. Rodina, H. W. Posamentier, and K. F. Aleshina (2024), Arctic cretaceous tectonic and igneous mega-province (TIMP): Regional domains and geodynamics, *Journal of Geodynamics*, *160*(102031), 102,031, https://doi.org/10.1016/j.jog.2024.102031.

Norwegian Polar Institute (2025), Geological map of Svalbard 1:100 000 (S100 Geological Map Data), https://doi.org/10.21334/NPOLAR.2025.509227A0.

Ntaflos, T., and W. Richter (2003), Geochemical constraints on the origin of the Continental Flood Basalt magmatism in Franz Josef Land, Arctic Russia, *European Journal of Mineralogy*, *15*(4), 649–663, https://doi.org/10.1127/0935-1221/2003/0015-0649.

Oakey, G. N., and R. W. Saltus (2016), Geophysical analysis of the Alpha–Mendeleev ridge complex: Characterization of the High Arctic Large Igneous Province, *Tectonophysics*, *691*, 65–84, https://doi.org/10.1016/j.tecto.2016.08.005.

Odlum, M., O. A. Anfinson, E. M. Poulaki, G. E. Shephard, D. F. Stockli, and C. Gaina (2019), Thermal record of deformation, exhumation, and fluid-rock interactions along the Billefjorden Fault Zone, Pyramiden, Svalbard, in *Chapman Conference on Large-scale Volcanism in the Arctic: The Role of the Mantle and Tectonics*, AGU.

Ogata, K., K. Senger, A. Braathen, J. Tveranger, and S. Olaussen (2014), Fracture systems and mesoscale structural patterns in the siliciclastic mesozoic reservoir-caprock succession of the longyearbyen CO2 lab project: Implications for geological CO2 sequestration in central spitsbergen, svalbard, *Norwegian Journal of Geology*, *94*, 121–154.

Olaussen, S., G. B. Larssen, W. Helland-Hansen, E. P. Johannessen, A. Nøttvedt, F. Riis, B. Rismyhr, M. Smelror, and D. Worsley (2019), Mesozoic strata of Kong Karls Land, Svalbard, Norway; a link to the northern Barents Sea basins and platforms, *Norwegian Journal of Geology*, *98*(4), 1–69, https://doi.org/10.17850/njg98-4-06.

Olaussen, S., S.-A. Grundvåg, K. Senger, I. Anell, P. Betlem, T. Birchall, A. Braathen, W. Dallmann, M. Jochmann, E. P. Johannessen, G. Lord, A. Mørk, P. T. Osmundsen, A. Smyrak-Sikora, and L. Stemmerik (2025), Svalbard Composite Tectono-Sedimentary Element, Barents Sea, *Geological Society London Memoirs*, *57*(1), 472–495, https://doi.org/10.1144/m57-2021-36.

Olesen, O., M. Brönner, J. Ebbing, J. Gellein, L. Gernigon, J. Koziel, T. Lauritsen, R. Myklebust, C. Pascal, M. Sand, D. Solheim, and S. Usov (2010), New aeromagnetic and gravity compilations from Norway and adjacent areas: methods and applications, *Geological Society London Petroleum Geology Conference Series*, *7*(1), 559–586, https://doi.org/10.1144/0070559.

Osadetz, K. G., and P. R. Moore (1988), Basic volcanics in the Hassel formation [Mid-Cretaceous] and associated intrusives, Ellesmere Island, district of Franklin, Northwest Territories, *Tech. Rep. M44-87/21E*, Geological Survey of Canada.

Percival, L. M. E., L. R. Tedeschi, R. A. Creaser, C. Bottini, E. Erba, F. Giraud, H. Svensen, J. Savian, R. Trindade, R. Coccioni, F. Frontalini, L. Jovane, T. A. Mather, and H. C. Jenkyns (2021), Determining the style and provenance of magmatic activity during the Early Aptian Oceanic Anoxic Event (OAE 1a), *Global and Planetary Change*, *200*(103461), 103,461, https://doi.org/10.1016/j.gloplacha.2021.103461.

Piepjohn, K., W. von Gosen, and F. Tessensohn (2016), The Eurekan deformation in the Arctic: an outline, *Journal of the Geological Society*, *173*(6), 1007–1024, https://doi.org/10.1144/jgs2016-081.

Polteau, S., B. W. H. Hendriks, S. Planke, M. Ganerød, F. Corfu, J. I. Faleide, I. Midtkandal, H. S. Svensen, and R. Myklebust (2016), The Early Cretaceous Barents Sea Sill Complex: Distribution, 40Ar/39Ar geochronology, and implications for carbon gas formation, *Palaeogeography, Palaeoclimatology, Palaeoecology*, *441*, 83–95, https://doi.org/10.1016/j.palaeo.2015.07.007.

Priyanto, W. S., and B. J. Coakley (2025), Seismic insight on basement structure of the extinct mid-oceanic ridge in Canada Basin, arctic ocean, *Geochemistry, Geophysics, Geosystems: G(3)*, *26*(12), https://doi.org/10.1029/2024gc012023.

Rabbel, O., O. Galland, K. Mair, I. Lecomte, K. Senger, J. B. Spacapan, and R. Manceda (2018), From field analogues to realistic seismic modelling: a case study of an oil-producing andesitic sill complex in the Neuquén Basin, Argentina, *Journal of the Geological Society*, *175*(4), 580–593, https://doi.org/10.1144/jgs2017-116.

Rodes, N., A. M. R. Sartell, J. Whattam, E. Lindell, and Svalbox Team (2023), Svalbox-DOM_2023-0023, https://doi.org/10.5281/ZENODO.8311422.

Rodes, N., T. Mosociova, A. M. R. Sartell, K. Senger, and Svalbox Team (2024a), Svalbox-DOM_2022-0005, https://doi.org/10.5281/ZENODO.11191036.

Rodes, N., K. Senger, T. Mosočiová, A. M. Sartell, and Svalbox Team (2024b), Svalbox-DOM_2022-0027, https://doi.org/10.5281/ZENODO.12699304.

Rohde, R. A., and R. A. Muller (2005), Cycles in fossil diversity, *Nature*, *434*(7030), 208–210, https://doi.org/10.1038/nature03339.

Sartell, A. (2021), The igneous complex of Ekmanfjorden, Svalbard: an integrated field, petrological and geochemical study, Master's thesis, Lund University, Lund, Sweden.

Sartell, A. M. R., U. Söderlund, K. Senger, H. J. Kjøll, and O. Galland (2025), A review of the spatiotemporal evolution of the High Arctic Large Igneous Province, and a new U-Pb age of a mafic sill complex on Svalbard, *Geochemistry, Geophysics, Geosystems: G(3)*, *26*(12), https://doi.org/10.1029/2024gc011842.

Saumur, B. M., K. Dewing, and M.-C. Williamson (2016), Architecture of the Canadian portion of the High Arctic Large Igneous Province and implications for magmatic Ni–Cu potential, *Canadian Journal of Earth Sciences*, *53*(5), 528–542, https://doi.org/10.1139/cjes-2015-0220.

Saumur, B. M., M.-C. Williamson, and J. H. Bédard (2022), Targeting Ni-Cu mineralization in the Canadian High Arctic large igneous province: integrating geochemistry, magmatic architecture and structure, *Mineralium deposita*, *57*(2), 207–233, https://doi.org/10.1007/s00126-021-01054-3.

Saunders, A. D., S. M. Jones, L. A. Morgan, K. L. Pierce, M. Widdowson, and Y. G. Xu (2007), Regional uplift associated with continental large igneous provinces: The roles of mantle plumes and the lithosphere, *Chemical Geology*, *241*(3-4), 282–318, https://doi.org/10.1016/j.chemgeo.2007.01.017.

Senger, K., and O. Galland (2022), Stratigraphic and spatial extent of HALIP magmatism in central Spitsbergen, *Geochemistry, Geophysics, Geosystems: G(3)*, *23*(11), https://doi.org/10.1029/2021gc010300.

Senger, K., S. Roy, A. Braathen, S. Buckley, K. Bælum, L. Gernigon, R. Mjelde, R. Noormets, K. Ogata, S. Olaussen, S. Planke, B. Ruud, and J. Tveranger (2013), Geometries of doleritic intrusions in central Spitsbergen, Svalbard: an integrated study of an onshore-offshore magmatic province with implications for CO2 sequestration, *Norwegian Journal of Geology*, *93*, 143–166.

Senger, K., S. Planke, S. Polteau, K. Ogata, and H. Svensen (2014a), Sill emplacement and contact metamorphism in a siliciclastic reservoir on Svalbard, Arctic Norway, *Norwegian Journal of Geology*, *94*, 155–169.

Senger, K., J. Tveranger, K. Ogata, A. Braathen, and S. Planke (2014b), Late Mesozoic magmatism in Svalbard: A review, *Earth-Science Reviews*, *139*, 123–144, https://doi.org/10.1016/j.earscirev.2014.09.002.

Senger, K., J. Millett, S. Planke, K. Ogata, C. Haug Eide, M. Festøy, O. Galland, and D. A. Jerram (2017), Effects of igneous intrusions on the petroleum system: a review, *First Break*, *35*(6), https://doi.org/10.3997/1365-2397.2017011.

Senger, K., P. Brugmans, S.-A. Grundvåg, M. Jochmann, A. Nøttvedt, S. Olaussen, A. Skotte, and A. Smyrak-Sikora (2019), Petroleum, coal and research drilling onshore Svalbard: a historical perspective, *Norwegian Journal of Geology*, https://doi.org/10.17850/njg99-3-1.

Senger, K., P. Betlem, T. Birchall, S. J. Buckley, B. Coakley, C. H. Eide, P. P. Flaig, M. Forien, O. Galland, L. Gonzaga, Jr, M. Jensen, T. Kurz, I. Lecomte, K. Mair, R. H. Malm, M. Mulrooney, N. Naumann, I. Nordmo, N. Nolde, K. Ogata, O. Rabbel, N. W. Schaaf, and A. Smyrak-Sikora (2020), Using digital outcrops to make the high Arctic more accessible through the Svalbox database, *Journal of Geoscience Education*, *69*, 1–15, https://doi.org/10.1080/10899995.2020.1813865.

Senger, K., P. Betlem, S.-A. Grundvåg, R. K. Horota, S. J. Buckley, A. Smyrak-Sikora, M. M. Jochmann, T. Birchall, J. Janocha, K. Ogata, L. Kuckero, R. M. Johannessen, I. C. Lecomte, S. M. Cohen, and S. Olaussen (2021), Teaching with digital geology in the high Arctic: Opportunities and challenges, *Geoscience Communication*, *4*(3), 399–420, https://doi.org/10.5194/gc-4-399-2021.

Senger, K., D. Kulhanek, M. T. Jones, A. Smyrak-Sikora, S. Planke, V. Zuchuat, W. J. Foster, S.-A. Grundvåg, H. Lorenz, M. Ruhl, K. K. Sliwinska, M. L. Vickers, and W. Xu (2023), Deep-time Arctic climate archives: high-resolution coring of Svalbard's sedimentary record – SVALCLIME, a workshop report, *Scientific Drilling*, *32*, 113–135, https://doi.org/10.5194/sd-32-113-2023.

Senger, K., G. Shephard, F. Ammerlaan, O. Anfinson, P. Audet, B. Coakley, V. Ershova, J. I. Faleide, S.-A. Grundvåg, R. K. Horota, K. Iyer, J. Janocha, M. Jones, A. Minakov, M. Odlum, A. Sartell, A. Schaeffer, D. Stockli, M. A. Vander Kloet, and C. Gaina (2024), Arctic

Tectonics and Volcanism: a multi-scale, multi-disciplinary educational approach, *Geoscience Communication*, *7*(4), 267–295, https://doi.org/10.5194/gc-7-267-2024.

Senger, K., P. Betlem, A. Braathen, S. Olaussen, and G. Sand (2025), Longyearbyen CO_2 lab project—from a vision of a CO_2-neutral Svalbard to a geoscience data eldorado, *Arctic Science*, *11*, 1–26, https://doi.org/10.1139/as-2024-0019.

Shen, S.-Z., J. L. Crowley, Y. Wang, S. A. Bowring, D. H. Erwin, P. M. Sadler, C.-Q. Cao, D. H. Rothman, C. M. Henderson, J. Ramezani, H. Zhang, Y. Shen, X.-D. Wang, W. Wang, L. Mu, W.-Z. Li, Y.-G. Tang, X.-L. Liu, L.-J. Liu, Y. Zeng, Y.-F. Jiang, and Y.-G. Jin (2011), Calibrating the end-Permian mass extinction, *Science (New York, N.Y.)*, *334*(6061), 1367–1372, https://doi.org/10.1126/science.1213454.

Shephard, G. E., R. D. Müller, and M. Seton (2013), The tectonic evolution of the Arctic since Pangea breakup: Integrating constraints from surface geology and geophysics with mantle structure, *Earth-Science Reviews*, *124*, 148–183, https://doi.org/10.1016/j.earscirev.2013.05.012.

Shipilov, E. V., and Y. V. Karyakin (2010), New data on basaltoid magmatism of western Spitsbergen, *Doklady earth sciences*, *430*(2), 252–257, https://doi.org/10.1134/s1028334x10020236.

Silantyev, S. A., S. F. Karpenko, Y. A. Kostitsyn, O. G. Bogdanovskii, and P. I. Fedorov (2004), Intraplate magmatism of the De Long Islands: A response to the propagation of the ultraslow-spreading Gakkel Ridge into the passive continental margin in the Laptev Sea, *Russian Journal of Earth Sciences*, *6*(3), 153–183, https://doi.org/10.2205/2004es000150.

Simonov, V. A., Y. V. Karyakin, and A. V. Kotlyarov (2019), Physical and chemical conditions of basaltic magmatism at the Franz Josef land archipelago, *Geochemistry International*, *57*(7), 761–789, https://doi.org/10.1134/s0016702919070103.

Sklyarov, E. V., Y. V. Karyakin, N. S. Karmanov, and N. D. Tolstykh (2016), Platinum-group minerals in dolerites from Alexandra Land Island (*Franz Josef Land Archipelago*), *Russian Geology and Geophysics*, *57*(5), 834–841, https://doi.org/10.1016/j.rgg.2016.04.006.

Smelror, M., and G. B. Larssen (2016), Are there Upper Cretaceous sedimentary rocks preserved on Sørkapp Land, Svalbard?, *Norwegian Journal of Geology*, *96*(2), 147–158, https://doi.org/10.17850/njg96-2-05.

Smelror, M., G. B. Larssen, S. Olaussen, A. Rømuld, and R. Williams (2018), Late Triassic to Early Cretaceous palynostratigraphy of Kong Karls Land, Svalbard, Arctic Norway, with correlations to Franz Josef Land, Arctic Russia, *Norwegian Journal of Geology*, https://doi.org/10.17850/njg004.

Smyrak-Sikora, A., J. Janocha, C. Lie, M. Buelhoff, and Svalbox Team (2024), Svalbox-DOM_2022-0018, https://doi.org/10.5281/ZENODO.12624872.

Spacapan, J. B., A. D´Odorico, O. Palma, O. Galland, K. Senger, R. Ruiz, R. Manceda, and H. A. Leanza (2020), Low resistivity zones at contacts of igneous intrusions emplaced in organic-rich formations and their implications on fluid flow and petroleum systems: A case study in the northern Neuquén Basin, Argentina, *Basin Research*, *32*(1), 3–24, https://doi.org/10.1111/bre.12363.

Spall, H. (1968), Anomalous paleomagnetic poles from late Mesozoic dolerites from Spitsbergen, *Earth and Planetary Science Letters*, *4*(1), 73–78, https://doi.org/10.1016/0012-821x(68)90057-5.

Steel, R. J., and D. Worsley (1984), Svalbard's post-Caledonian strata — an atlas of sedimentational patterns and palaeogeographic evolution, in *Petroleum Geology of the North European Margin*, pp. 109–135, Springer Netherlands, Dordrecht, https://doi.org/10.1007/978-94-009-5626-1_9.

Steinberger, B., and T. H. Torsvik (2008), Absolute plate motions and true polar wander in the absence of hotspot tracks, *Nature*, *452*(7187), 620–623, https://doi.org/10.1038/nature06824.

Sun, S.-S., and W. F. McDonough (1989), Chemical and isotopic systematics of oceanic basalts: implications for mantle composition and processes, *Geological Society Special Publication*, *42*(1), 313–345, https://doi.org/10.1144/gsl.sp.1989.042.01.19.

Svensen, H., S. Planke, A. Malthe-Sørenssen, B. Jamtveit, R. Myklebust, T. Rasmussen Eidem, and S. S. Rey (2004), Release of methane from a volcanic basin as a mechanism for initial Eocene global warming, *Nature*, *429*(6991), 542–545, https://doi.org/10.1038/nature02566.

Svensen, H., G. Bebout, A. Kronz, L. Li, S. Planke, L. Chevallier, and B. Jamtveit (2008), Nitrogen geochemistry as a tracer of fluid flow in a hydrothermal vent complex in the Karoo Basin, South Africa, *Geochimica et cosmochimica acta*, *72*(20), 4929–4947, https://doi.org/10.1016/j.gca.2008.07.023.

Svensen, H. H., M. T. Jones, and T. A. Mather (2023), Large igneous provinces and the release of thermogenic volatiles from sedimentary basins, *Elements (Quebec, Quebec)*, *19*(5), 282–288, https://doi.org/10.2138/gselements.19.5.282.

Sømme, T. O., A. G. Doré, E. R. Lundin, and B. O. Tørudbakken (2018), Triassic–Paleogene paleogeography of the Arctic: Implications for sediment routing and basin fill, *AAPG Bulletin*, *102*(12), 2481–2517, https://doi.org/10.1306/05111817254.

Tarduno, J. A., D. B. Brinkman, P. R. Renne, R. D. Cottrell, H. Scher, and P. Castillo (1998), Evidence for extreme climatic warmth from late cretaceous arctic vertebrates, *Science (New York, N.Y.)*, *282*(5397), 2241–2244, https://doi.org/10.1126/science.282.5397.2241.

Tegner, C., M. Storey, P. M. Holm, S. B. Thorarinsson, X. Zhao, C.-H. Lo, and M. F. Knudsen (2011), Magmatism and Eurekan deformation in the High Arctic Large Igneous Province: 40Ar–39Ar age of Kap Washington Group volcanics, North Greenland, *Earth and Planetary Science Letters*, *303*(3-4), 203–214, https://doi.org/10.1016/j.epsl.2010.12.047.

Thorarinsson, S. B., P. M. Holm, H. Duprat, and C. Tegner (2011a), Silicic magmatism associated with Late

Cretaceous rifting in the Arctic Basin—petrogenesis of the Kap Kane sequence, the Kap Washington Group volcanics, North Greenland, *Lithos*, *125*(1-2), 65–85, https://doi.org/10.1016/j.lithos.2011.01.013.

Thorarinsson, S. B., P. M. Holm, S. Tappe, L. M. Heaman, and C. Tegner (2011b), Late Cretaceous–Palaeocene continental rifting in the High Arctic: U–Pb geochronology of the Kap Washington Group volcanic sequence, North Greenland, *Journal of the Geological Society*, *168*(5), 1093–1106, https://doi.org/10.1144/0016-76492011-018.

Thorarinsson, S. B., P. M. Holm, H. I. Duprat, and C. Tegner (2012), Petrology and Sr–Nd–Pb isotope geochemistry of Late Cretaceous continental rift ignimbrites, Kap Washington peninsula, North Greenland, *Journal of Volcanology and Geothermal Research*, *219-220*, 63–86, https://doi.org/10.1016/j.jvolgeores.2012.01.011.

Thórarinsson, S. B., U. Söderlund, A. Døssing, P. M. Holm, R. E. Ernst, and C. Tegner (2015), Rift magmatism on the Eurasia basin margin: U–Pb baddeleyite ages of alkaline dyke swarms in North Greenland, *Journal of the Geological Society*, *172*(6), 721–726, https://doi.org/10.1144/jgs2015-049.

Trettin, H. P. (1996), Chemical analyses of Upper Cretaceous volcanics and related(?) sills, northwestern Ellesmere Island, District of Franklin, *Tech. Rep. Open File, 3274, 30*, Geological Survey of Canada.

Tullius, D. N., A. L. Leier, J. M. Galloway, A. F. Embry, and P. K. Pedersen (2014), Sedimentology and stratigraphy of the lower cretaceous Isachsen formation: Ellef ringnes island, sverdrup basin, Canadian arctic archipelago, *Marine and Petroleum Geology*, *57*, 135–151, https://doi.org/10.1016/j.marpetgeo.2014.05.018.

Tyrrell, G. W., and K. S. Sandford (1934), XXI.—geology and petrology of the dolerites of Spitsbergen, *Proceedings of the Royal Society of Edinburgh*, *53*, 284–321, https://doi.org/10.1017/s0370164600015649.

Van Wagoner, N. A., M.-C. Williamson, P. T. Robinson, and I. L. Gibson (1986), First samples of acoustic basement recovered from the alpha ridge, Arctic ocean: New constraints for the origin of the ridge, *Journal of Geodynamics*, *6*(1-4), 177–196, https://doi.org/10.1016/0264-3707(86)90038-4.

Vickers, M. L., G. D. Price, R. M. Jerrett, and M. Watkinson (2016), Stratigraphic and geochemical expression of Barremian–Aptian global climate change in Arctic Svalbard, *Geosphere*, *12*(5), 1594–1605, https://doi.org/10.1130/ges01344.1.

Vincenz, S. A., D. Cossack, S. J. Duda, K. Birkenmajer, M. Jeleńska, M. Kadziałko-Hofmokl, and J. Kruczyk (1981), Palaeomagnetism of some late Mesozoic dolerite dykes of South Spitsbergen, *Geophysical Journal International*, *67*(3), 599–614, https://doi.org/10.1111/j.1365-246x.1981.tb06940.x.

Vincenz, S. A., M. Jeleńska, K. Aiinehsazian, and K. Birkenmajer (1984), Palaeomagnetism of some late Mesozoic dolerite sills of East Central Spitsbergen, Svalbard Archipelago, *Geophysical Journal International*, *78*(3), 751–773, https://doi.org/10.1111/j.1365-246x.1984.tb05069.x.

Wang, K., T. Plank, J. D. Walker, and E. I. Smith (2002), A mantle melting profile across the Basin and Range, SW USA, *Journal of Geophysical Research*, *107*(B1), https://doi.org/10.1029/2001jb000209.

Wesenlund, F., S.-A. Grundvåg, V. S. Engelschiøn, O. Thießen, and J. H. Pedersen (2022), Multi-elemental chemostratigraphy of Triassic mudstones in eastern Svalbard: Implications for source rock formation in front of the World's largest delta plain, *The Depositional Record*, *8*(2), 718–753, https://doi.org/10.1002/dep2.182.

Williamson, M.-C., G. E. Shephard, K. Boggild, R. Carey, P. B. Hamilton, D. Kellett, D. Miggins, A. A. P. Koppers, D. H. C. Wilton, D. J. MacDonald, D. Weis, S. Zhang, B. L. Cousens, S. E. Jackson, D. C. Petts, C. M. Lawley, E. Massey, L. M. Larsen, W. Jokat, and J. Harris (2026), A sample dredged from the Alpha Ridge records evidence of an emergent volcanic setting at 90 Ma, *Communications Earth & Environment*, *7*(1), https://doi.org/10.1038/s43247-025-02981-z.

Zhang, T., J. Dyment, and J. Y. Gao (2019), Age of the Canada Basin, Arctic ocean: Indications from high-resolution magnetic data, *Geophysical Research Letters*, *46*(23), 13,712–13,721, https://doi.org/10.1029/2019gl085736.

Zhang, Y., J. G. Ogg, D. Minguez, M. W. Hounslow, S. Olaussen, F. M. Gradstein, and S. Esmeray-Senlet (2021), Magnetostratigraphy of U-Pb–dated boreholes in Svalbard, Norway, implies that magnetochron M0r (a proposed Barremian-Aptian boundary marker) begins at 121.2 ± 0.4 Ma, *Geology*, *49*(6), 733–737, https://doi.org/10.1130/g48591.1.

Zhou, Y., Y. Li, W. Zheng, S. Tang, S. Pan, J. Chen, X.-F. He, J. Shen, and T. J. Algeo (2024), The role of LIPs in Phanerozoic mass extinctions: An Hg perspective, *Earth-Science Reviews*, *249*(104667), 104,667, https://doi.org/10.1016/j.earscirev.2023.104667.

Zuchuat, V., A. R. N. Sleveland, R. J. Twitchett, H. H. Svensen, H. Turner, L. E. Augland, M. T. Jones, O. Hammer, B. T. Hauksson, H. Haflidason, I. Midtkandal, and S. Planke (2020), A new high-resolution stratigraphic and palaeoenvironmental record spanning the End-Permian Mass Extinction and its aftermath in central Spitsbergen, Svalbard, *Palaeogeography, Palaeoclimatology, Palaeoecology*, *554*(109732), 109,732, https://doi.org/10.1016/j.palaeo.2020.109732.

Śliwińska, K. K., M. E. Jelby, S.-A. Grundvåg, H. Nøhr-Hansen, P. Alsen, and S. Olaussen (2020), Dinocyst stratigraphy of the Valanginian–Aptian Rurikfjellet and Helvetiafjellet formations on Spitsbergen, Arctic Norway, *Geological Magazine*, *157*(10), 1693–1714, https://doi.org/10.1017/s0016756819001249.